University of Helsinki
Department of Chemistry
Finland

CAPILLARY ELECTROCHROMATOGRAPHY: A VERSATILE INSTRUMENTAL TECHNIQUE FOR NANODOMAIN INTERACTION STUDIES

Lucia D'Ulivo

ACADEMIC DISSERTATION

To be presented, with the permission of
the Faculty of Science of the University of Helsinki
for public criticism in Chemicum, Auditorium A110,
(A.I. Virtasen aukio 1, Helsinki)
on January 29th, at 12 o'clock noon.
Helsinki 2010

Custos

Prof. Dr. Marja-Liisa Riekkola

Laboratory of Analytical Chemistry

Department of Chemistry

University of Helsinki

Finland

Reviewers

Prof. Dr. Pat Sandra

Pfizer Analytical Research Center

Department of Organic Chemistry

Ghent University

Belgium

and

Dr. Václav Kašička

Institute of Organic Chemistry & Biochemistry

Academy of Science of the Czech Republic

Czech Republic

Opponent

Prof. Dr. Ernst Kenndler

Max F. Perutz Laboratories, Medical University of Vienna

Inst. Med. Biochem., Vienna Biocenter (VBC)

Vienna, Austria

ISBN 978-952-10-5968-1 (paperback)

ISBN 978-952-10-5969-8 (PDF)

http://ethesis.helsinki.fi/

Helsinki University Printing House, 2010

Table of Contents

Preface

This thesis is based on research carried out in the Laboratory of Analytical Chemistry of the Department of Chemistry, University of Helsinki, during the years 2005-2010. Funding was provided by graduate School of Chemical Sensors and Microanalytical Systems (CHEMSEM) and the Academy of Finland, Research Council for Natural Sciences and Engineering.

I would like to warmly thank Professor Marja-Liisa Riekkola to have believed in me and given me the possibility to carry out my doctoral studies in the Laboratory of Analytical Chemistry. I'm grateful to Professor Ernst Kenndler for accepting to act as opponent. I thank Dr. Václav Kašička and Professor Pat Sandra to have revised my doctoral thesis and supplied valuable comments. I'm also in debit with Kathleen Ahonen for carefully and patiently revising the papers presented here as well as the final thesis.

Then, I would like to thank my colleagues which whom I shared this period. I'm especially grateful to Dr. Ruth Shimmo (formerly Kuldvee) that had patiently introduced me to the open tubular capillary electrochromatography. A warm thank to Joanna Witos and Kati Vainikka, which shared the office with me, and to Géraldine Cilpa for their positive characters and for making the working days more pleasant. As a collegue, I'm also grateful for their help in the laboratory, for useful discussions and for the great work in team.

I'm grateful to Matti Jussila and Pentti Jyske to fix all the problems occurred with the instruments and/or the software. I thank Liisa Heino to provide the chemicals and the supplies needed for the experiments. I'm also grateful to Merit Hortling for her effectiveness and for her help with several bureaucratic procedures, about which I was often totally puzzled.

Also, a great thank to present and former laboratory staff and co-workers: Ai-Jun, Anne, Antti, Arvind, Gebrenegus, Giovanni, Juhani, Jaakko, Jaana, Jana, Jari, Jaroslav, Jevgeni, Jie, Joonas, José, Kari, Laura, Maria, Minna, Maarit, Nanyin, Pepe, Simo, Susanne, Tapio, Totti, Tuulia, Yi.

A special thank to Professor Petri T. Kovanen and Dr. Katariina Öörni, our collaborators from the Wihuri Research Institute, that have provided the low-density lipoproteins needed for the studies. Moreover, thanks for our stimulating meetings and for useful discussions, I learnt so much from you.

I would like to remember our collaborators from Attana AB, Stockholm, namely Dr. Björn Ingemarsson and Dr. Julien Saint-Guirons. Thanks for introducing me to the quartz crystal microbalance technique and for the valuable discussions during our joint project.

I'm also grateful to Dr. Kristoffer Meinander for helpful discussion concerning atomic force microscopy images.

A warm thank to all the friends I met in Finland: Nadia, Silvia, Francesco, Felice, Andrea Ambrosioni, Valentina, Rossella, Andrea Bacioccola, Francesca, Roberto, Simone, Anne, Tamara, Harri, Katariina, Fanny, Marianna, Jan and Beatriz. Thanks to share this adventure with me and to make my stay better! In particular, a special thought for Nadia, Silvia and Gigi that have been stood by me during the toughest moments.

Then my dear, great friends Barbara and Laura: I think a whole book may not be long enough to tell how much you count for me! Thanks for your friendship that has survived despite the distance and the personal vicissitudes.

I cannot forget my friends in Italy: Francesca Aversa, Francesca Galli, Mariapia, and the others that have supported me during this period abroad.

I would like to thank the persons working at the IPCF, in Pisa: Massimo, Roberto, Emanuela and, in particular, Emilia that has taught me so much and has encouraged me during this experience abroad.

I cannot forget my lovely, big, family that I missed so much during these years. *Mamma e papa', grazie per il vostro supporto, per il vostro amore, per avermi lasciata sempre libera di scegliere, senza imposizione alcuna. Capisco che questi anni di lontananza siano stati duri anche per voi e ho capito che lasciare crescere i propri figli e' un mestiere difficile, ma per questo vi stimo ancora di piu'. Per non parlare dei miei nonni, Piera, Moreno, Dora e Massimiliano, a cui sono legati i miei piu' cari ricordi d'infanzia. Mia zia Serena, una delle persone che meglio mi capisce, una seconda madre con cui condivido una grande empatia. I miei cugini Gabriele, Simona e Mariapia: siete come dei fratelli per me. Ed ancora: Manuela e Raffaello, siete stati e siete ancora parte integrante della mia famiglia e della mia vita*. You are all so dear to me!

Finally, last but not least, my beloved Nicola. Maybe, I do not need to say you how much you are for me. Anyway, I think if I'm here, defending my thesis, it's mostly because of you, supporting and

driving me with all your love and your optimism. I actually wonder if I would have been able to go through these four years by myself. So, my dear Nicola, this thesis is also yours.

Abstract

This doctoral thesis describes the development of a miniaturized capillary electrochromatography (CEC) technique suitable for the study of interactions between various nanodomains of biological importance.

The particular focus of the study was low-density lipoprotein (LDL) particles and their interaction with components of the extracellular matrix (ECM). LDL transports cholesterol to the tissues through the blood circulation, but when the LDL level becomes too high the particles begin to permeate and accumulate in the arteries. Through binding sites on apolipoprotein B-100 (apoB-100), LDL interacts with components of the ECM, such as proteoglycans (PGs) and collagen, in what is considered the key mechanism in the retention of lipoproteins and onset of atherosclerosis. Hydrolytic enzymes and oxidizing agents in the ECM may later successively degrade the LDL surface. Metabolic diseases such as diabetes may provoke damage of the ECM structure through the non-enzymatic reaction of glucose with collagen.

In this work, fused silica capillaries of 50 μm i.d. were successfully coated with LDL and collagen, and steroids and apoB-100 peptide fragments were introduced as model compounds for interaction studies. The LDL coating was modified with copper sulphate or hydrolytic enzymes, and the interactions of steroids with the native and oxidized lipoproteins were studied. Lipids were also removed from the LDL particle coating leaving behind an apoB-100 surface for further studies. The development of collagen and collagen–decorin coatings was helpful in the elucidation of the interactions of apoB-100 peptide fragments with the primary ECM component, collagen. Furthermore, the collagen I coating provided a good platform for glycation studies and for clarification of LDL interactions with native and modified collagen.

All methods developed are inexpensive, requiring just small amounts of biomaterial. Moreover, the experimental conditions in CEC are easily modified, and the analyses can be carried out in a reasonable time frame.

Other techniques were employed to support and complement the CEC studies. Scanning electron microscopy and atomic force microscopy provided crucial visual information about the native and modified coatings. Asymmetrical flow field-flow fractionation enabled size measurements of the modified lipoproteins. Finally, the CEC results were exploited to develop new sensor chips for a

continuous flow quartz crystal microbalance technique, which provided complementary information about LDL–ECM interactions.

This thesis demonstrates the potential of CEC as a valuable and flexible technique for surface interaction studies. Further, CEC can serve as a novel microreactor for the *in situ* modification of LDL and collagen coatings. The coatings developed in this study provide useful platforms for a diversity of future investigations on biological nanodomains.

List of abbreviations

AFM	atomic force microscopy
AGE	advanced glycation end product
ApoB-100	apolipoprotein B-100
AsFlFFF	asymmetrical flow field-flow fractionation
BGE	background electrolyte
BSA	bovine serum albumin
CE	capillary electrophoresis
CEC	capillary electrochromatography
CGE	capillary gel electrophoresis
CITP	capillary isotachophoresis
C6S	chondroitin 6-sulphate
DAG	diacylglycerol
DIEA	*N*,*N*-diisopropylethylamine
Dihydro-SM	*N*-lauroyl-*D*-*erythro*-sphinganylphosphorylcholine
DLS	dynamic light scattering
DMF	*N*,*N*-dimethylformamide
DMSO	dimethyl sulphoxide
ECM	extracellular matrix
EDC	1-ethyl-3-(3-dimethylaminopropyl) carbodiimide hydrochloride
EDTA	ethylenediaminetetraacetic acid

EOF	electroosmotic flow
FFF	field-flow fractionation
FlFFF	flow field-flow fractionation
GAG	glycoaminoglycans
HCTU	O-(6-chlorobenzotriazol-1-yl)-*N*,*N*,*N´*,*N´*-tetramethyluronium hexafluorophosphate
HDL	high density lipoprotein
HEPES	4-(2-hydroxyethyl)-1-piperazineethanesulphoric acid
HPLC	high pressure liquid chromatography
i.d.	inner diameter
IDL	intermediate-density lipoprotein
LC	liquid chromatography
LDL	low-density lipoprotein
LIF	laser induced fluorescence
MALDI	matrix-assisted laser desorption/ionization
MEEKC	microemulsion electrokinetic chromatography
MEKC	micellar electrokinetic chromatography
MS	mass spectrometry
MWCO	molecular weight cut-off
$NeuP_1$	neutral peptide fragment of apolipoprotein B-100 with 12 amino acids
$NeuP_2$	neutral peptide fragment of apolipoprotein B-100 with 11 amino acids

NHS	*N*-hydroxysuccinimmide
NMM	4-methylmorpholine
NMR	nuclear magnetic resonance
NP	negative peptide fragment of apolipoprotein B-100 with 17 amino acids
o.d.	outer diameter
PBS	phosphate buffered saline
PC	phosphatidylcholine
PG	proteoglycan
PG_m	proteoglycan monomer
PLA_2	phospholipase A_2
PMSF	phenylmethylsulphonyl fluoride
POPC	1-palmitoyl-2-oleyl-*sn*-glycero-3-phosphatidylcholine
PP	positive peptide fragment of apolipoprotein B-100 with 19 amino acids
PP_2	positive peptide fragment of apolipoprotein B-100 with 42 amino acids
PS	polystyrene
QCM	quartz crystal microbalance
SEM	scanning electron microscopy
SM	sphingomyelin
SMase	sphingomyelinase
SM mimics	microemulsions prepared from commercial lipids
SPR	surface plasma resonance

Sulpho-NHS	sulpho-*N*-hydroxysuccinimmide
TFA	trifluoroacetic acid
TIS	triisoprolylsilane
TOF	time of flight
VLDL	very-low-density lipoprotein

List of symbols

β	phase ratio
C_M	concentration of mobile phase
C_S	concentration of stationary phase
Δf	frequency shift
E	electric field strength
e	elementary charge
ε	permittivity in solution
d_f	thickness of the stationary phase
k	retention factor
K_D	distribution coefficient
K_d	binding constant
$k_{OT\text{-}CEC}$	retention factor in open tubular capillary electrochromatography
L_{det}	detection length
L_{tot}	total length
m_M	mass of the mobile phase
m_S	mass of the stationary phase
μ_{eo}	electroosmotic mobility
μ_{ep}	electrophoretic mobility
μ_{tot}	total mobility
η	dynamic viscosity

r	Stokes radius
r_c	column radius
t_{eo}	migration time of the EOF marker
t_m	migration time of the analyte
V	applied voltage
v_e	electrophoretic velocity
v_{eo}	electroosmotic velocity
V_M	volume of the mobile phase
V_S	volume of the stationary phase
z	number of elementary charges
ζ	zeta potential

List of original papers

This doctoral thesis is based on the papers listed below, hereafter referred to by their Roman numerals [I-VI].

I R. Kuldvee, L. D'Ulivo, G. Yohannes, P. W. Lindenburg, M. Laine, K. Öörni, P. Kovanen, M.-L. Riekkola, *Anal. Chem.*, 78 (2006) 2665-2671. Open tubular capillary electrochromatography: technique for oxidation and interaction studies on human low-density lipoproteins. Copyright American Chemical Society 2006

II L. D'Ulivo, G. Yohannes, K. Öörni, P. T. Kovanen, M.-L. Riekkola, *Analyst*, 132 (2007) 989-996. Open tubular capillary electrochromatography: a new technique for *in situ* enzymatic modification of low density lipoprotein particles and their protein-free derivatives. Copyright The Royal Society of Chemistry 2007

III L. D'Ulivo, J. Chen, K. Meinander, K. Öörni, P. T. Kovanen, M.-L. Riekkola, *Anal. Biochem.*, 383 (2008) 38-43. In situ delipidation of low-density lipoproteins in capillary electrochromatography yields apolipoprotein B-100-coated surfaces for interaction studies. Copyright Elsevier Science 2008

IV L. D'Ulivo, J. Witos, K. Öörni, P. T. Kovanen, M.-L. Riekkola, *Electrophoresis*, 30 (2009) 3838-3845. Capillary electrochromatography: a tool for mimicking collagen surface interactions with apolipoprotein B-100 peptides. Copyright Wiley-VCH 2009

V L. D'Ulivo, J. Witos, K. Öörni, P. T. Kovanen, M.-L. Riekkola, submitted for publication in *Anal. Chim. Acta*, (2009). Capillary electrochromatography: useful microreactor for collagen I glycation and interaction studies with low-density lipoprotein particles.

VI L. D'Ulivo, J. Saint-Guirons, B. Ingemarsson, M.-L. Riekkola, *Anal. Bioanal. Chem.* (2009) DOI 10.1007/s00216-009-3371-y. Quartz crystal microbalance, a valuable tool for elucidation of weak interactions between biomolecules. Copyright Springer-Verlag 2009

The contribution of the author:

Paper I: part of the experimental work related to capillary electrochromatography

Paper II: experimental work related to capillary electrochromatography and writing of the article

Paper III: experimental work related to capillary electrochromatography and writing of the article

Paper IV: experimental work related to capillary electrochromatography and writing of the article

Paper V: experimental work related to capillary electrochromatography and writing of the article

Paper VI: experimental work and writing of the article

1 Introduction

The emerging field of nanoscience and nanotechnologies is ushering in a new era of nanodevices and nanodomain research. With the pressing need for miniaturized devices capable of carrying out analyses in shorter time and with lower consumption of compounds, nanoscience is assuming an important place alongside the conventional analytical techniques. In bioanalysis, in particular, where only small amounts of analytes are available, miniaturized systems that minimize sample consumption are essential. Miniaturized instruments are also finding important applications in clinical analysis, vastly speeding up routine tests of physiological samples.

With atherosclerosis one of the main causes of morbidity and mortality in industrialized countries, research on the disease has been increasing at a rapid pace. Close attention is being paid to lipoproteins and, in particular, to low-density lipoproteins (LDL), which are imputed as the main cause of atherosclerosis. Innumerable studies have been carried out with the aim of comprehending their modality of accumulation and modification in the arteries.

Several procedures are available for lipoprotein isolation and characterization. Understanding of lipoprotein structure is crucial for clarifying the modality of interaction of lipoproteins with the arterial extracellular matrix (ECM) and with the enzymes located there. Slab gel electrophoresis was one of the first techniques employed for the separation and characterization of LDL and other plasma lipoproteins (**1,2**). Techniques such as liquid chromatography (LC) and asymmetrical flow field-flow fractionation (AsFlFFF) have also made a great contribution to the separation of lipoproteins. In addition, column microtiters have been helpful in the clarification of interactions between LDL and ECM components such as proteoglycans. Fluorescence and UV spectrometers have been employed for the determination of kinetics and the degree of LDL oxidation (**3**,**4),** while AsFlFFF has proven useful for measuring the sizes of lipoproteins after their oxidation and enzymatic modification (**5**) Although all these techniques have played an important role in LDL isolation, and in providing reliable information about the modality of LDL interactions and modifications, there are also a number of drawbacks. LDLs are huge molecules, and samples are highly complex, which means that experienced staff is required for the task of isolation. In addition, earlier studies have mostly been carried out in vials or with use of techniques that, although valuable, require high consumption of material. For these reasons, there is a great need for faster and miniaturized techniques that save time and sample material without sacrificing reliability. The size

of LDLs and their complex interactions with the ECM pose a challenging task for the developer of new tools. The advent of capillary electrophoresis (CE) and microchip electrophoresis has opened up new possibilities for miniaturization and for novel studies. (**6,7**)

In CE, analytes are separated in an electric field according to their charge, size and shape of their molecules. In comparison with other separation techniques, such as high pressure liquid chromatography (HPLC), CE has the advantage that runs are performed in shorter time and resolution is better. CE is actually one of a family of techniques, of which micellar electrokinetic chromatography (MEKC), microemulsion electrokinetic chromatography (MEEKC) and capillary electrochromatography (CEC) also allow the separation of uncharged analytes. (**8-14**) CEC can further be considered a special case of capillary liquid chromatography, where the movement of the mobile phase through a capillary that is filled, packed or coated with a stationary phase is achieved by electroosmotic flow. (**15-18**) Because the retention of the analyte on a stationary phase depends upon both electrophoretic migration and chromatography, CEC offers great flexibility and potential for elucidation of the interactions of nanodomains of biological importance.

The aim of this doctoral work was to develop microsystems that enable interaction studies between biomaterials and biomarkers involved in the development of pathologies in human beings. Special emphasis was put on the possibility of carrying out *in situ* studies with these miniaturized tools, with the attached benefits of time saving, decreased sample consumption and enhanced reliability. CEC was selected as the technique of choice because the presence of a stationary phase enhances its versatility. CEC also allows easy and rapid changes in experimental parameters, such as pH, temperature and background electrolyte composition.

LDL particles were used as stationary phase in CEC to understand how they are modified when exposed to copper sulphate (I) or enzymes in the capillary (II). In addition, flushing of LDL coating with non-ionic surfactant almost totally removed the lipids, leaving a fresh apolipoprotein apoB-100 surface suitable for further investigations (III). In studies I, II and III, neutral steroids that can promote the development of atherosclerosis, were employed as model compounds. The interactions between LDL and uncharged steroids are mainly based on hydrophobicity, and changes in the coating charge density affect the affinity of the coating for the model compounds. Because LDL–ECM interactions play an important role in the onset and progression of atherosclerosis, a method of preparing collagen and collagen–decorin coatings was developed as well (IV). Selected apoB-100

peptide fragments were used as marker compounds for the evaluation of apoB-100 interactions with collagens I and III. Calculated retention factors (*k*) employed to describe the strength of affinity indicated the importance of decorin for the interactions and for the entrapment of LDL by the ECM. Since atherosclerosis has frequently been linked to diabetes, capillaries coated with collagen I were glycated *in situ* to provide a platform for interaction studies between native and oxidized LDL and glycated collagen I (V). The results obtained by CEC were exploited in studies on a continuous flow quartz crystal microbalance (QCM), which gave both supportive and complementary information on LDL–ECM interactions (VI).

All methods employed required only small amounts of compounds and provided results in a reasonable time period. The flexibility and versatility of CEC as a tool suitable for interaction studies were clearly demonstrated.

Scanning electron microscopy (SEM), atomic force microscopy (AFM) and AsFlFFF were employed as supportive and complementary techniques. The specific targets of my study were the following:

- To develop a low-density lipoprotein (LDL) coating in a capillary for clarification, by CEC, of modifications to LDL upon *in situ* oxidation with copper sulphate (I)
- To study the suitability of the LDL-coated capillary as a microreactor in *in situ* treatment of LDL with hydrolytic enzymes (II)
- To delipidate *in situ* LDL particles acting as stationary phase in the capillary and so isolate the apolipoprotein B-100 (apoB-100) surface for use in interaction studies with biological marker compounds (III)
- To coat the capillaries with collagen I, collagen III, collagen I-decorin and collagen III-decorin, and to clarify the interactions with selected apoB-100 peptide fragments (IV)
- To develop a method for *in situ* glycation of collagen I enabling interaction studies with native and oxidized LDL (V)
- To apply the results obtained with the LDL and collagen coatings in CEC to studies on QCM chip surfaces, and so calculate numerical values for the interactions (VI)

2 Low-density lipoprotein particles and cardiovascular diseases

Retention of low-density lipoprotein (LDL) particles in the arteries is considered the main cause of atherosclerosis. In this chapter, the onset of atherosclerosis, the structure of LDLs and the modality of LDL entrapment in the arteries are described.

2.1 Atherosclerosis and cardiovascular diseases

Atherosclerosis is a chronic inflammation of the arteries and a disorder of the lipid methabolism. (**19**-**21**) The capillary wall consists of three concentric layers: intima, media and adventitia. The intima is the inner layer of the capillary wall and lies in direct contact with the blood circulation. Atherosclerosis, which is associated with high levels of cholesterol in the blood, originates from the accumulation of LDL in the arteries. (**22**-**24**) LDL can then interact with the components of the extracellular matrix (ECM) and become entrapped in the intima. (**25**-**29**) Later, it may be modified by enzymes and/or oxidizing agents, with resultant aggregation and fusion. (**30,31**) These events activate macrophages and may arouse a chronic inflammatory response. (**32**-**34**) After undergoing modification, and possibly aggregation and fusion as well, LDLs have strengthened affinity for arterial proteoglycans (PGs), and the retention of LDLs in the *intima* is enhanced. (**35**,**36**) Once formed, the atherosclerotic plaque (atheroma) can continue to grow, with consequent thickening of the arteries and narrowing of the lumen. The circulation becomes obstructed and blood pressure rises as a compensatory response. The probability of tissue ischemia, ictus and infarct increases in pace. Together with cancer, atherosclerosis is a primary cause of premature death in Western countries. A sedentary life-style, reduced bodily activity and a fat-rich diet are considered to be the main triggers of this disease. Genetic defects, such as mutation of the apoB-100 site, may contribute by impairing the removal of LDL from the blood circulation, with consequent accumulation in the artery. (**37**-**39**) For these reasons, clarification of the mechanisms leading to the formation of atherosclerotic plaques has become a key concern of medical research.

2.2 Low-density lipoprotein (LDL)

Plasma LDLs are spherical particles with an estimated diameter of about 22 nm (**40**) and, like other lipoproteins, they are involved in the transport of cholesterol in the blood circulation. LDLs originate from the metabolism of chylomicrons and very-low-density lipoprotein (VLDL) particles, which are synthesised by the intestine and the liver, respectively, and transport the lipids to the tissues. (**41**) As lipids are released, the density of the lipoproteins increases; VLDLs are converted to intermediate-

density lipoproteins (IDL) and eventually to LDL. The conversion of IDLs to LDLs proceeds particularly through the removal of triglycerides, performed by hepatic lipase. (**22**)

LDLs consist of a hydrophobic core of triglycerides and free and esterified cholesterol, which is surrounded by a monolayer of phospholipids, mostly made up of phosphatidylcholine (PC) and sphingomyelin (SM) (**40**,**30**). Unlike VLDLs, LDLs contain only one protein, namely, apolipoprotein B-100 (apoB-100), which wraps the particle like a ribbon, while also taking contact with the hydrophobic core. (**42**-**44**) The huge molecular mass (about 512 kDa) and the hydrophobicity make the isolation and characterization of apoB-100 extremely challenging. (**45**-**47**) ApoB-100, which contains the LDL receptor-binding domain, plays a crucial role in the reuptake of the lipoproteins from the blood circulation, and defective apoB sequences are the cause of inherited hypercholesterolemia. (**39**,**48**)

A high plasmatic level of LDL is considered a risk factor for the development of atherosclerosis and cardiovascular diseases. In view of this, several methods have been developed to separate lipoproteins and estimate their precise amount in the plasma. Slab gel electrophoresis (**1,2**) was one of the first techniques for the separation and quantification of lipoproteins. Ultracentrifugation (**49**) and, although low in accuracy, the Friedewald method (**50**) have routinely been used to separate and to determine the cholesterol content of lipoproteins, respectively. Nuclear magnetic resonance (NMR) spectroscopy has been proposed for the characterization and precise quantification of plasma lipoproteins. (**51**) However, the drawbacks of relatively high cost, lengthy procedures and the large amount of samples required, have pushed the quest for reasonably priced miniaturized techniques. Flow field-flow fractionation (flow FFF) has been helpful in the separation and size determination of lipoproteins in human plasma. (**52**) Moreover, important studies have been carried out by anion-exchange HPLC, where lipoproteins are separated and the amounts of cholesterol determined by enzymatic essay. (**53**) The advent of CE has opened doors for the development of miniaturized techniques. Capillary gel electrophoresis (CGE) was used as long ago as 1986 for the separation of serum lipoproteins, (**54**), and since then CE has been successfully coupled with mass spectrometry for quantification of serum levels of apolipoproteins (**3**). In addition, capillary isotachophoresis (CITP) has been beneficial for the identification of atherogenic LDL in the whole plasma. (**55**-**60**)

2.3 Extracellular matrix

The extracellular matrix (ECM) is a highly complex environment built up of several different components, which, by forming a tight net, support the tissues and deliver nutrients to the cells. Of the many ECM components, there are two main ones involved in the development of atherosclerosis: PGs and collagen.

Proteoglycan monomer (PGm), consisting of a core protein with one or more glycosaminoglycan (GAG) chains, comprises the basic unit of PGs. PGs can be distinguished into several families according to the type of GAG that predominates in the monomer. (**61**,**62**) In our laboratory, we have focused on decorin and chondroidin-6-sulphate (C6S) PGs, which, respectively, belong to the small leucine-rich and chondroitin sulphate families.

Collagen is the most abundant protein in the human body. Although several types of collagen have been classified, all of them share the common repetitive sequence Gly-X-Y, where X is usually proline and Y hydroxyproline, and the triple helix structure where three polypeptide α-chains are twisted around each other. (**63-65**) Collagen I and III are the most abundant types in the arteries, and they are usually present in association with arterial PGs, in particular with decorin. (**66,67**) This small leucine-rich PG seems to be involved in collagen fibril formation and organization, and its absence appears to result in the formation of loose fibrils. (**68-70**)

2.4 Interactions of LDL particles with extracellular matrix components, their retention and modifications

In the pathological condition of hypercholesterolemia, LDL particles diffuse through the endothelial cell layer, interact with components of the ECM and become entrapped in the intima. A specific site on apoB-100 (residues 3359-3377), particularly rich in lysine and arginine, probably mediates the binding by interacting with the sulphate groups of PGs (**71**,**72**) and the negative charged residues of collagen. Furthermore, it has been shown that decorin enhances the binding of LDLs to collagen, and promotes their retention in the ECM. (**73**,**25**) The entrapped LDL particles may then be modified by oxidizing agents, such as Cu^{2+} and Fe^{2+}, or hydrolytic enzymes located in the intima. (**74**,**75**) The major enzymes involved in LDL degradation are α-chymotrypsin, phospholipase A_2 (PLA_2) and sphingomyelinase (SMase) (**30**,**76,77**). α-Chymotrypsin is a proteolytic enzyme that hydrolyses apoB-100. (**78**) Since apoB-100 is important in maintaining LDL integrity, even partial loss of the

apolipoprotein can provoke significant rearrangements in the phospholipid monolayer and in the lipid core, with possible aggregation and fusion of the particles. PLA_2 and SMase are lipolytic enzymes, catalysing the hydrolysis of phosphatidylcholine and SM, respectively. The degradation of phosphatidylcholine yields lysophosphatidylcholine and fatty acids, which, in the presence of bovine serum albumin (BSA), are removed from lipoprotein surfaces. The hydrolysis of SM produces ceramide and phosphocholine, the latter polar enough to easily leave the LDL surface. SMase provokes aggregation and then fusion of the LDL particles, PLA_2 only aggregation. (**30**,**79**,**80**) Oxidizing agents, such as Cu^{2+}, are able to react with both the lipid and protein parts of LDL, provoking aggregation and fusion. (**30**)

Modified LDL particles have increased affinity for arterial PG. The stronger LDL–PG interactions appear to be related to the rearrangement of apoB-100 that occurs during modification, exposing new binding sites with active lysine residues. (**81**,**82**)

2.5 Modification of extracellular matrix components in diabetes

Diabetes is a complex multifunctional disease, characterized by a high level of glucose in the blood circulation. Diabetes has severe consequences: not least, diabetes increases the risk of atherosclerosis and cardiovascular diseases. (**83**) The complications of diabetes are mostly associated with the reaction of glucose with the long-lived proteins of the human body and the modification and loss of functionality of these proteins. Like other structural proteins, those forming the ECM may be modified. Glycation of collagen I has attracted special attention (**84**). The glycation reaction involves an aldehydic group of the sugar and an amino group, usually of a lysine residue, of the protein. The so-formed Schiff base may successively rearrange into an Amadori product, which further attacks other amino groups and finally yields advanced glycation end-products (AGEs). AGEs, as reactive molecules, can react further with proteins and have been imputed as the main cause of diabetes complications. (**85,86**) AGEs can react with collagen I, with such severe consequences as decrease in solubility, resistance to collagenase, and cross-link formation. (**87**,**88**) These structural changes cause severe alterations of collagen functionality, which may affect the retention of LDLs in the ECM. (**89**,**90**)

3 Techniques used in the studies

Although CEC was selected as the method of choice in this study, other techniques were employed as well, to provide supporting or complementary information. A description of the techniques that were used is given in the following sections.

3.1 Capillary electromigration techniques

Separations in capillary electromigration techniques are achieved in narrow capillaries under high electric field strength. Capillary electromigration techniques can be divided into two groups: capillary electrophoretic techniques and electrically driven capillary chromatographic techniques. The division is base on different separation principles, in some cases overlapping. A schematic representation of capillary electromigration techniques is shown in the scheme below:

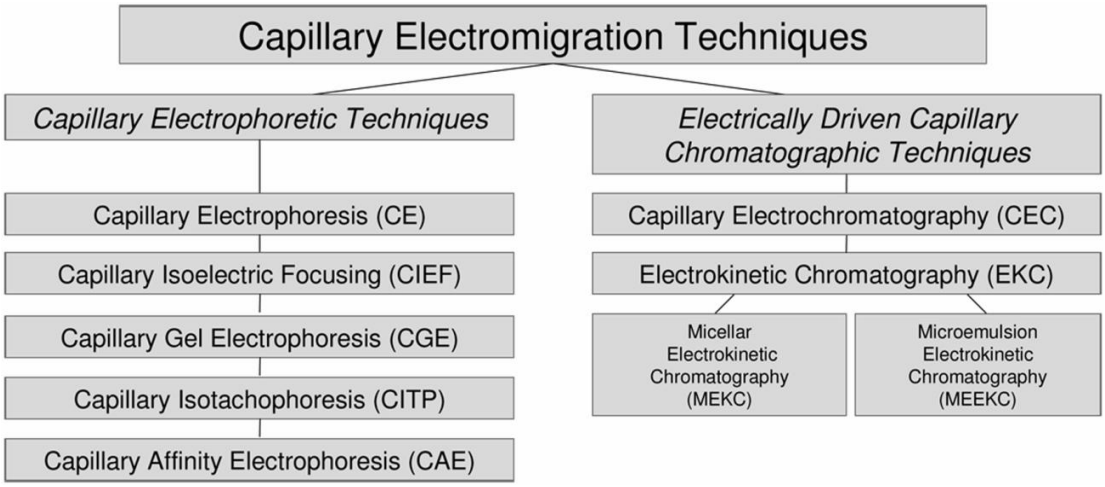

In electrophoresis, analytes migrate under the influence of an electric field and separation is based on their different charges, sizes and molecular shape. The electrophoretic velocity of the analyte can be expressed as:

$$v_{ep} = \mu_{ep} \cdot E = \mu_{ep} \frac{V}{L_{tot}} \qquad (1)$$

where E is the electric field strength, V the applied voltage, L_{tot} the total length of the capillary and μ_{ep} the electrophoretic mobility of the analyte, which is given by the following equation:

$$\mu_{ep} = \frac{ze}{6\pi\eta r} \qquad (2)$$

where z is the number of the elementary charges of the ion, e the elementary charge, η the dynamic viscosity of the solution and r the Stokes radius of the ion. Fused silica capillaries are characterized by the presence of silanol groups, which start to be deprotonated above pH about 2. The positive ions of the background electrolyte interact with the capillary wall, generating a double layer and a potential difference between the wall and the bulk liquid. When voltage is applied, the ions in the positively charged diffuse layer move towards the cathode and, because they are hydrated, they drag along the molecules of the bulk liquid, generating electroosmotic flow (EOF). Because the thickness of the diffuse layer is much less than the radius of the capillary, the electroosmotic flow adopts a flat profile (so-called plug flow). Although the presence of electroosmotic flow may contribute to the separation, it is not always needed (e.g., in isoelectric focusing), and sometimes may be completely undesired. In the separation of small molecules, uncoated fused silica capillaries are usually preferred and EOF is exploited. However, to prevent surface adsorption of the analytes or matrix components, and to eliminate or control the electroosmotic flow, surface coating or chemical modification of the silanol groups may be required. Neutral and charged coatings have been successfully used in a variety of applications. In coated capillaries, the EOF can be used as a surface charge indicator.

In CE, the total velocity (v_{tot}) of a charged analyte can be given as:

$$v_{tot} = v_{ep} + v_{eo} \tag{3}$$

where v_{ep} and v_{eo} are the electrophoretic and electroosmotic velocities, respectively. v_{eo} can be expressed as:

$$v_{eo} = \mu_{eo} \cdot E = \mu_{eo} \frac{V}{L_{tot}} \tag{4}$$

where μ_{eo} represents the electroosmotic mobility that is given by the following equation:

$$\mu_{eo} = -\frac{\varepsilon\zeta}{\eta} \tag{5}$$

where ε is the permittivity of the solution and ζ the zeta potential. Another expression affords the experimental determination of the EOF mobility:

$$\mu_{eo} = \frac{L_{tot} L_{\det}}{V t_{eo}} \quad (6)$$

where t_{eo} is the migration time for the EOF marker, and L_{tot} and L_{det} are the total and detection lengths of the capillary, respectively. (**91**) In the case of an uncharged compound, the term μ_{ep} is equal to zero, and the uncharged analyte migrates together with the EOF. As evident from equation (3) uncharged compounds cannot be separated by CE. Fortunately, electrically driven techniques, such as micellar electrokinetic chromatography, microemulsion electrokinetic chromatography and capillary electrochromatograpy, can then be employed.

Principle of capillary electrochromatography

In capillary electrochromatography (CEC), the technique of interest in this work, the capillary is either filled or coated with a stationary phase, and the retention time of the analytes depends on both electrophoretic migration and chromatographic retention. The retention factor (k) of an uncharged analyte can be evaluated with the same formula as used in LC:

$$k = \frac{t_m - t_{eo}}{t_{eo}} \quad (7)$$

where t_m and t_{eo} are the migration times of the analyte and EOF marker, respectively. (**92**) When the amount of immobilized stationary phase is known, the distribution coefficient (K_D) can be calculated according to the following equation:

$$K_D = \frac{C_S}{C_M} = \frac{m_S / V_S}{m_M / V_M} = \frac{m_S \cdot V_M}{m_M \cdot V_S} = k\beta \quad (8)$$

where C_M, m_M and V_M are the concentration, mass and volume of the mobile phase, while C_S, m_S and V_S are the concentration, mass and volume of the stationary phase. The phase ratio β can be expressed as

$$\beta = \frac{r_c}{2 d_f} \quad (9)$$

where r_c is the column radius and d_f the thickness of the stationary phase.

Because equation (7) is not valid in the case of charged analytes running in a coated capillary, the following equation (**93**,**94**) must be applied:

$$k_{OT-CEC} = \left(1 - \frac{v_{ep}}{v_{ep} + v_{eo}}\right) k - \frac{v_{ep}}{v_{ep} + v_{eo}} \qquad (10)$$

Instrumentation for capillary electromigration techniques

The CE apparatus (Fig. 1) consists of the capillary, inlet and outlet reservoirs, and typically of an on-capillary UV detector, located before the outlet. Two electrodes are dipped into each reservoir and a power supply provides the electricity needed for the separation. Both the capillary cassette and the vial carousel can be thermostatted. Although other capillary materials such as teflon and pyrex are available, fused silica is by far the most common material. Capillary dimensions are typically an inner diameter (i.d.) from 15 to 100 μm and total length (L_{tot}) from 20 to 80 cm. The field strength can range from 200 to 1000 V/cm.

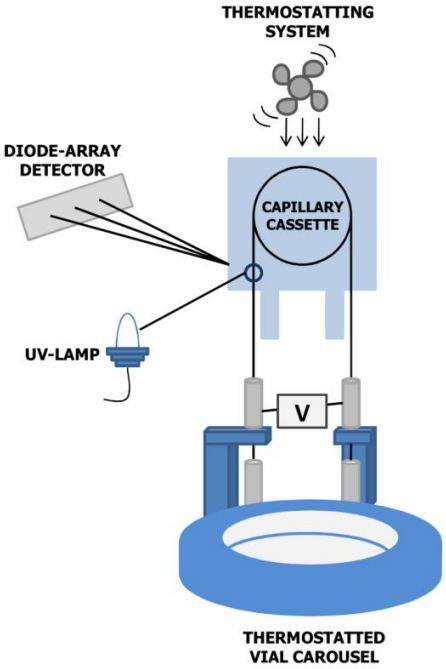

Figure 1. *Schematic representation of CE apparatus.*

Capillary electromigration instruments are versatile and can be coupled with any of several detectors: UV/VIS, diode array, MS, laser induced fluorescence (LIF), NMR, dynamic light scattering (DLS) and conductivity detector, to mention the most common ones. Several studies have shown the applicability of capillary electromigration techniques to the analysis of biological samples. Analyses of cell coatings, blood and urine are just a few examples of tasks that can be performed with capillary electromigration techniques. (**95-98**)

3.2 Scanning electron microscopy

Scanning electron microscopy (SEM) can be employed to examine the external structure of almost anything that can be viewed in a dissecting light microscope. Scanning electron microscopy examines structures by bombarding the specimen with a scanning beam of electrons. The slow-moving secondary electrons that the specimen generates are successively collected, amplified, and displayed on a cathode ray tube. The electron beam and the cathode ray tube scan synchronously to produce an image of the surface of the specimen. (**99**) Before the measurement, the sample must be dried and made conductive to electricity, if it is not already.

3.3 Atomic force microscopy

Atomic force microscopy (AFM) measures forces between a probe and the surface of interest through changes in the deflection of a flexible cantilever attached to the probe. Changes in sample topography affect the probe–sample interaction profile and thereby the response of the cantilever. (**100-104**)

The contact and tapping modes are the most widely applied of the several modes of operation. In the contact mode the probe tip is in continuous contact with the surface, while in the tapping mode it oscillates up and down as it scans over the surface. (**104**) The tapping mode is gentler than the contact mode and is more suitable for the investigation of soft matter, such as polymers and biological material. AFM offers the possibility to visualize the surface in 2D or 3D, and it can give both qualitative and quantitative information on many physical properties including size, morphology, surface texture and roughness. Information on size, surface area and volume distributions can be obtained as well. A wide range of particle sizes can be characterized in the same scan, from about 1 nanometer (nm) to about 8 micrometers (μm). AFM can also be employed under different conditions (air, liquid, pH).

3.4 Quartz crystal microbalance technique

The quartz crystal microbalance (QCM) technique belongs to the family of acoustic biosensors that are based on quartz crystal resonators. The QCM is a mass-sensing device whose signal transduction mechanism depends on the piezoelectric effect of the quartz crystal. The crystals are typically a few tenths of a millimetre thick and cut AT form (35^{o} 10' angle from the Z-axis). Gold electrodes are coated on upper and lower sides of the crystal (Fig. 2), which is then integrated into a cuvette or flow cell. (**105-107**)

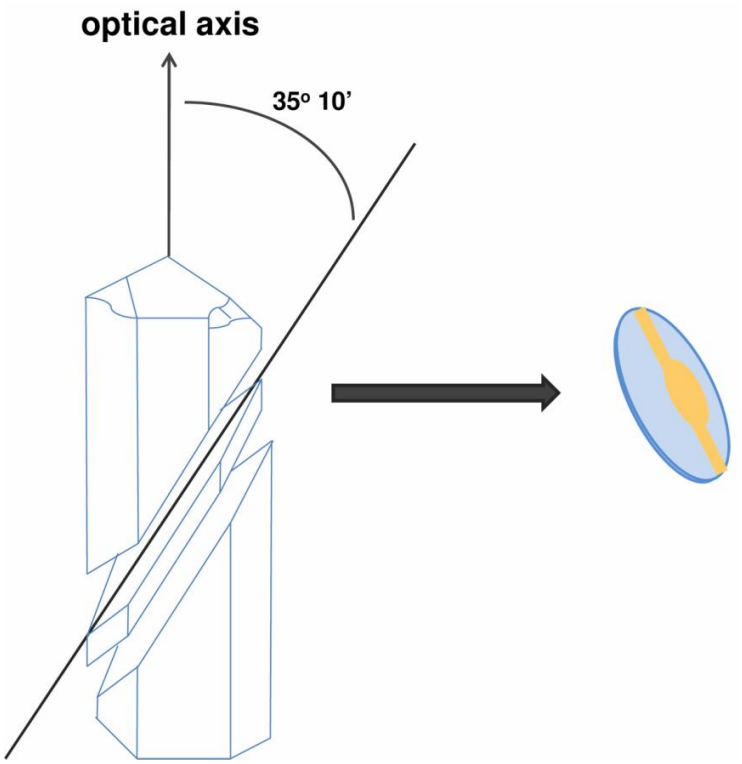

Figure 2. *Fabrication of an AT-cut quartz crystal for QCM. The final crystal, coated on either side with gold electrodes, is shown on the right.*

Because quartz is a piezoelectric material, the application of an alternating electric field through two metal electrodes generates a mechanical oscillation of a certain frequency. When a mass is bound to the crystal, the frequency decreases and the shift can be recorded with an oscillometer. There is a linear relationship between the frequency shift and the mass adsorbed on the surface. (**108**)

The QCM has been widely applied to the study of biochemical processes and the development of biomimetic systems and biosensors. (**109-111**) Molecules of interest (ligands) are directly immobilized on the gold surface for study of the interactions with specific analytes. The gold surface can also be modified with polystyrene, biotin, silicon dioxide or carboxyl group to promote the immobilization of specific molecules.

Relative to optical biosensors, such as surface plasma resonance (SPR) sensors, QCM provides some clear advantages. Since the acoustic sensor response is sensitive to the charge of receptor–ligand complexes and the changes in visco-elastic properties, more detailed information is obtained about interactions. (**112,113**) The QCM technique allows the direct injection of crude samples, which usually provoke significant non-specific binding response in SPR devices. QCM also has higher mass sensitivity (on the order of fg/mm^2) than SPR (pg/mm^2).

3.5 Field-flow fractionation

Field-flow fractionation (FFF) is a major analytical technique for the separation and characterization of macromolecules and particles. Giddings (**114**) introduced field-flow fractionation (FFF) for the separation of macromolecules and colloids. DNA, viruses and other macromolecules and complexes, including lipoproteins, ribosomes and liposomes, have all been separated by FFF (**5**, **115**).

In contrast to flow FFF (FlFFF), where two walls are permeable to the flow, in asymmetrical flow FFF (AsFlFFF) only one wall is permeable. AsFlFFF has recently also been realized in miniaturized scale. (**5**) Whereas in FlFFF the main and the cross flow enter the channel from two separate inlets, in AsFlFFF the incoming flow from a single channel inlet is split into an axial component (the main flow) and a perpendicular component (cross flow). Normal, steric and hyperlayer modes can be applied in AsFlFFF.

In AsFlFFF, particles or macromolecules are separated on the basis of differences in diffusion coefficients. The movement of the cross flow across the separation channel propels larger particles with lower diffusion coefficients closer to the channel wall. In normal mode, the larger molecules will therefore be eluted more slowly than the smaller ones.

4 Experimental

The chemicals, equipment and methods employed are briefly described in this chapter. The details can be found in papers I-VI.

4.1 Chemicals

The chemicals and reagents used in the studies are reported in Table 1. Because of the huge molecular size of apoB-100, selected peptide fragments carrying a site of interaction for PGs were selected for the studies. The negative and the neutral peptide fragments were used as negative controls. More information about the peptide fragments is given in Table 2.

4.2 Instruments and equipment

The instruments and other equipment employed in the work are reported in Tables 3 and 4, respectively.

4.3 Methods

The methods employed in the studies are reported in the following sections.

4.3.1 Isolation of human LDL

Human LDL (d=1.019–1.050 g/mL) was isolated from the plasma of healthy volunteers by sequential ultracentrifugation in the presence of 3 mM EDTA (**116-118**). Briefly, solid KBr was added to plasma to adjust the density to 1.019 g/mL. The floated VLDL and IDL fractions were removed, and the density of the infranatant solution was adjusted to 1.050 g/mL with solid KBr. After ultracentrifugation for 72 h at 35 000 rpm in a Beckman Coulter Type 50.2 Ti rotor (148 000 gmax), LDL was recovered from the top of the centrifuge tubes, recentrifuged (d=1.060 g/mL) for 24 h at 35 000 rpm in a Beckman Coulter Type 80 Ti rotor (115 000 gmax), and dialysed extensively against LDL buffer (1 mM EDTA and 150 mM sodium chloride in water, pH 7.4, adjusted with sodium hydroxide). The amount of LDL is expressed in terms of its protein concentration, which was determined by the method of Lowry *et al.*, with bovine serum albumin (BSA) as standard. (**119**) When needed, EDTA was removed from LDL in a PD-10 desalting column equilibrated with Dulbecco's phosphate buffered saline.

Table 1. List of chemicals used in the experiments.

Compound	Supplier	Notes	Paper
Acetic acid	Sigma Chemical Co.	Solvent 99.7%	I
Apolipoprotein B-100 (apoB-100) peptide fragments	Mehilahti Protein Chemistry Facility		IV, VI
17-α-Progesterone	Sigma-Aldrich	Marker compound	I
α-Chymotrypsin	Sigma-Aldrich	Hydrolytic enzyme	II
Bovine serum albumin (BSA)	Sigma-Aldrich	Serum protein	II
β-Estradiol	Sigma-Aldrich	Marker compound	I-III
Cholesterol	Avanti Polar Lipids		II
Cholesteryl linoleate	Sigma-Aldrich		II
Chondroitin 6-sulphate (C6S)	Sigma-Aldrich		VI
Collagen I	Sigma-Aldrich		IV-VI
Collagen III	Sigma-Aldrich		IV
Copper Sulphate	Merck	Oxidizing agent	I
d-Aldosterone	Sigma Chemical Co.	Marker compound	I, II
Decorin	Sigma-Aldrich		IV
1-Ethyl-3-(3-dimethylaminopropyl) carbodiimide hydrochloride (EDC)	Sigma-Aldrich	Carboxyl activating agent	VI
D-Glucose 6-phosphate sodium salt	Fluka		
Dimethyl sulphoxide (DMSO)	Oy FF-Chemicals Ab	Marker compound	I
Dimethyl sulphoxide (DMSO)	LabScan Ltd Co.	Marker compound	II-V
Dulbecco's phosphate-buffered saline	Bio Whittaker	Physiological buffer	I, II
Ethylenediaminetetraacetic acid (EDTA) sodium salt	Sigma Chemical Co.	Chelant agent	I, II, V
N-Hydroxysulphosuccinimide sodium salt (sulpho-NHS)	Sigma-Aldrich		VI
Membrane for dialysis	Spectrapor		IV, V
N-Lauroyl-D-*erythro*-sphinganylphosphorylcholine (dihydro-SM)	Avanti Polar Lipids		II
N-Lauroyl-D-*erythro*-sphingosylphosphorylcholine (SM)	Avanti Polar Lipids		II
Nonidet P-40	Roche Diagnostic	Nonionic surfactant	III
OptiPhase HiSafe	Wallac Oy	Liquid scintillation cocktail	I
1-Palmitoyl-2-oleyl-*sn*-glycero-3-phosphatidylcholine (POPC)	Avanti Polar Lipids		II
Phenylmethylsulphonyl fluoride (PMSF)	Sigma-Aldrich		II
Phosphate buffered saline (PBS)	Sigma-Aldrich	Tablets	VI
Phospholipase A_2 (PLA_2)	Sigma-Aldrich	Hydrolytic enzyme	II
Progesterone	Merck	Marker compound	I-III
Sodium cyanoborohydride	Sigma-Aldrich	Reducing agent	VI
Sodium meta-periodate	Thermo Scientific	Oxidizing agent	VI
Sphingomyelinase (SMase)	Sigma-Aldrich	Hydrolytic enzyme	II
Testosterone	Merck	Marker compound	I-III
tert-Butoxycarbonyl-L-[S]-methionine *N*-hydroxysuccinimidyl ester	Amersham Biosciences	^{3}H labeling reagent	I

Table 2. Information about apoB-100 peptide fragments.

	Peptide with 19 amino acids	**Peptide with 42 amino acids**	**Peptide with 17 amino acids**	**Peptide with 12 amino acids**	**Peptide with 11 amino acids**
Abbreviation	PP	PP_2	NP	$NeuP_1$	$NeuP_2$
Primary sequence	RLTRKRGLKLATALS LSNK	LSLSLNADLRLKNGNLSLSL NADLRLKNGNLSLSLNADL RLK	DEDDDFSKWN FYYSPQS	RQIDDID VRFQK	SLTSASG LALA
Residues in apoB-100	3359-3377	Contains part of the residues of PP	3987-4003	4094-4105	3359-3369
Net charge[a]	+6	+3	-4	0	0

[a] value at pH 7.4

Table 3. Instruments used for the experiments.

Equipment	**Model and Manufacturer**	**Notes**	**Paper**
Atomic force microscope (AFM)	Autoprobe CP Research, ThermoMicroscopes	MikroMasch NSC21 triangular Si cantilevers, tapping mode	III
Atomic force microscope (AFM)	Veeco Instruments Multimode V	Veeco RFESP rectangular phosphorus-doped Si cantilevers	IV, V
AsFlFFF	Constructed in-house	UV/visible detector	I, II
CE	^{3D}CE system, Agilent	diode array detector	I-V
QCM	Attana A100®, Attana AB		VI
Scanning electron microscope (SEM)	Hitachi S4800	1.0 kV acceleration voltage	I
Zetasizer	3000 HAS, Malvern Instruments		I

Table 4. Other equipment used in the studies.

Equipment	Model and Manufacturer	Notes	Paper
Commercial kit for cholesterol determination	Roche Diagnostics		II
Gold-plated quartz crystals	Attana AB	10 MHz	VI
Liquid scintillation counter	1219 Rackbeta, LKB, Wallac Oy		I
Millipore filters	Bedford	0.2-0.46 μm pore size	I-VI
Millipore water purification system	Millipore S.A.		I-V
PD-10 desalting columns	Amersham Biosciences		I
pH meter	Jenway 3030		II-V
pH meter	Radiometer PHM 220 Lab		I-V
Shaking bath 58-16	Serial no. 19999-6, Techne Inc.		I, V
Uncoated fused silica capillaries	Composite Metal Services Ltd.	50 μm i.d., 375 μm o.d.	I
Uncoated fused silica capillaries	Optronis GmbH	50 μm i.d., 375 μm o.d.	II-V
Water bath	HETO		II
Water bath	Lauda Ercoline		I

4.3.2 Preparation of LDL-derived microemulsions (microemulsions) and microemulsions from commercial lipids (SM mimics)

Lipids for microemulsions were extracted from 1 mL of LDL (4.3–5.0 mg/mL) by the method of Bligh and Dyer. (**120**) SM mimics were prepared by mixing, in appropriate ratio, commercial lipids that mimic the lipid composition of LDL (Table 5). The lipids were dissolved in methanol, stored at -20 ^{o}C and mixed in the appropriate ratio immediately before use.

The microemulsions and the SM mimic solutions were evaporated under a stream of nitrogen. PBS and phosphate buffer were added to microemulsions and SM mimics, respectively. The solutions

were sonicated six times under nitrogen at 40–45 ^{o}C, for 5 min, and then centrifuged to eliminate the residues of titanium. Particle sizes measured by AsFlFFF at pH 7.4 and 25 ^{o}C were 113 nm for microemulsions and 99 nm for SM mimics. The amounts of microemulsions and SM mimics were expressed as cholesterol concentration, determined with a commercial kit.

Table 5. Commercial lipids and percentages used for the preparation of SM mimics.

Lipids	**Percent of total (w/w)**
POPC	20%
SM[a]	9%
Cholesterol	14%
Cholesteryl linoleate	57%

[a] For the preparation of SM mimics without 4,5-*trans* double bonds dihydro SM was employed.

4.3.3 Buffer preparation

The buffers are listed in Table 6. The pH was adjusted with 1 M HCl or NaOH. Before use, the buffers were filtered through 0.2–0.45 μm Millipore filters by means of a Millipore vacuum system. The details of the buffer preparation can be found in the relevant papers.

Table 6. Buffers used in the studies.

Buffer	**pH**	**Ionic strength**	**Paper**
Acetate	4.0-5.0	20 mM	I, III
Borate	8.5	100 mM	I
HEPES	7.4	20 mM	IV
Phosphate	3.2, 6.0-7.4	20 mM	I-VI
PBS	7.4	10 mM	VI

4.3.4 Synthesis of apoB-100 peptide fragments

PP (RLTRKRGLKLATALSLSNK), PP_2 (LSLSLNADLRLKNGNLSLSLNADLRLKNGNLSLSLNADLRLK), NP (DEDDDFSKWNFYYSPQS), $NeuP_1$ (RQIDDIDVRFQK) and $NeuP_2$ (SLTSASGLALA) were synthesised by standard solid-phase synthesis via Fmoc (9-fluorenylmethoxycarbonyl) chemistry on Wang resin preloaded with C-terminal amino acid (Applied Biosystems). Synthesis was done in 25 mmol scale on a MultiPep synthesiser (Intavis Ag) using double coupling and activation with 1:1:2 amino acid / O-(6-chlorobenzotriazol-1-yl)-*N*,*N*,*N´*,*N´*-tetramethyluronium hexafluorophosphate (HCTU) / 4-methylmorpholine (NMM). Amino acids with standard side chain protecting groups (Novabiochem) were used in 4-fold excess to resin to ensure maximal coupling under the pre-activation with 0.5 M HCTU / 4 M NMM (Fluka) in *N*,*N*-dimethylformamide (DMF, Rathburn Chemicals). Peptide chains that were unreacted after the coupling and subsequent DMF wash cycles were capped by acetylation in 50 mM acetic anhydride / 130 mM *N*,*N*-diisopropylethylamine (DIEA) in DMF. Fmoc deprotection after each amino acid cycle was done twice with 25% piperidine in DMF. The synthesis product was dried on resin and cleaved in 5 ml of cleavage mix: 95% trifluoroacetic acid (TFA) / 2.5% triisoprolylsilane (TIS) / 2.5% H_2O to remove the side-chain protecting groups and detach the peptide. After 2 h incubation at room temperature, the resin eluate was filtered, and the solution containing the newly synthesised peptide was evaporated under nitrogen flow (99.99%) to approximately 20% of the volume. Peptide was precipitated with 10-fold volume of tert-butyl methyl ether, centrifuged in an explosion-proof centrifuge, washed once with ether, solubilized in water, and lyophilized. Peptide powder was resolubilized in dimethylsulphoxide (DMSO, Riedel-de Haën) and purified in a C18 reversed-phase column (Supelco Discovery wide-pore) with 10 column volumes of 0–70% acetonitrile / H_2O gradient. The purified peptide of interest was quality controlled by MALDI-TOF/TOF mass spectrometry (AutoFlex III, Bruker). About 5 pmol of the solubilized peptide was mixed with saturated α-cyano-4-hydroxycinnamic acid matrix solution (1 part of 0.1% trifluoro acetic acid in water to 2 parts of MS grade acetonitrile). If necessary, each peptide was further de-novo sequenced by TOF/TOF.

4.3.5 Preparation and modification of coatings

Before each coating, the capillary was preconditioned by flushing 20 min with 1 M HCl, 10 min with 0.1 M HCl, 25 min with MilliQ water and 5 min with background electrolyte (BGE). The

coating methods are summarized in Table 7. LDL and collagen I coatings were modified *in situ*. Table 8 presents a list of the developed treatments and the optimized conditions.

Table 7. Coating methods developed in the studies.

Coating	**Biomaterial**	**Concentration (mg/mL)**	**Conditions**	**Buffer**	**Paper**
LDL	LDL	0.1	Pressure 50 mbar, 40 min; wait 15 min; flush 15 min buffer; 25/37 ^{o}C	20 mM phosphate pH 7.4	I-III
Collagen I	Collagen I	0.5	Pressure 50 mbar, 40 min; wait 2 h; flush 30 min buffer; 25/37 ^{o}C	20 mM phosphate pH 7.4	IV, V
Collagen III	Collagen III	0.3	Pressure 50 mbar, 40 min; wait 2 h; flush 30 min buffer; 25/37 ^{o}C	20 mM HEPES pH 7.4, 135 mM NaCl	IV
Collagen I–decorin	Collagen I, decorin	0.5, 0.025	Pressure 50 mbar, 40 min; wait 2 h; flush 30 min buffer; 37 ^{o}C	20 mM phosphate pH 7.4, 135 mM NaCl	IV
Collagen III–decorin	Collagen III, decorin	0.3, 0.015	Pressure 50 mbar, 40 min; wait 2 h; flush 30 min buffer; 37 ^{o}C	20 mM HEPES pH 7.4, 135 mM NaCl	IV
Micro-emulsions	Lipid micro-emulsions derived from LDL lipids	1	Pressure 50 mbar, 40 min; wait 15 min; flush 15 min buffer; 37 ^{o}C	20 mM phosphate pH 7.4	II
SM mimics	Pseudo lipid micro-emulsions	1	Pressure 50 mbar, 40 min; wait 15 min; flush 15 min buffer; 37 ^{o}C	20 mM phosphate pH 7.4	II

Table 8. Procedures for *in situ* modification of coatings.

Modified coating	**Original coating**	**Reagent/Treatment agents**	**Treatment conditions**	**Paper**
Oxidized LDL	LDL	$CuSO_4$ (5 μM in phosphate buffer)	Pressure 50 mbar, 5 min; wait 0.5-12 h; rinsing with 1 mM EDTA	I
ApoB-100-hydrolysed LDL	LDL	α-Chymotrypsin (0.187 mg/mL in PBS)	Pressure 50 mbar, 10 min; wait 55 min; flushing 25 min BGE	II
SM-hydrolysed LDL	LDL	Sphingomyelinase (0.185 U/mL in PBS)	Pressure 50 mbar, 5 min; wait 55 min; flushing 25 min 10 mM EDTA	II
DAG-hydrolysed LDL	LDL	Phospholipase A_2 (0.00187 mg/mL, BSA 2% v/v)	Pressure 50 mbar, 5 min; wait 55 min; flushing 40 min 10 mM EDTA	II
ApoB-100	LDL	Nonidet P-40 (0.1 mM in water)	Flushing 25 min; flushing 25 min water; flushing 40 min BGE	III
Glycated Collagen I	Collagen I	D-Glucose 6-phosphate	Pressure 50 mbar 40 min; wait 8-24 h; pressure 50 mbar 10 min BGE	V

4.3.6 Study of coatings and coating interactions

DMSO was employed as EOF marker to obtain information about the charge of the coatings. The retention factors (k) and distribution coefficients (K_D) were calculated for steroids, apoB-100 peptide fragments and LDL, which served as important biomarkers. Successive runs (n=3-6) were carried

out, and EOF mobilities and k and K_D values were evaluated with equations (6), (7) and (8), respectively. Instead of equation (7), equation (10) was used to calculate the retention factors of charged analytes. Before each run, the capillary was flushed for 2 min with the BGE. Most runs were carried out under the following conditions: voltage +20 kV, injection 2-5 s by 50 mbar pressure, temperature 25–37 ^{o}C. For the evaluation of k of apoB-100 peptide fragments, runs were carried out at 50 mbar pressure with no voltage (paper IV). Details about the samples are reported in Table 9.

Table 9. Description of samples.

Sample	**Stock solution concentration (mg/mL)**	**Storage temperature (^{o}C)**	**Final concentration injected (mg/mL)**	**Paper**
ApoB-100 peptide fragments	2.0 (in water)	-20	0.005–0.5	IV, VI
β-Estradiol	0.5 (in methanol)	+4	0.05–0.071	I–III
C6S	10.0 (in water)	+4	0.0001–0.03	VI
d-Aldosterone	0.5 (in methanol)	+4	0.02–0.071	I–III
DMSO	11.1 (in water)	+4	1.6–1.9	I–V
LDL	1.0-11.4 (in Dulbecco's phosphate buffered saline)	+4	0.5	V
Progesterone/17-α-progesterone	0.5 (in methanol)	+4	0.05–0.071	I–III
Testosterone	0.5 (in methanol)	+4	0.02–0.071	I–III

Study of coating lifetime

Studies on coating lifetime were carried out for apoB-100 (paper III), collagen I, collagen III, collagen I–decorin and collagen III–decorin coatings (paper IV). The coatings were obtained, as described in section 4.3.5. The stability of the coatings was evaluated by following the EOF

repeatability daily and the EOF reproducibility during 7–8 days. For the repeatability and reproducibility studies, six and three successive runs, respectively, were carried out by injecting DMSO as EOF marker. For apoB-100 coatings, the repeatability and reproducibility of *k* values of steroids were evaluated as well. The running conditions were the following: +20 kV, injection 2 s at 50 mbar pressure, temperature 25 or 37 ^{o}C, BGE 20 mM phosphate or HEPES pH 7.4.

Measurement of isoelectric point of the coating

Isoelectric points were determined only for apoB-100 coatings (paper III). Coating of the capillary with apoB-100 was carried out as explained in section 4.3.5. The capillary was then flushed for 10 min with the BGE at different pH values. The buffers were 20 mM phosphate (pH 6.0, 6.5, 7.4) and acetate (pH 4.0, 4.5, 5.0). DMSO was used as EOF marker. Running conditions were the following: ±20 kV, injection 2 s at 50 mbar pressure, temperature 25 ^{o}C.

Asymmetrical flow field-flow fractionation studies

AsFlFFF was used to determine the size of LDL after oxidative or enzymatic modifications. The carrier liquid used in AsFlFFF was 20 mM phosphate (pH 3.2, 6.5, 7.4) and acetate (pH 4.0, 5.0) buffer. The actual channel thickness was calculated at 20 ^{o}C, from BSA solution in 8.5 mM phosphate buffer with 150 mM NaCl solution. The BSA solution had a diffusion coefficient of 6.21×10^{-7} cm^2/s. (**121**) The main and cross-flow rates were 1.8 and 1.4 mL/min, respectively.

In-vial oxidation (paper I) and enzymatic treatment (paper II) of LDL for AsFlFFF experiments were performed in an Eppendorf plastic container and EDTA-free PBS, and incubation was done in a horizontal shaking bath operating at 25 cycles/min. Details of the conditions employed are reported in Table 10.

Radioactivity measurements

Radioactivity measurements were carried out to obtain information on the distribution of the LDL particles on the capillary wall. LDL particles were labelled with ^{3}H according to Bolton and Hunter's procedure (**122**), except that *N*-hydroxysuccinimmide (NHS) was substituted for the Bolton and Hunter reagent.

Table 10. Experimental conditions for in-vial oxidation and enzymatic treatment of LDL.

	LDL oxidation	**SMase-modified LDL**	**PLA_2-modified LDL**	**α-Chymotrypsin-modified LDL**
Incubation temperature	37 °C	25/37 °C	25/37 °C	25/37 °C
Incubation time	16-24 h	Overnight (~16 h)	Overnight (~16 h)	Overnight (~16 h)
LDL amount	2 µL (stock solution 4.6 mg/mL[a])	16 µL (stock solution 6.2 mg/mL[a])	16 µL (stock solution 6.2 mg/mL[a])	16 µL (stock solution 6.2 mg/mL[a])
Modifying agent	$CuSO_4 \cdot 5H_2O$ (23 µL of 5 µmol/L stock solution)	SMase (2.7 µL of 3.68 U/mL stock solution)	PLA_2 (1 µL of 0.01 mg/mL stock solution)	α-chymotrypsyn (10 µL of 1 mg/mL stock solution)
Terminating agent	EDTA (2 µL of 1 mM stock solution)	EDTA (2.5 µL of 0.4 M stock solution)	EDTA (2.5 µL of 0.4 M stock solution)	PMSF (0.5 µL of 0.2 M stock solution)

[a] Expressed as protein concentration.

LDLs (5–10 mg/mL in 0.1 M borate buffer pH 8.5) were added to the labelling reagent, which had been precooled in a vessel on ice. The reaction was stopped after 30 min by adding 100 mL of glycine (0.2 M in 0.1 M borate buffer pH 8.5). The tagged LDL sample was purified on a PD-10 desalting column and dialysed against LDL buffer. Three different lengths (38.5, 77 and 192.5 cm) of capillaries were coated with the ^3H LDL, according to the procedure described in section 4.3.5. The preconditioning, the rinsing with ^3H LDL and the final BGE flushing were increased proportionally to the capillary length. The capillaries of longer size were then cut into pieces of 38.5 cm length, and all coated capillaries were flushed with freshly made piranha acid (3:1 (v/v) sulphuric acid and hydrogen peroxide) for 60 min. The ^3H LDL coating was then collected and dissolved in 2

mL of MilliQ and 3 mL of OptiPhase HiSafe 3 scintillation cocktail and left for at least 1 h. Radioactivity was measured with a liquid scintillation counter (^{3}H window: channels 5–364) over a period of 10 min. The counting efficiency of the ^{3}H standard was estimated at 22.6 %.

Scanning electron microscopy and atomic force microscopy studies

For the SEM and AFM studies of coatings, the polyimide layer of the outside of the fused silica capillary was burned off and the underlying surface was cleaned with methanol and treated with acid. After that, the surface was coated with the material of interest as described in section 4.3.4. Modification of the surface was carried out according to the procedure described in the relative paper (see also section 4.3.5). Capillaries were stored in either 20 phosphate or HEPES buffer pH 7.4 until the AFM measurements. Details of the types of coating submitted to SEM and AFM studies are given in the sketch below.

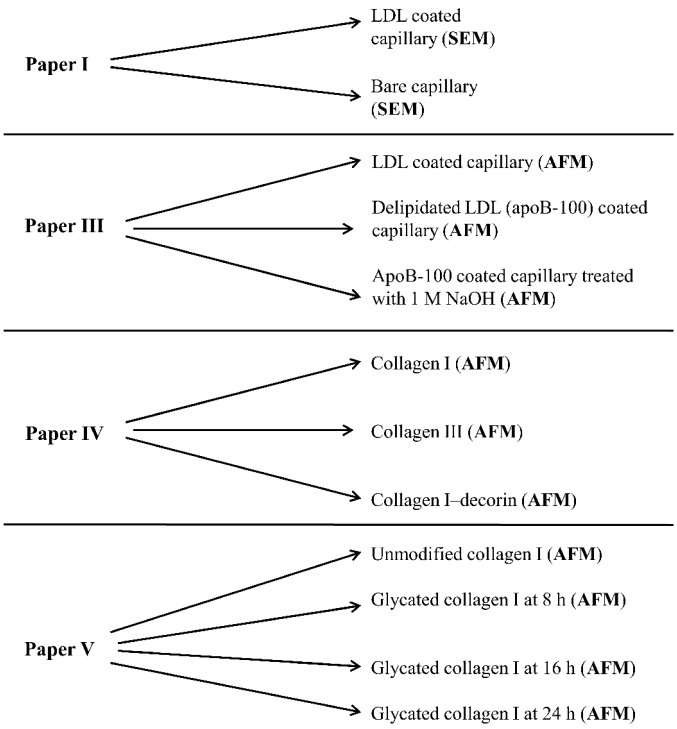

4.3.7 Quartz crystal microbalance studies

QCM experiments were carried out only in study VI. Gold-plated QCM polystyrene (PS) crystals were coated with positive apoB-100 peptide fragments (PP and PP_2) of 19 and 42 amino acids and carboxyl-derivatized collagen I and C6S.

For the experiments with polystyrene sensor chip, solutions of PP, BSA and $NeuP_2$ were prepared in 10 mM PBS, pH 7.4, at concentrations of 0.8 mg/ml, 1 mg/ml and 0.8 mg/ml, respectively. A volume of 20 µl of PP, BSA or $NeuP_2$ solution was deposited on the polystyrene surface and left to incubate for 16 hours at + 4 ^{o}C to permit maximum adsorption of the ligands. A different adsorption protocol was used for PP_2. The peptide solution was prepared in DMSO to a concentration of 1 mg/ml, deposited on the polystyrene surface and left to incubate for 1 h at room temperature. Before measurement, the chips were rinsed with running buffer. For the experiments with carboxyl sensor chips (Attana AB, Stockholm, Sweden), collagen I or C6S were immobilized by amine or aldehyde coupling according to the manufacturer's recommendations.

Briefly, before the immobilization of collagen I, the sensor was pre-wetted *ex situ* with 20 µl of MilliQ water, inserted into an Attana A100® QCM biosensor (Attana AB, Stockholm, Sweden) and left to stabilize. The immobilization was performed at a flow rate of 25 µl/min in running buffer (10 mM HEPES pH 7.4, 150 mM NaCl, 0.005% Tween™). The surface was activated by making three consecutive injections of a freshly-prepared mixture of 0.2 M 1-ethyl-3-(3-dimethylaminopropyl) carbodiimide hydrochloride (EDC) and 0.05 M sulpho-NHS (1:1), each for 400 s. The amine coupling was then carried out by performing two or three injections of collagen I solution (0.050 mg/mL in 10 mM acetate buffer pH 4) for 200 sec. Finally, the remaining activated carboxyl groups on the surface were deactivated with two injections of 1 M ethylene diamine pH 8.5 (400 s/ each).

C6S was immobilized on carboxyl sensor chips (Attana AB) by aldehyde coupling. *cis*-Diols of C6S were first oxidized into aldehyde groups using sodium meta-periodate according to the supplier's recommendations (Thermo Scientific) in order to enable efficient coupling. Oxidized C6S was then immobilized on carboxyl sensor chip via aldehyde coupling according to the manufacturer's recommendations (Attana AB). Briefly, the immobilization was carried out at a flow rate of 10 µL/min in HEPES buffer. Activation of the surface was performed by injecting a freshly made mixture of 0.2 M EDC and 0.05 M sulpho-NHS (1:1) for 300 s. Carbohydrazide (5 mM) was coupled to the activated surface prior to injection of the aldehyde-containing C6S. C6S (0.5 mg/mL) was covalently bound to carbohydrazide; this was further stabilized by injection of cyanoborohydride (0.1 M in acetate buffer pH 4.0).

Binding of the analyte to the sensor was monitored by frequency logging, and the frequency shifts (Δf) were recorded with the Attester™ software (Attana AB, Stockholm, Sweden). The experiments were carried out at room temperature.

Before the measurements, the derivatized PS and carboxyl crystals were equilibrated with the running buffer (PBS, HEPES or phosphate buffer pH 7.4) in the flow-through QCM system. With the exception of the BSA control and collagen I–derivatized chips, the surfaces were blocked with BSA (2 mg/mL in PBS). A continuous flow of running buffer (PBS or phosphate pH 7.4) was employed in all experiments (flow rate 25 μL/min). The selected analytes were C6S (max concentration 30 μg/mL) for the PS-derivatized chips, and PP and $NeuP_2$ (max concentration 250 μg/mL) for the carboxyl–derivatized chips.

For the evaluation of the dissociation constant (K_d), increasing concentrations of PP and C6S were injected over the surfaces and Δf values recorded with the Attester™ software. The kinetic data were then analysed with the software ClampXP (**123**).

5 Results and discussion

The starting point for all research described in this thesis was the discovery, made in the Laboratory of Analytical Chemistry, that capillaries for electrochromatography can be coated with lipoproteins. (**124**) In addition to lipoproteins, coating methods were developed and optimized for microemulsions, collagen and collagen–decorin. The suitability of these biomaterial-based stationary phases for *in situ* oxidation, delipidation, glycation and interaction studies was then explored. The results and discussion presented below summarize the results of the work. Capillary electrochromatographic results were supported and complemented with scanning electron microscopy, asymmetrical flow field flow fractionation and atomic force microscopy studies. The results obtained by CEC were exploited in continuous flow quartz crystal microbalance studies to obtain further information on the interactions between selected extracellular components and low-density lipoproteins.

5.1 Coating of capillaries with biomaterials

The development of stable biomaterial coatings was the first step in the studies. The good and repeatable results laid the basis for *in situ* studies. Figure 3 shows a schematic representation of the immobilization of biomaterials on the inner surface of a fused silica capillary. As already mentioned, the inner surface of a fused silica capillary is covered with silanol groups that start to be dissociated at above pH about 2 and make the capillary wall negatively charged. Negative charges attract basic proteins and other positively charged analytes causing them to adsorb on the capillary wall. Since the fused silica surface is hydrophobic in nature, it also favours the adsorption of hydrophobic parts of proteins and other biological materials. These features were exploited for the immobilization of biological materials, namely, LDL, microemulsions, collagen I, collagen III, collagen I–decorin and collagen III–decorin, on the inner surface of the silica capillary. The variety of biomaterials studied, differing in chemical nature and properties, presented a challenge for the development of suitable coating procedures.

5.1.1 Development of LDL and microemulsion coatings

As shown in Table 7, LDL and microemulsions required a shorter coating time than did collagen and collagen–decorin. LDL and microemulsions are spherical particles that have electrostatic and hydrophobic interactions with the capillary wall.

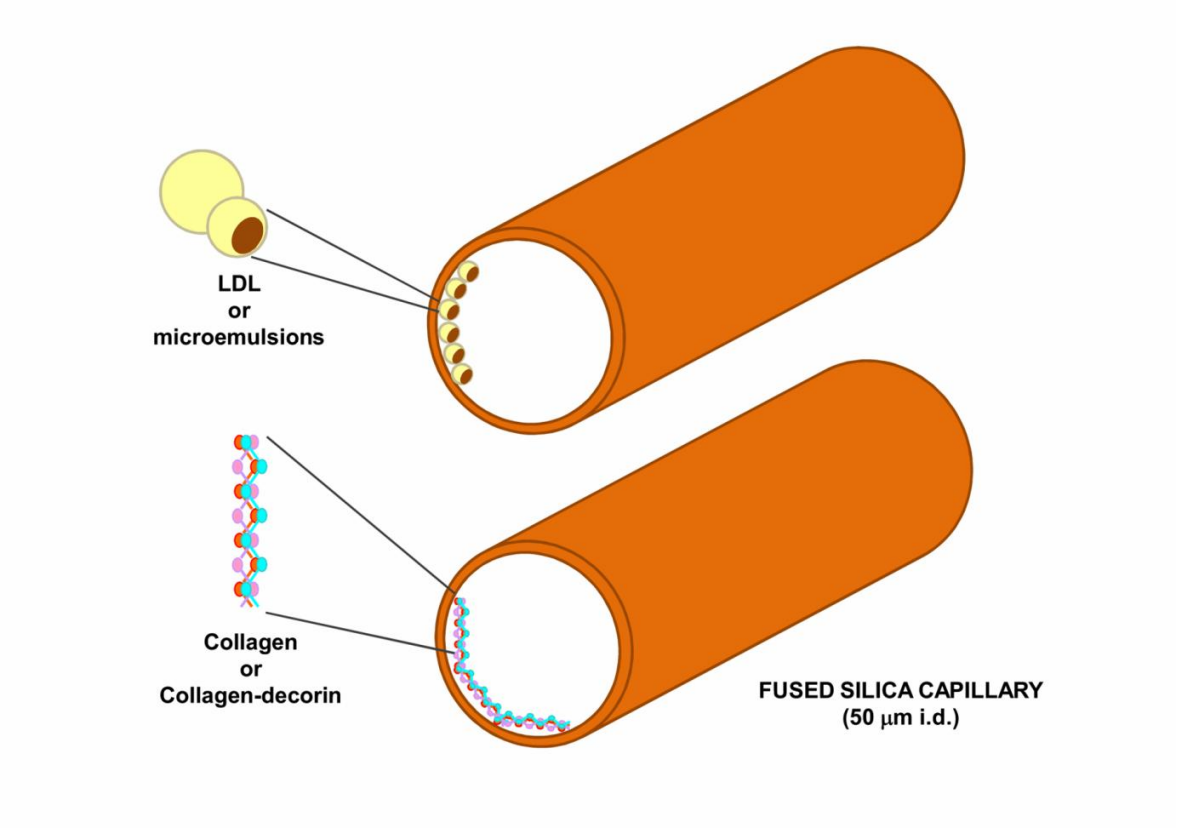

***Figure 3**. Schematic representation of the immobilization of biomaterials onto the inner wall of a fused silica capillary.*

Owing to their shape, the particles arrange themselves as a monolayer on the silica surface. Optimization of the conditions for LDL coatings is reported in paper I. Even though a wide range of LDL concentrations (**124**) could be used, 0.1 mg/mL was considered as the optimal concentration, ensuring good LDL coverage of the capillary. At lower concentrations degradation was possible, while at higher concentrations a larger sample was required with no improvement in the coating. In previous studies carried out in our laboratory, LDL coating was shown to be stable in a pH range of 4.5–7.4. (**124**)

5.1.2 Development of collagen and collagen–decorin coatings

The great complexity of collagen molecules and their capacity for self-assembly under certain conditions made the development of collagen I and collagen III coatings particularly challenging. Even though collagen I and III adsorb on several surfaces, (**125-127**) it was a highly demanding task

to develop a stable and repeatable coatings on the fused silica wall of a capillary. First, dialysis was crucial for obtaining a homogeneous collagen solution. The buffer had to be carefully selected and the time required for coating preparation optimized. As a rule, the buffer used for the dialysis had to be the same as that in the coating solution. Phosphate buffer pH 7.4 was selected for collagen I, while HEPES with 135 mM NaCl was more suitable for collagen III. For both buffers, the pH was 7.4 and the ionic strength 20 mM. The addition of NaCl was essential for the stabilization of the collagen III coating, but NaCl completely destabilized the collagen I coating. A possible explanation is the difference in the structure of collagen I and III. Type I is less hydrophilic than type III and easily interacts with the hydrophobic fused silica capillary. Collagen I also interacts through electrostatic interactions, which may be suppressed by the presence of salt. Collagen III contains a higher degree of hydroxyproline and, being more hydrophilic than type I, adsorbs less readily on hydrophobic surfaces. We assume, therefore, that collagen III can form salt bridges with the negatively charged silica wall when NaCl is present in the medium. (**128**,**129**). In addition, just as in the phospholipid coatings, protonation of the amines of HEPES probably enhances the formation and stability of collagen III coatings. (**130**) A final important detail was the choice of the membrane molecular weight cut-off (MWCO) used in the dialysis. A MWCO of 12–24 kDa was selected to ensure that the dialysis would be completed in a reasonable time frame. A lower MWCO was tested, but the dialysis process was less repeatable and much more time consuming. The time required for dialysis depended on the type of collagen (3 h for collagen I and overnight for collagen III) and could be related to structural differences. Furthermore, since collagen self-assembly commences at about 25 ^{o}C, (**131**) the dialysis was carried out at 4 ^{o}C to avoid any monomer aggregation. On the other hand, the temperature selected for the coating was 25 or 37 ^{o}C, in order to ensure monomer assembly and fibril formation. During the coating process, the capillary was not simply rinsed with the collagen solution but left filled for a certain time. Thus, the waiting interval was optimized to 2 h, during which the collagen monomers had sufficient time to adsorb on the capillary wall and self-assemble into fibrils.

The development of collagen–decorin coatings was less challenging, once the collagen coatings had been optimized. First, the capillary coated with collagen was simply rinsed with decorin, and the capillary was left filled for several hours (e.g., overnight). Although a stable coating was achieved, note was taken of the observation of Bierbaum and coworkers that premixing of collagen with decorin results in tight and ordered fibrils. (**69**) Further requirements for stable collagen–decorin

coatings were physiological temperature (37 ^{o}C) and the presence of NaCl. Unlike LDL and microemulsion coatings, collagen and collagen–decorin coatings were highly sensitive to changes in pH, and their stability could not be ensured at pH above 7.4.

5.1.3 Stability and coating-to-coating reproducibility

The stability of the coating was tested by checking the EOF mobility after six successive runs. The coating-to-coating reproducibility was evaluated by coating three different capillaries with LDL, microemulsions, collagen I, collagen III, collagen I–decorin or collagen III–decorin and checking the EOF mobilities (Table 11). DMSO was selected as EOF marker because it did not interact with any of the biomaterials used in the coatings.

Table 11. Coating-to-coating reproducibility (n=3) and EOF mobilities [10^{-4} cm^2 V^{-1} s^{-1}] for three different capillaries coated with LDL, microemulsions, collagen I, collagen III, collagen I-decorin or collagen III-decorin. Experiments were performed at 37 ^{o}C.[a]

	LDL	**Microemulsions**	**Collagen I**	**Collagen III**	**Collagen I-decorin**	**Collagen III-decorin**
Capillary 1	2.53 (2.3%)	4.30 (0.7%)	1.68 (0.9%)	2.53 (1.4%)	3.09 (0.4%)	3.29 (0.6%)
Capillary 2	2.44 (2.0%)	4.14 (1.2%)	1.44 (5.6%)	2.23 (0.6%)	2.70 (0.7%)	4.35 (0.3%)
Capillary 3	2.49 (1.4%)	4.29 (0.7%)	1.77 (2.8%)	5.81 (1.4%)	2.62 (1.4%)	2.20 (0.6%)
Paper	I, II, III	II	IV, V	IV	IV	IV

[a] RSD values are given in parenthesis

The RSD values reported in Table 11 confirm the good stability of all the coatings. The use of freshly coated capillaries is recommended, nevertheless, to ensure reliable results. In capillaries coated with collagen, physiological temperature and the presence of decorin were advantageous in stabilizing the coating, probably because fibril formation and organization are then favoured. The LDL coatings showed the best coating-to-coating reproducibility, followed by the other biomaterials in the order LDL>microemulsions>collagen I-decorin>collagen I>collagen III-decorin>collagen III. The hydrophobic nature and spherical shape of LDL and microemulsion particles are important for the coating reproducibility. On the other hand, the capacity for self-assembly and the heterogeneity of collagen fibrils make coating reproducibility harder to achieve. For this reason, addition of decorin, which participates in the monomer assembly and collagen fibril formation, improved the reproducibility of the coatings. The lower stability of collagen III than of collagen I coatings on the hydrophobic fused silica surface is due to the greater hydrophilicity.

The successfully coated columns served as excellent chromatographic tools for the separation of analytes and for interaction studies with model compounds of biological interest. Retention factors (k) and, where possible, distribution coefficients (K_D), were calculated to obtain information about interactions and about the affinity of the selected analytes to the different biomaterials.

5.2 Development of methods for modification and *in situ* reactions of biomaterial coatings

The use of coated capillaries as miniaturized reactors was a key innovative feature of this research. Details of the methods employed can be found in Table 8. The following sections discuss the methods and the results achieved.

5.2.1 Oxidation of LDL coating

The *in situ* oxidation of the LDL in LDL-coated capillaries is reported in paper I. The oxidation was speed up at the physiological temperature of 37 ^{o}C, and it achieved a plateau after 5 h; at 25 ^{o}C it was still progressing at 5 h. Since the pH of the bodily environment is decreased during inflammation, the influence of acidic pH on oxidation was studied. Oxidation was enhanced at higher pH values, such as 6.5 and 7.4, and was slower at pH 4.0, 4.5 and 5.5. This same finding was obtained in previous studies, where the capability of copper to bind the protein part of LDL was mentioned as possible explanation. (**132**,**133**)

5.2.2 Enzymatic modification of LDL coating

The feasibility to use CEC with LDL-coated capillaries as a microreactor to carry out enzymatic modification of lipoproteins was investigated in study II. To clarify the role of lipids in the enzymatic reactions, also microemulsion-coated capillaries were submitted to enzymatic treatment. The influence of temperature was explored by carrying out all experiments at both 25 and 37 ^{o}C. It is good to remember that the peak transition temperature of the core lipids of LDL ranges from 29 to 38 ^{o}C, (**134**) meaning that the temperature employed dramatically affects the results. Indeed, totally different trends were sometimes observed when the experiments were carried out at 25 ^{o}C, where the lipid core is relatively rigid, and at 37 ^{o}C.

Of all the methods with different enzymes, the reaction with PLA_2 was the most difficult to optimize. After several trials, it was realized that the presence of fatty-acid-free BSA in the reaction buffer was critical for removing the produced fatty acids and, thus, speeding up the process. (**135-137**) Several experiments with longer treatment times, and hour-by-hour observation of the kinetics, revealed that the reaction is usually completed after just 1 h.

5.2.3 *In situ* delipidation of LDL

An important criterion in the selection of the delipidating agent was that the conformation of apoB-100 should be preserved. Organic solvents and ionic surfactants are helpful in the removal of lipids from LDL particles, (**138**,**139**) but they also provoke the denaturation of apoB-100. Thus, nonionic surfactants, which delipidate LDL with much less damage to the protein structure, appeared more suitable. According to computational studies carried out by Johs and co-workers, **(140)** Nonidet P-40 removes lipids without loss of the secondary structure of apoB-100. Their studies strongly support our choice of Nonidet P-40 for the *in situ* delipidation of LDL particles (Fig. 4).

5.2.4 *In situ* glycation of collagen I

The feasibility of using CEC for *in situ* glycation of collagen I coated onto a capillary inner surface was clarified. First, the sugar was selected from the available monosaccharides and polysaccharides. Although glucose would be the better match physiologically, D-glucose-6-phosphate was selected because of its higher reactivity with the amino groups. (**89**). Collagen was non-enzymatically glycated in vial by incubating it with glucose and then coated onto the capillary. Unfortunately, the poor coating repeatability forced this protocol to be abandoned.

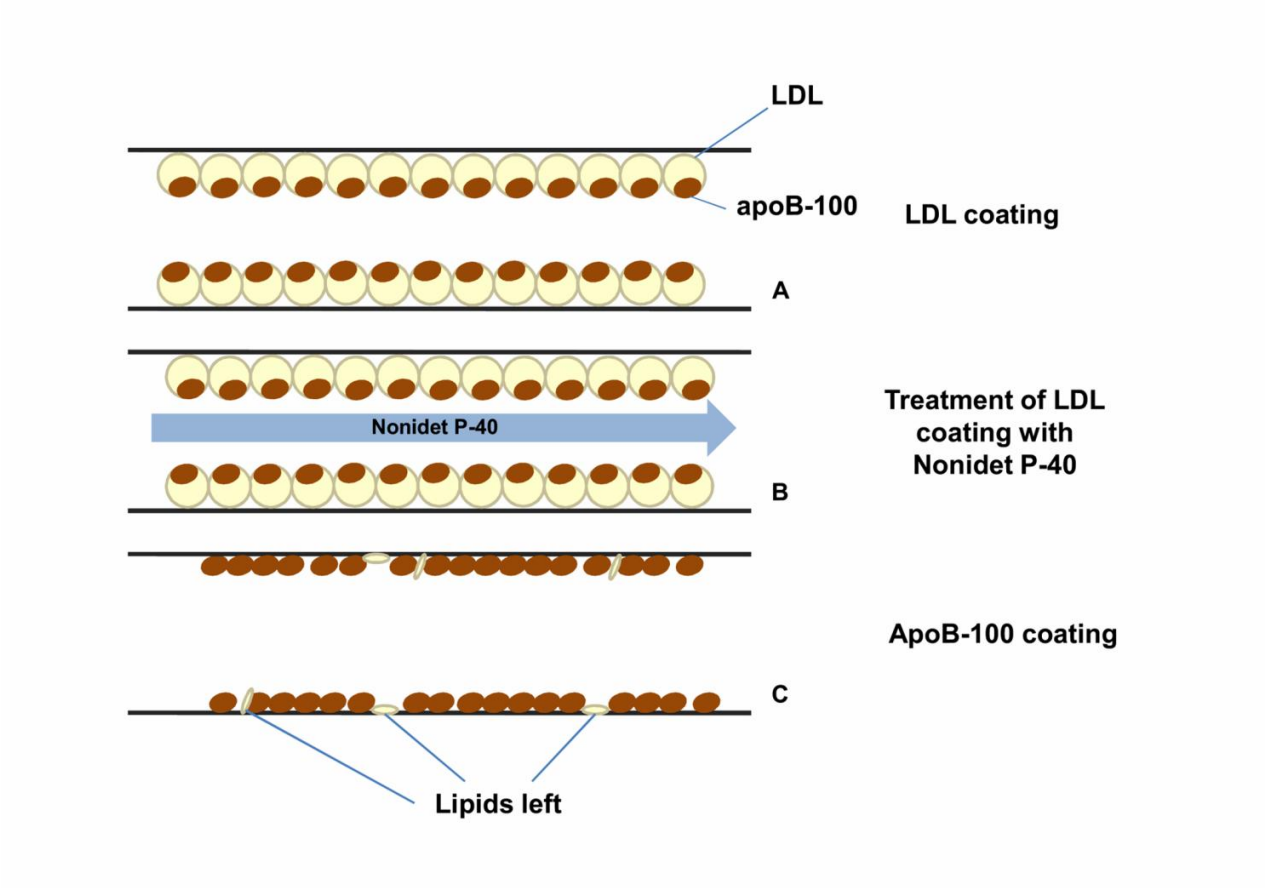

Figure 4. *In situ delipidation of LDL particles, in which the apoB-100 is isolated and present in the form of a coating. LDL coating A) before delipidation, B) with Nonidet P-40 and C) after delipidation.*

Subsequently, the glycation was carried out *in situ* by rinsing the collagen I-coated capillary with the glucose solution. Because non-enzymatic protein glycation is a slow process, whose consequences do not become manifest for many years, the sugar concentration (5.2 mg/mL) was much higher than the physiological concentration to ensure that significant collagen modification would be obtained in a reasonable time. The glycation reaction was followed during time periods of 8, 16, and 24 h, which were long enough to provide modifications in collagen I surfaces (Fig. 5).

5.2.5 Preparation of sensor chips in QCM

Polystyrene-derivatized gold-plated QCM crystals, which are widely used for protein immobilization, (**107**,**141**) were selected for PP and PP_2 adsorption.

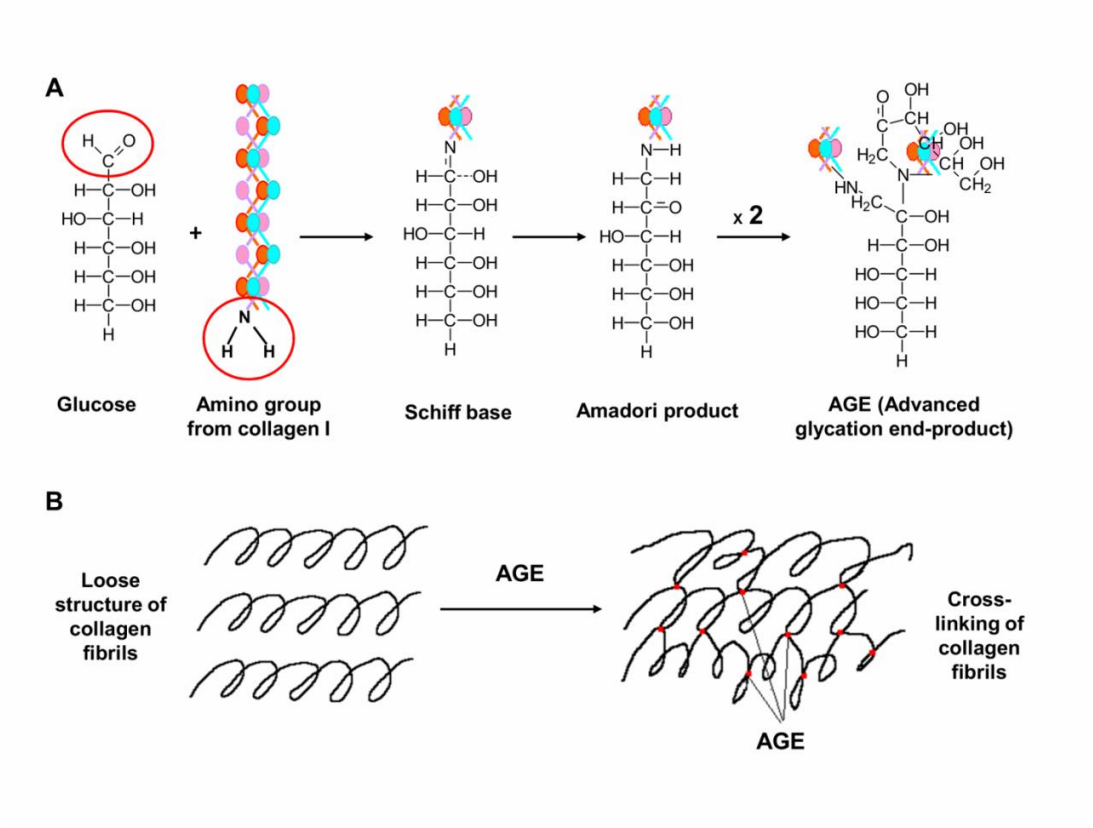

Figure 5. *Mechanism of glycation (A) and effect of glycation on the structure of collagen I (B).*

A good and stable coverage of PP and PP_2 was obtained on this surface. Although collagen I adsorbs well on hydrophobic surfaces, (**128,142**,**143**), reliable immobilization of collagen I on the polystyrene chip surface was not obtained. Thus, amino-coupling of collagen I on the carboxyl crystal was selected as an alternative. In this procedure (paper VI), the carboxyl groups of the derivatized surface were activated with a mixture of EDC and sulpho-NHS. Collagen I was then coupled through its amino groups, while the carboxyl groups were left free for interaction with the analyte (PP). The carboxyl chip was also used for the immobilization of C6S through aldehyde coupling.

5.3 Measurements of EOF mobility

The EOF mobilities, which were determined in all studies with equation (6), gave information about the coating charges and stability. In view of its negligible interactions with the coatings, DMSO was selected as EOF marker and detected at 214 nm.

5.3.1 Oxidized LDL coatings

LDL oxidation was carried out both in vial and in the capillary. In one experiment, LDLs were oxidized by $CuSO_4$ in vial and the capillary was coated with the oxidized LDL particles. In the second, the oxidation was carried out *in situ* in the LDL-coated capillary. In both cases, the EOF mobility of the coating increased proportionally to the oxidation of LDLs, and a plateau was reached when the oxidation was completed. (Fig. 6, Fig. 5 paper I). This finding is in agreement with earlier electrophoretic separation studies where the electrophoretic mobility of oxidized LDLs was higher than that of native lipoproteins. (**144**-**146**) Although the results obtained for in-vial and *in situ* oxidized LDL particles were closely similar, the *in situ* approach was preferred because of its simplicity, the ease with which the experimental conditions could be changed and the shorter time frame.

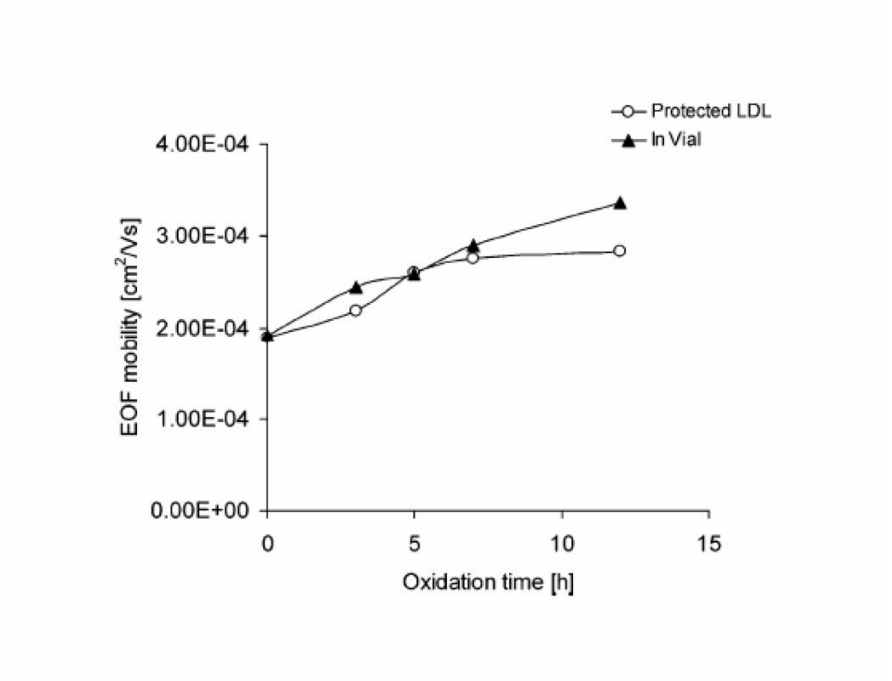

Figure 6. *Comparison of average EOF mobilities after different oxidation times in vial and in capillary. Oxidation was carried out with 5 mM $CuSO_4$ solution, at pH 7.4 and 25 ^oC. Running conditions: 38.5 cm L_{tot}, 30 cm L_{det}, temperature 25 ^oC, inj. 5 s at 50 mbar, voltage 20 kV, BGE 20 mM phosphate buffer pH 7.4, detection at 214 nm.*

5.3.2 LDL coatings after enzymatic modification

As described in section 2.4, the three enzymes that were used—SMase, PLA_2 and α-chymotrypsin—modify the LDL surface in different ways (Fig. 7). The EOF mobilities for LDL coatings modified with these enzymes and for microemulsion coatings modified with SMase are presented below.

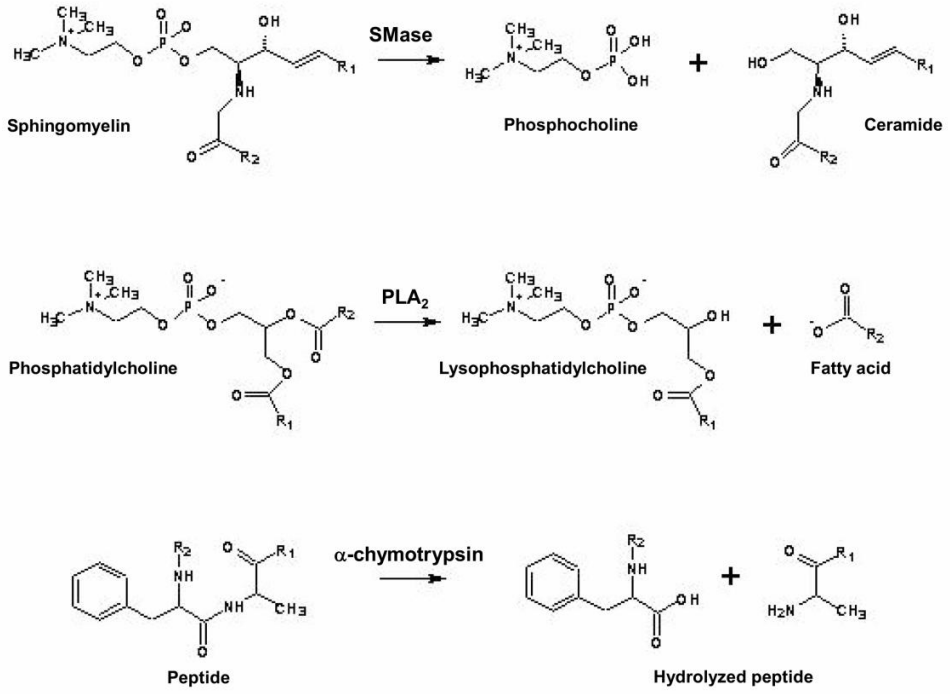

Figure 7. *Schematic representation of reactions involving SMase, PLA_2 and α-chymotrypsin.*

LDL modified with SMase

At both 25 and 37 ^{o}C, the EOF mobility increased after treatment of the LDL coating with SMase. As expected, physiological temperature speeded up the reaction (Fig. 8, Fig. 1(a) paper II). A possible reason for the increase in EOF is that the loss of phosphocholine provokes a rearrangement of the lipids and apoB-100 on the LDL surface, with a consequent increase in negative charges and EOF mobility.

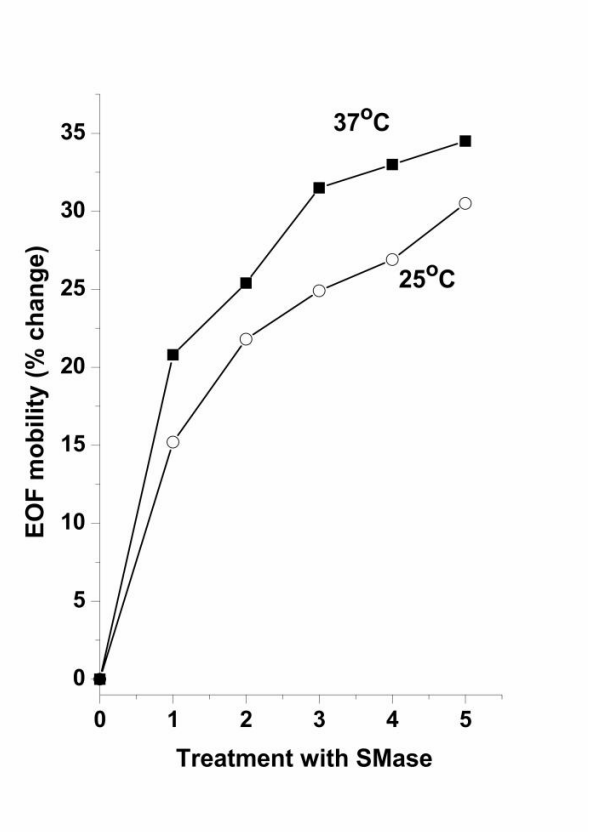

***Figure 8**. Comparison of EOF mobilities (n=6) at 25 °C and 37 °C in capillaries with immobilized LDL particles treated in five steps with SMase. Comparison is presented as percentage change. In each treatment step, SMase was injected at 50 mbar pressure for 5 min and the capillary was left filled with the enzyme solution for 55 min, after which the treatment was stopped by flushing 25 min with 10 mM EDTA. BGE 20 mM phosphate buffer pH 7.4.*

LDL modified with PLA_2

Totally different trends were observed after the treatment with PLA_2. After just 1 h, the EOF mobility was increased significantly at 37 °C and decreased at 25 °C (Fig. 9, Fig. 3(a) paper II). LDL incubation with PLA_2 at 37 °C has been shown to cause the hydrolysis of nearly 50% of the phospholipids. (**82,147**) The formation of smaller, denser particles with 25% lower surface area, and consequent increase in the charge/surface ratio of LDL, might explain the increase in mobility at 37 °C. The greater rigidity of the lipid core at 25 °C would result in slower reorganization of the

unesterified cholesterol and phospholipids on the LDL surface and so to the different trend at lower temperature.

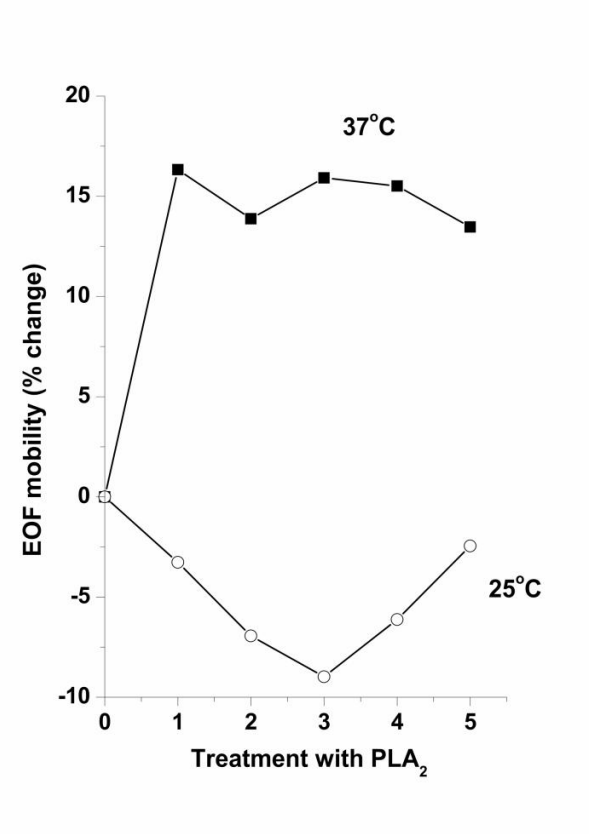

***Figure 9**. Comparison of EOF mobilities (n=6) at 25 °C and 37 °C in capillaries with immobilized LDL particles treated in five steps with PLA_2. Comparison is presented as percentage change. In each treatment step, PLA_2 was injected to the capillary at 50 mbar pressure for 5 min and the capillary was left filled with the enzyme solution for 55 min, after which the treatment was stopped by flushing with 10 mM EDTA for 40 min. BGE 20 mM phosphate buffer pH 7.4.*

LDL modified with α-chymotrypsin

After treatment with α-chymotrypsin, the negative charges of the LDL coating increased at both 25 and 37 °C (Fig. 10, Fig. 4(a) paper II). A similar result was obtained by Bernfeld *et al.* (**148**) for proteolysed lipoproteins in paper electrophoresis.

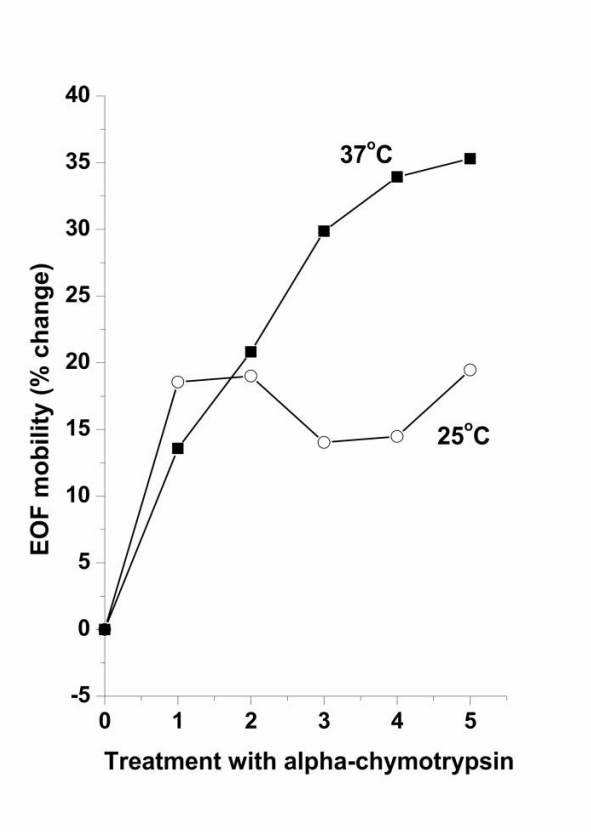

Figure 10. *Comparison of electroosmotic flow mobilities (n=6) at 25 °C and 37 °C in capillaries immobilized with LDL particles treated in five steps with α-chymotrypsin. Comparison is presented as percent change. In each treatment step, α-chymotrypsin was injected by pressure at 50 mbar for 10 min and the capillary was left filled with the enzyme solution for 55 min, after which the enzyme was removed by flushing 25 min with BGE at pH 7.4. BGE 20 mM phosphate buffer pH 7.4.*

Microemulsions modified with SMase

To better clarify the action of SMase on the lipid part of LDL, the capillary was coated with lipid microemulsions derived from LDL (microemulsions) and from commercial lipids (SM mimics). In the dihydro-SM mimics, SM was replaced by dihydro-SM. The coating procedure was identical with that used for LDL, but for simplicity, the experiments were carried out only at the physiological temperature of 37 °C. Parallel studies with PLA_2 could not be carried out because the BSA needed to remove the fatty acids adsorbs on the coating. The results were comparable with those obtained with

LDL: the EOF mobility was increased for all modified coatings (Fig. 11, Fig. 6(a) paper II), and the same conclusion can be drawn.

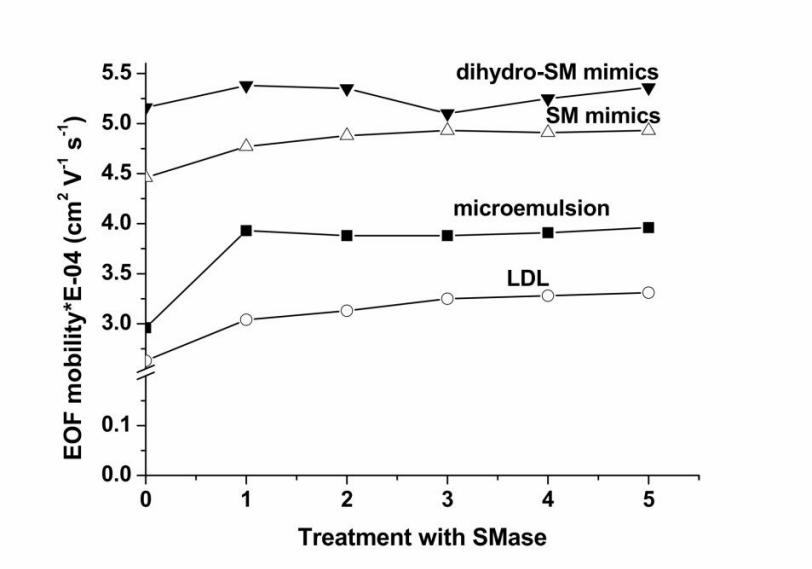

Figure 11. *Electroosmotic flow mobilities (n=6) in capillaries coated with LDL (o), lipid microemulsions derived from LDL lipids (microemulsions, <), lipid microemulsions mimicking the lipid composition of LDL (SM mimics, r) and mimics in which sphingomyelin was replaced by dihydrosphingomyelin (dihydro-SM mimics, q) measured at 37 °C as a function of SMase treatment time. The SMase treatment conditions are as given in the caption of Fig. 8.*

5.3.3 Delipidated LDL (apoB-100) coating

The EOF mobility was determined before and after delipidation of the LDL coating. After delipidation, the EOF mobility was slightly increased, (Fig. 12, Fig. 1 paper III) reflecting the greater amount of negative charges on the apoB-100-coated capillary than on the capillary coated with native LDLs. Repeated DMSO runs were also carried out to evaluate the stability of the apoB-100 coating. According to the relative standard deviation (RSD) values, the apoB-100 coating showed both good repeatability and good reproducibility. RSD values (n=6) indicated a coating lifetime of 5 days. However, the intraday EOF mobilities indicated the reliable lifetime of the coated capillary to be a maximum of three days. When the coating-to-coating reproducibility was evaluated on four different capillaries, the average RSD of the EOF mobilities was 6.3 %.

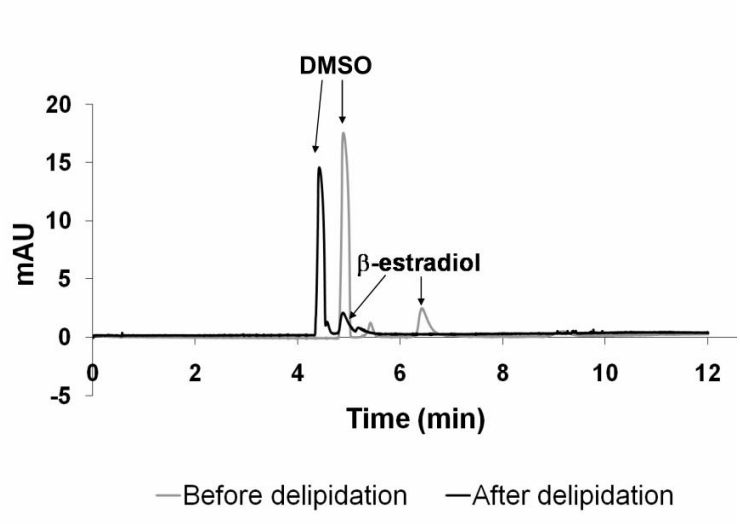

Figure 12. *Electropherograms for β-estradiol before and after delipidation of the LDL coating with Nonidet P-40. DMSO was used as EOF marker. Running conditions:* L_{tot} *38.5 cm,* L_{det} *30 cm, voltage +20 kV, sample injection 2 s at 50 mbar, capillary temperature 25 °C, detection wavelength 214 nm, running buffer phosphate at pH 7.4 (I=20 mM).*

5.3.4 Collagen and collagen–decorin coatings

The EOF mobilities were compared at 37 ^{o}C for four different capillaries coated with collagen I, collagen III, collagen I–decorin and collagen III–decorin. The mobility increased in the order collagen I < collagen I–decorin < collagen III < collagen III–decorin (Fig. 13, Fig. 1 paper IV). The substantially higher mobility for the collagen III than the collagen I coating may be due to the larger percentage of hydroxyproline, which is a characteristic for type III. The EOF mobilities were usually higher when decorin was included in the coating, indicating enhanced negative charges.

5.3.5 Glycated collagen I coating

Substantial increase in the EOF mobility was observed after the glycation of collagen I (Fig. 14). The increase was proportional to the time of glycation, in the following order: 8 h < 16 h < 24 h. This result is attributable to the reaction of D-glucose-6-phosphate with the amino groups of the lysine residues on collagen I, and the resulting neutralization of the positive charges and increase of the negative net charge of the coating.

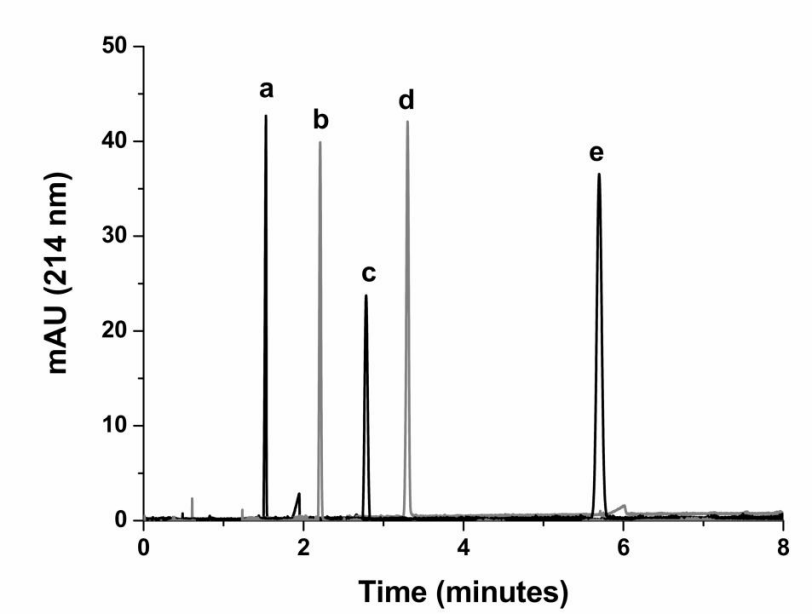

Figure 13. *Electropherograms of electroosmotic marker DMSO in an (a) uncoated capillary, (b) collagen III–decorin-coated capillary, (c) collagen III-coated capillary, (d) collagen I–decorin-coated capillary, and (e) collagen I-coated capillary. Running conditions: +20 kV, injection for 2 s at 50 mbar, 37 ^{o}C, 20 mM phosphate buffer or HEPES pH 7.4, L_{tot} 38.5 cm, L_{det} 30 cm, detection wavelength 214 nm.*

Furthermore, the RSD values for the glycated collagen I coatings (n=3, range 0.1–1.2%) demonstrated that that surface was more stable than the surface of the native collagen I (n=3, range 0.8–7.4%).

5.4 Measurements of retention factors (*k*) and distribution coefficients (K_D)

Retention factors (*k*) and distribution coefficients (K_D) were calculated according to equations (7) and (8), respectively. Both values describe the affinity of the analytes for the coating. In the case of charged analytes, equation (10) was used instead of equation (7). K_D offers more information than *k* because it takes into account the thickness of the stationary phase. Unfortunately, K_D could not always be evaluated; this was especially true for collagen and collagen–decorin where, owing to the unevenness of the coatings, the average thickness could not be estimated.

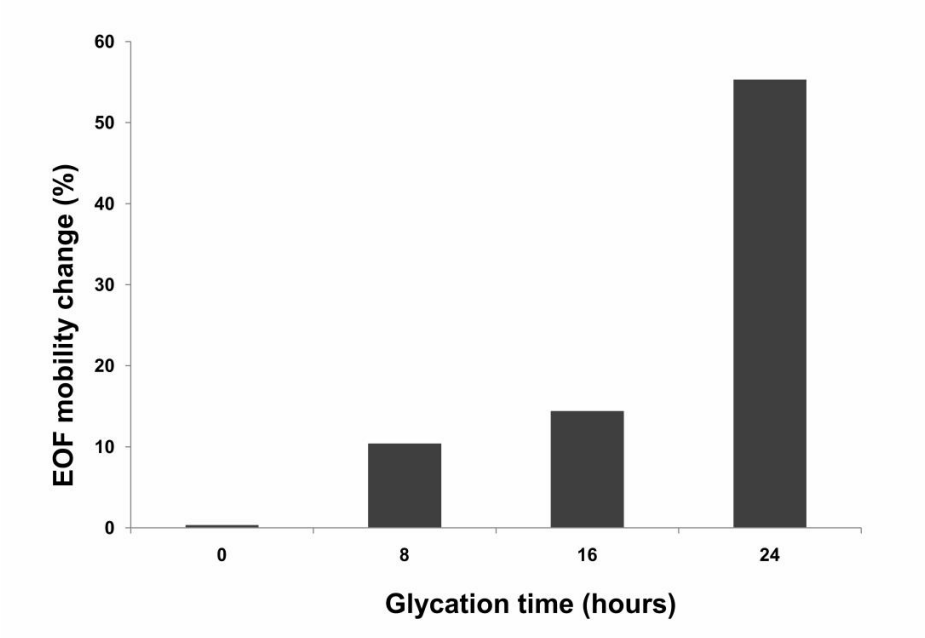

Figure 14. *Increase of the EOF mobility (as percentage change) in a capillary with collagen I coating after glycation with D-glucose-6-phosphate for different periods of time. BGE 20 mM phosphate buffer pH 7.4. More information about the glycation procedure is given in the Experimental section.*

5.4.1 Unmodified and oxidized LDL coatings

The retention factors of four different steroids (d-aldosterone, testosterone, β-estradiol and progesterone) were helpful in understanding the modifications of LDL that took place during the oxidation. Since steroids are neutral compounds, separation is based solely on their hydrophobic interaction with the stationary phase. Of the four steroids tested, d-aldosterone was the least hydrophobic. Its interaction with the LDL particle coating was very weak, and it migrated together with the EOF marker. Accordingly, retention factors were calculated only for testosterone, β-estradiol and progesterone. The *k* values of all these steroids increased with the degree of oxidation (Table 12, Table 1 paper I). Copper can react with both the lipid and protein parts of LDL. It has been proposed that the degradation and release of apoB-100 fragments might assist the hydrophobic core to penetrate the particle surface. (**30**) If true, this could explain the increase of the hydrophobicity of the coating and the *k* values of the steroids as a function of the oxidation time.

Table 12. Effect of LDL oxidation time on the retention factors (*k*) of steroids. Oxidation of LDL coating, pH 7.4, 37 °C.[a]

Oxidation time (h)	**EOF mobility 10^4 (cm^2/sV)**	**Retention factor (*k*)**		
		Testosterone	**β-Estradiol**	**Progesterone**
0	3.11 (1.7)	0.09 (0.8)	0.22 (0.9)	0.67 (1.3)
1	3.41 (0.6)	0.09 (0.6)	0.22 (0.3)	0.72 (0.9)
2	3.67 (1.6)	0.11 (1.1)	0.27 (1.3)	0.89 (1.6)
3	3.89 (0.2)	0.13 (0.3)	0.29 (7.3)	0.98 (1.3)
4	4.00 (1.5)	0.14 (2.2)	0.34 (2.6)	1.04 (3.9)
5	4.07 (0.5)	0.14 (1.5)	0.36 (1.7)	1.05 (3.6)
Change of EOF mobility/*k* value (%)	26	34	50	42

[a] The RSD values of six parallel experiments are given in parenthesis

5.4.2 LDL coatings after enzymatic modification

Because all the steroids exhibited similar behaviour in the interaction studies with biomaterial coatings, progesterone, the most hydrophobic steroid, was selected as model compound in the further studies. Hence, only the retention factor of progesterone was employed as indicator of the interactions.

LDL modified with SMase

After SMase treatment of 2 h, the retention factor of progesterone was significantly increased at 37 °C, but it was slightly decreased at 25 °C (Fig. 15, Fig. 1(b) paper II). As explained above in section 2.4, SMase hydrolyses SM, yielding phosphocholine and ceramide. Whereas water-soluble phosphocholine is released from the LDL particles, ceramide forms non–polar spots that augment the surface hydrophobicity. (**40**) This may explain why the *k* value increases as a function of the treatment time at 37 °C. At 25 °C, on the other hand, the rigidity of the lipid core (**134**) hampers the lateral diffusion of lipids on the surface and hydrophobicity decreases.

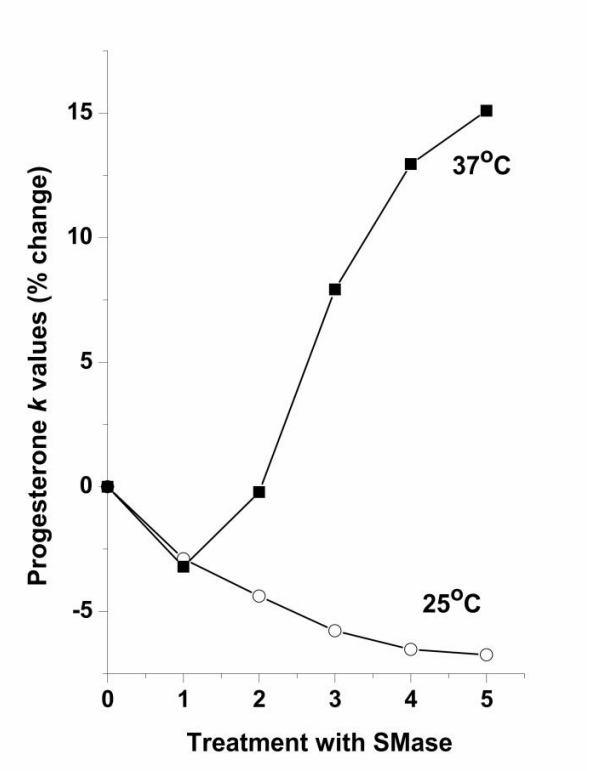

Figure 15. *Comparison of retention factors of progesterone (n=6) at 25 °C and 37 °C in capillaries with immobilized LDL particles treated in five steps with SMase. Comparison is presented as percentage change. In each treatment step, SMase was injected at 50 mbar pressure for 5 min and the capillary was left filled with the enzyme solution for 55 min, after which the treatment was stopped by flushing 25 min with 10 mM EDTA. BGE 20 mM phosphate buffer pH 7.4.*

LDL modified with PLA_2

In the modification of LDL with PLA_2, two different trends were observed depending on the temperature. After just 1 h treatment with PLA_2, the retention factor of progesterone increased markedly at 25 °C, but decreased at 37 °C (Fig. 16, Fig. 3(b) paper II). Once more, a possible explanation is the different fluidity of the lipid core, which at 25 °C is in relatively rigid and ordered state and prevents the lateral diffusion of the lipids.

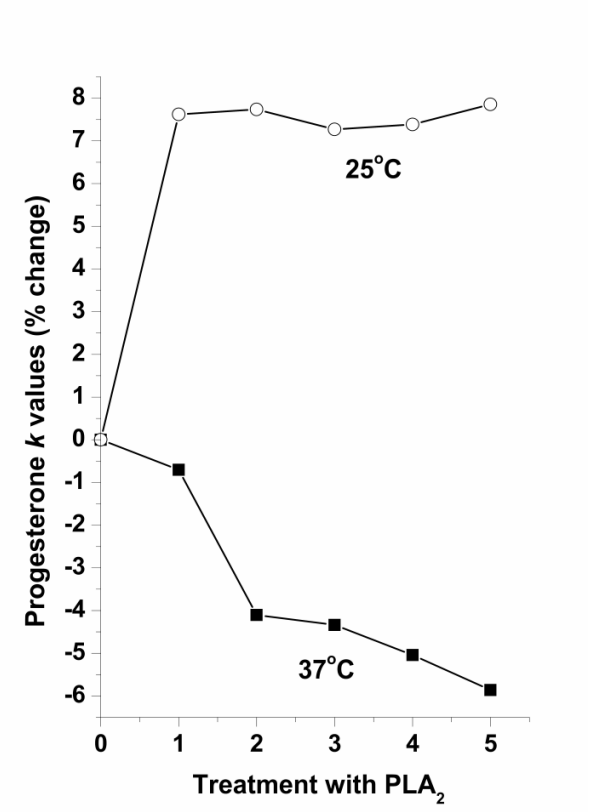

Figure 16. *Comparison of retention factors of progesterone (n=6) at 25 °C and 37 °C in capillaries with immobilized LDL particles treated in five steps with PLA_2. Comparison is presented as percentage change. In each treatment step, PLA_2 was injected to the capillary at 50 mbar pressure for 5 min and the capillary was left filled with the enzyme solution for 55 min, after which the treatment was stopped by flushing with 10 mM EDTA for 40 min. BGE 20 mM phosphate buffer pH 7.4.*

LDL modified with α-chymotrypsin

At both temperatures, 25 and 37 °C, the retention factor of progesterone decreased significantly as a function of treatment time with α-chymotrypsin (Fig. 17, Fig. 4(b) paper II). Because α-chymotrypsin hydrolyses the protein part of LDL, with consequent release of apoB-100 fragments, a rearrangement of the surface can follow and a decrease in hydrophobicity occurs.

Microemulsions modified with SMase

As noted above (see section 5.3.2), for simplicity all the experiments involving modification of microemulsions with SMase were carried out at 37 ^{o}C.

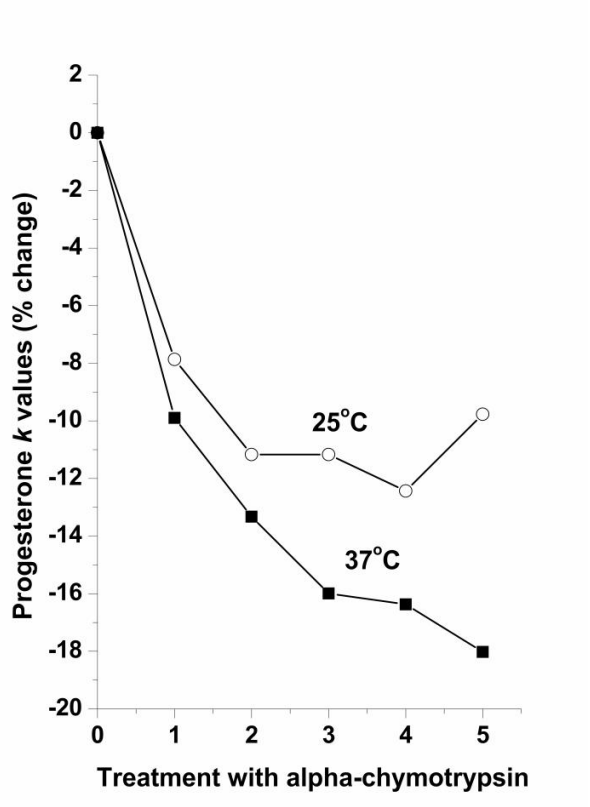

Figure 17. *Comparison of retention factors of progesterone (n=6) at 25 ^{o}C and 37 ^{o}C in capillaries with immobilized LDL particles treated in five steps with α-chymotrypsin. Comparison is presented as percentage change. In each treatment step, α-chymotrypsin was injected by pressure at 50 mbar for 10 min and left filled with the enzyme solution for 55 min, after which the enzyme was removed by flushing 25 min with BGE at pH 7.4. BGE 20 mM phosphate buffer pH 7.4.*

After the enzymatic treatment, the progesterone *k* values were decreased for both the microemulsion and SM mimic coatings (Fig. 18, Fig. 6(b) paper II). The decrease was particularly pronounced for microemulsions, even after one treatment. As noted in section 2.4, SMase hydrolyses sphingomyelin yielding ceramide and phosphocholine. According to the mathematical model proposed by Siskind and Colombini, (**149**,**150**) ceramide domains may form a hydrophilic pore structure, with consequent

decrease in the hydrophobicity of the surface. These kinds of domains are not produced with dihydroceramide where one double bond is reduced. Thus, to clarify the role of the double bond in the pore formation, an experiment was done in which the capillary was coated with dihydro-SM mimics rather than SM mimics. As can be seen from Fig. 18, there was no significant decrease in progesterone *k* values for the capillary coated with dihydro-SM mimics. Evidently, the absence of the double bond prevents the formation of hydrophilic pores and decrease of the surface hydrophobicity. A totally different trend was observed for the LDL coating after treatment with SMase. In this case, the progesterone *k* values increased as a function of treatment time, indicating increased hydrophobicity of the surface. It needs to be remembered, however, that microemulsions are devoid of apoB-100, so that the surface rearrangements can only be due to the lipids; in whole LDL, an important role is also played by the protein part.

5.4.3 Delipidated LDL (apoB-100) coating and interaction with steroids

The retention factor of all steroids tested (testosterone, β-estradiol and progesterone) markedly decreased after delipidation of the LDL coating (Fig. 19, Table 13; Fig. 2 and Table 1 paper III). Progesterone, the most hydrophobic steroid, showed a strong decrease in *k* value (80.5%), indicating successful removal of lipids from the LDL coating and the formation of a new stationary phase consisting of apoB-100.

Table 13. Retention factors (*k*) and RSDs for steroids before and after delipidation of LDL coating.

	Retention factor (*k*)			**RDS of retention factor (n=3)**		
	β-estradiol	**testosterone**	**progesterone**	**β-estradiol**	**testosterone**	**progesterone**
Before delipidation	0.31	0.11	0.87	1.3%	1.2%	0.9%
After delipidation	0.10	0.035	0.17	1.8%	1.7%	1.7%

The phase ratio (β) of the coatings increased from 631 (before delipidation) to 1179 (after delipidation), reflecting a strong decrease in the thickness of the stationary phase. The K_D values of

all steroids decreased after delipidation, and again the most dramatic drop was for progesterone (Table 14; Table 2 paper III). The higher K_D value of β-estradiol than of testosterone was probably due to the presence of one extra hydroxyl group in the structure of β-estradiol. As shown by Westphal et *al*., (**151**) the introduction of one hydroxyl group to a steroid may enhance the interaction with proteins, depending on the structure of the two molecules.

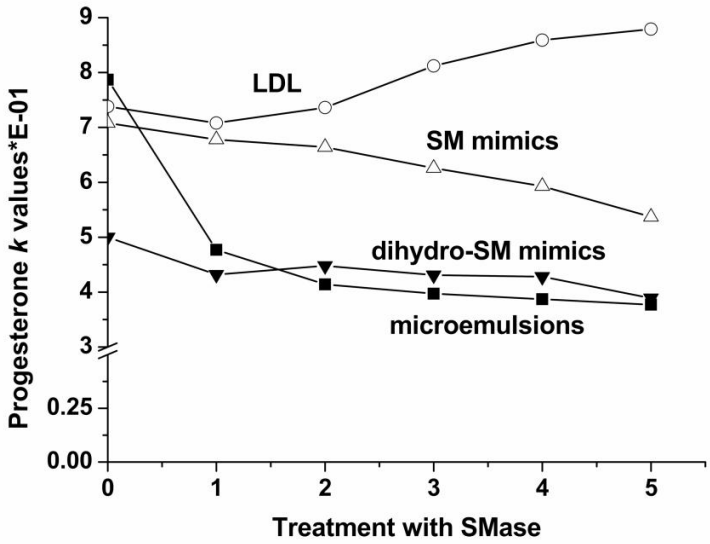

Figure 18. *Retention factors of progesterone (n=6) in capillaries coated with LDL (o), lipid microemulsions derived from LDL lipids (microemulsions, <), lipid microemulsions mimicking the lipid composition of LDL (SM mimics, r), and mimics in which sphingomyelin was replaced by dihydrosphingomyelin (dihydro-SM mimics, q) measured at 37 °C as a function of SMase treatment time. The SMase treatment conditions are described in Fig. 8.*

5.4.4 Interactions of apoB-100 peptide fragments with collagen and collagen–decorin coatings

Equation (7), which is widely used in chromatographic techniques, cannot be directly applied in our case because it does not take into consideration the electrophoretic mobility of charged analytes. Equation (10) was difficult to apply because the polarity must be reversed when running the negative peptide (NP), and the results were confusing. To draw some conclusions about the interactions of collagen coatings and apoB-100 peptides, experiments for determination of the *k* value were carried out in the absence of voltage. Under these conditions, equation (7) can be applied, since no driving

electrophoretic force is present. A longer capillary (200 cm L_{tot}, 191.5 L_{det}) was used to enhance the interactions between the peptide fragments and the coatings.

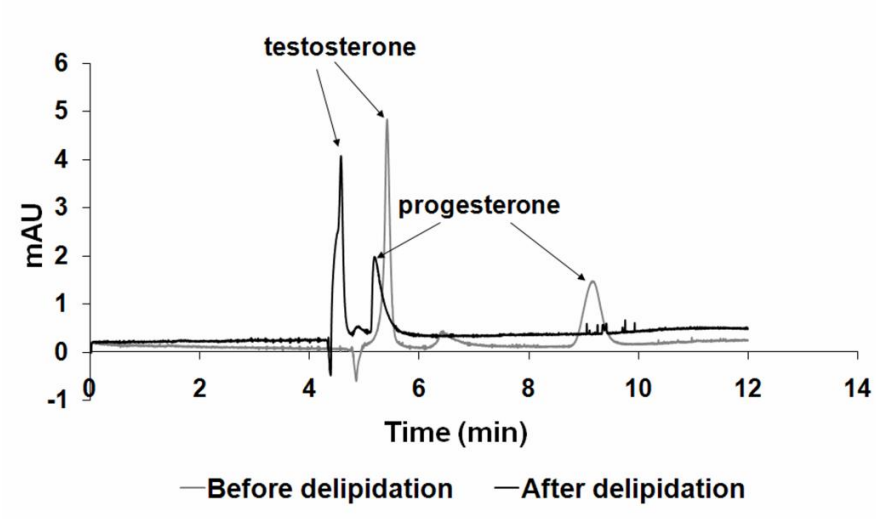

Figure 19. *Electropherograms of testosterone and progesterone separation before and after delipidation of LDL coating with Nonidet P-40. Running conditions: L_{tot} 38.5 cm, L_{det} 30 cm, voltage +20 kV, sample injection 2 s at 50 mbar, capillary temperature 25 °C, detection wavelength 245 nm, running buffer phosphate at pH 7.4 (I=20 mM).*

The results showed that interactions with all coatings were weakest with NP and $NeuP_2$ (Fig. 20, Table 15; Fig. 4 and Table 2 paper IV). A weak interaction was observed for $NeuP_1$, however, because some positive charges, counterbalanced by negative residues, are present.

Table 14. Distribution coefficients of steroids (K_D).

	β-estradiol	**testosterone**	**progesterone**
Before delipidation	196	69	549
After delipidation	118	41	201

The highest retention factor was obtained for PP, in particular when decorin was part of the coating. This confirms what has been observed in previous studies: that the positive residues lysine and arginine play a crucial role in the interactions between LDL and collagen I. (**71**,**72**) Furthermore, because the interactions are of an electrostatic nature, the presence of decorin, which is highly negatively charged, promotes the binding. (**73**,**25**) Finally, it should be noted that, in the absence of decorin, PP had a higher retention factor on the more negative collagen III coating than on the collagen I coating. This result further shows that ionic interactions could be driving the binding between LDL and collagens, and reinforces the proposal that lysine and arginine residues play a fundamental role.

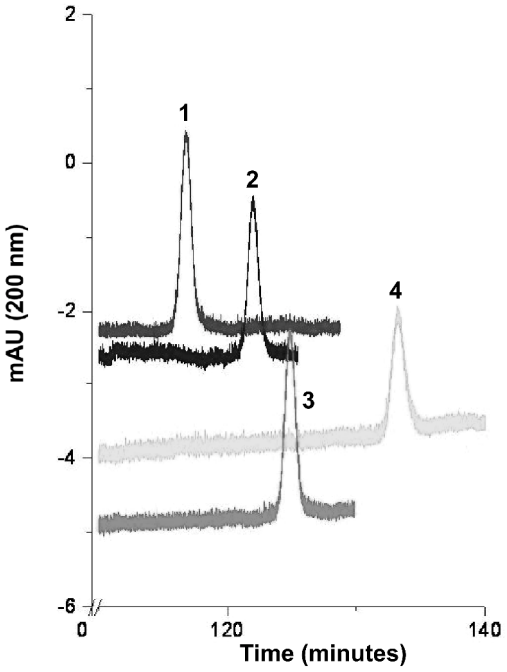

Figure 20. *Chromatographic retention of (1) negative peptide (NP), (2) neutral peptide 2 (NeuP$_2$), (3) neutral peptide 1 (NeuP$_1$) and (4) positive peptide (PP) in capillaries coated with collagen I. Running conditions: no voltage applied, 50 mbar pressure, injection for 2 or 5 s at 50 mbar, 37 ^oC, 20 mM phosphate buffer pH 7.4, L_{tot} 200 cm, L_{det} 191.5 cm, detection wavelength 200 nm.*

Table 15. Retention factors *k* (n=3) of apoB-100 peptide fragments: negative peptide (NP), neutral peptide 2 ($NeuP_2$), neutral peptide 1 ($NeuP_1$), positive peptide (PP), calculated for runs at 37 ^{o}C in capillaries coated with collagen I, collagen I–decorin, collagen III and collagen III–decorin.

Retention factors *k*				
	NP	**$NeuP_2$**	**$NeuP_1$**	**PP**
Collagen I coating	0.017	0.062	0.087	0.16
Collagen III coating	0.0030	0.0014	0.090	0.28
Collagen I–decorin coating	0.0057	0.028	0.066	0.65
Collagen III–decorin coating	0.54	0.55	Completely retained	Completely retained

5.4.5 Interactions of native and oxidized LDL and of PP with glycated collagen I coating

The retention factor of native LDL decreased as a function of treatment time with D-glucose-6-phosphate. (Fig. 21, Fig. 2 paper V) Thus, the more glycated the collagen, the fewer native LDL particles are retained in the capillary. Although we can assume that LDL interacts with collagen I mostly through electrostatic interactions between the positive lysine residues of apoB-100 and the negative residues of collagen, (**72**) these interactions cannot provide a total explanation of the results, since the trend would then be upwards. Feasibly, there is also a contribution from AGEs produced by glycated collagen fibrils reacting with the positive amino groups of lysine and leading to the formation of cross-links. (**152**,**153**) Thus, as glycation proceeds, collagen I becomes more negatively charged, the electrostatic repulsion between collagen I and native LDLs increases (native LDL is also negatively charged at pH 7.4), and the retention factors decrease.

To test this hypothesis, we injected the apoB-100 positive peptide fragment with 19 amino acids (PP), which contains precisely the residues involved in the interactions with PGs, and the neutral peptide fragment with 11 amino acids ($NeuP_2$). Surprisingly, there was no significant change in the retention factors of both PP and $NeuP_2$ as the glycation of collagen proceeded, suggesting that another site, not the one rich in positive residues, was playing a critical role in the interactions between LDL and the glycated collagen. For their part, oxidized LDL particles were completely retained in the capillary at each degree of glycation.

In this case, it is reasonable to suppose that, after treatment with $CuSO_4$, the lipoproteins begin to aggregate and fuse, with possible enhancement of the hydrophobic interactions with the coating. Moreover, fused LDL contains more than one apolipoprotein B, and this condition could be expected to further increase the interaction with collagen I. As well, previous studies have shown that the number of active lysine residues able to bind with LDL receptor and PGs may increase after oxidation, so enhancing the interaction with collagen I. (**30**,**81**,**154**)

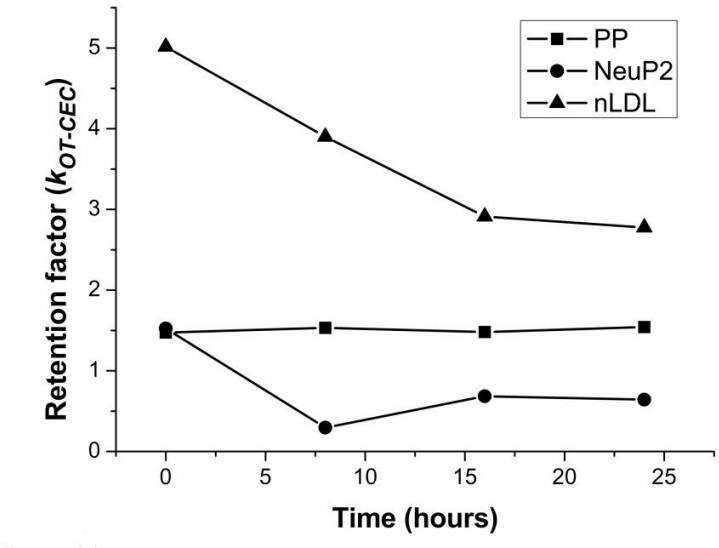

Figure 21. *Comparison of retention factors k (n=3) of native LDL (nLDL) and apoB-100 peptide fragments with 11 and 19 amino acids ($NeuP_2$ and PP) at 37 ^oC, in capillaries coated with untreated and glycated collagen I. Comparison is presented as percentage change.*

5.5 Determination of the isoelectric point

As demonstrated earlier, (**155**,**156**) CEC offers a way to easily and quickly determine the isoelectric point (pI) of a coating. The capillary is coated with the target material and the EOF mobility is measured at different pH values. The results are then plotted with pH on the x-axis and EOF mobility on the y-axis. The intercept of the fitting curve gives the pH value at which the EOF mobility equals zero, which corresponds to the isoelectric point of the coating. While it is clear that isoelectric points can only be determined for coatings that are stable over a wide pH range, there is also another requirement. This became clear in an unsuccessful attempt to estimate the pI value of the collagen I coating. Collagen is a self-assembly material, and even though the collagen I coating was fairly stable over a wide pH range, the fibrils presumably rearrange in conformations and patterns quite different from those occurring in physiological conditions.

The isoelectric point was successfully determined for the apoB-100 coating. To ensure that the hypothetical pI value of apoB-100 was covered, the pH range investigated was 4.0–7.4. The results showed the EOF mobility to increase as a function of pH (Fig. 22, Fig. 3 paper III). A second-order polynomial trend line fitted the data points very well, with an adjusted regression coefficient (adjusted R^2) equal to 0.99317. The EOF mobility was zero at ~pH 5.1, which means that the pI value of apoB-100 adsorbed on the capillary is about 5.1. This value is close to the value of 5.5, found for apoB-100 bound to lipids in LDL particles (**157**,**158**). Since the apoB-100 obtained through delipidation of LDL with Nonidet P-40 resembles the apoB-100 bound to lipids, (**140**) the obtained pI value is concluded to be reliable.

5.6. Supporting studies

Asymmetrical flow field-flow fractionation (AsFlFFF), scanning electron microscopy (SEM) and atomic force microscopy (AFM) studies were carried out to support and complement the results obtained by CEC. In addition, ζ-potential and radioactivity measurements were done at the start of the study. The results are briefly presented below.

5.6.1 Asymmetrical flow field-flow fractionation

Asymmetrical flow field-flow fractionation (AsFlFFF) measurements were helpful in clarifying the influence of oxidation and enzymatic treatment on the size of LDL particles (papers I and II). In oxidation studies with copper sulphate, a second peak centred at about 30 nm appeared after oxidation at 37 ^{o}C for 3 h indicating that LDL particles had aggregated or even fused.

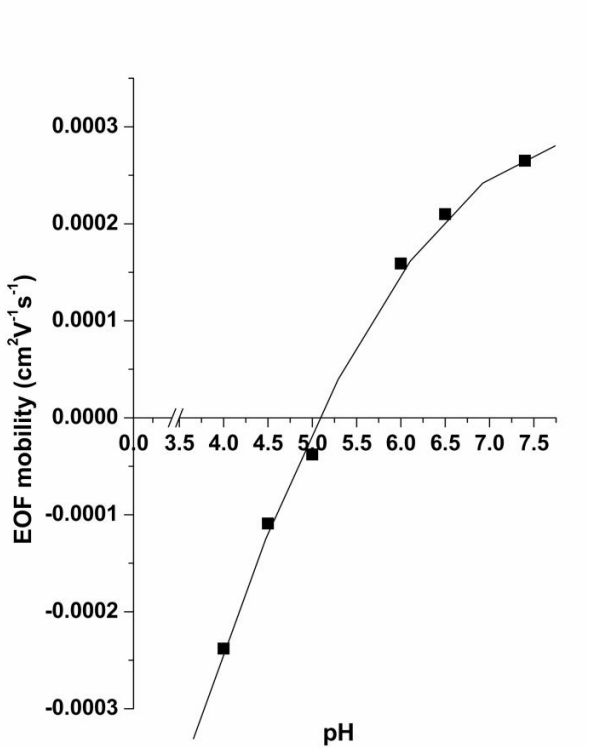

Figure 22. *Dependence of EOF mobility on pH in the apoB-100 coated capillary. The procedures used for coating and delipidation are described in the Methods section. Running conditions:* L_{tot} *38.5 cm,* L_{det} *30 cm, voltage ±20 kV, EOF marker DMSO, sample injection 2 s at 50 mbar, capillary temperature 25 °C, detection wavelength 214 nm. Running buffers: phosphate at pH 7.4, 6.5 and 6.0 and acetate at 4.0, 4.5 and 5.0 (I=20 mM).*

In the enzymatic studies, LDL particles were treated with SMase in vial for 24 h at 20, 25, 30 and 37 ^{o}C. A broad peak next to the LDL peak could be seen at 30 ^{o}C, and it became more pronounced at 37 ^{o}C (Fig. 23, Fig. 2 paper II). Only the LDL peak was seen at 20 and 25 ^{o}C confirming that no significant aggregation or fusion occurs below 30 ^{o}C. These results support the proposal (**5,30**) that SMase, by degrading sphingomyelin and by producing ceramide domains on the particle surface, induces aggregation and then fusion of LDL.

5.6.2 Scanning electron microscopy and atomic force microscopy studies

Visual information was crucial for understanding the topography of the coatings. Since opening the capillary without ruining or destroying the coating is practically impossible, the material was coated

on the outside of the silica capillary, and SEM and AFM images were recorded from the outer surface (see Experimental).

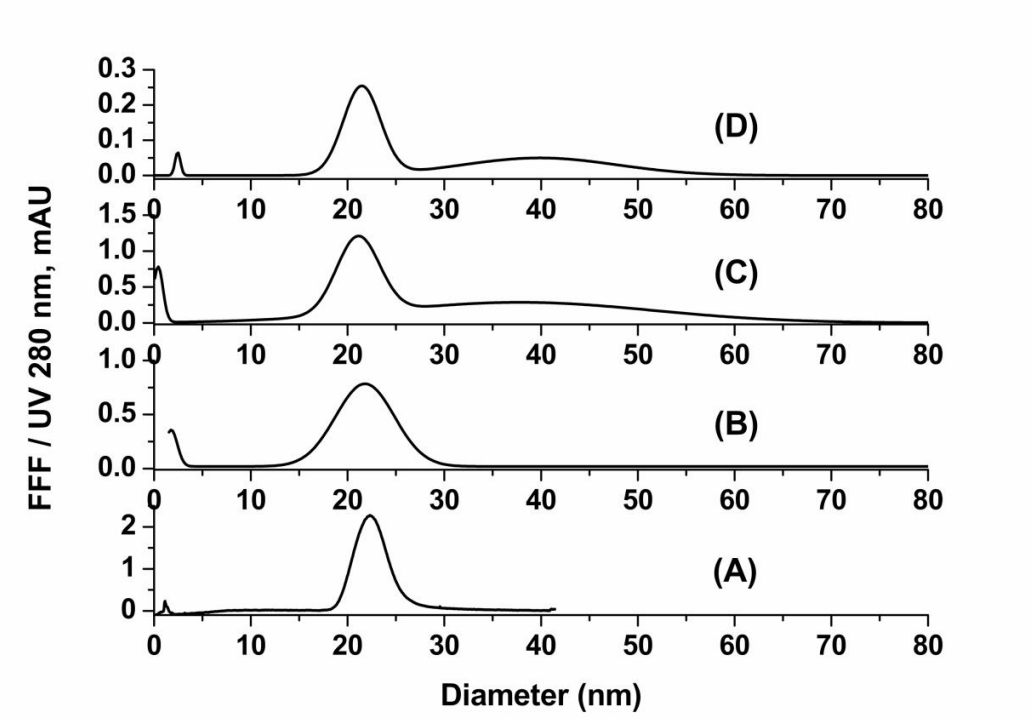

Figure 23. *Particle size distributions measured by AsFlFFF for LDL particles treated with SMase at pH 7.4. The incubations were carried out at various temperatures for 24 h (A) LDL 25 ^{o}C, (B) LDL-SMase 25 ^{o}C, (C) LDL-SMase 30 ^{o}C, and (D) LDL-Smase 37 ^{o}C. Carrier solution: 8.5 mM phosphate buffer, 0.02% NaN_3, 150 mM NaCl, pH 7.4, I 20 mM due to buffer. Relaxation focusing: frontal flow rate 0.1 mL min^{-1}, flow inward from outlet 3.2 mL min^{-1}, injection 1.0 mL min^{-1}for 5 min, relaxation time 12 min. Flow rates during elution: 1.0 and 2.0 mL min^{-1} for the main and cross-flow rates; UV detection at 280 nm.*

Scanning electron microscopy

SEM was used to obtain images of the LDL coating on the silica wall (paper I). Appreciable differences were noticed between the coated and uncoated capillaries, but the resolution was too low to determine the number of particles bound. Radioactivity measurements were employed to determine the number of particles (see section 5.6.4).

Atomic force microscopy

AFM was employed to obtain visual information about LDL, apoB-100, collagen, collagen–decorin and glycated collagen I coatings (papers III, IV, V).

Atomic force microscopy images of LDL and apoB-100 coatings

For study of LDL and apoB-100 coatings (paper III), three different capillaries were coated on the outside and the coating was delipidated according to the procedure described in the Experimental section. The surfaces examined were a) an LDL-coated capillary, b) a delipidated LDL (apoB-100)-coated capillary, c) and d) an apoB-100-coated capillary after treatment with NaOH (Fig. 24, Fig. 4 paper III). Figure 24a shows a 4x4 μm area coated with particles of fairly broad size distribution. The calculated average thickness of the coating was 19.8±2.3 nm, which is close to the average diameter of LDL. Figure 24b shows a 4x4 μm area coated with particles of smaller average size than particles of LDL. The average thickness was just 10.6±0.9 nm. This reduction in thickness supports the conclusion that delipidation of LDL particles results in a successful apoB-100 coating. In the experiments corresponding to Fig. 24c (height image) and 24d (phase image), capillaries were rinsed with NaOH to remove the apoB-100 coating obtained via the delipidation. A few features of average height 4.3±0.4 nm were still present after NaOH rinsing.

Atomic force microscopy images of collagen and collagen–decorin coatings

As shown in Fig. 25 (Fig. 3 paper IV), 2D-AFM images were recorded for collagen I (a), collagen I-decorin (b) and collagen III (c). Again, the outside of the capillary was coated as described in the Experimental section. Fibrils in the collagen I and collagen III images vary in thickness and are randomly distributed on the silica surface. Collagen III fibrils appear to be much thinner than those of collagen I. The higher hydrophilicity of collagen III than of collagen I (**108**) may explain the different degree of coverage on the hydrophobic fused silica. As can be seen in Fig. 25b, when decorin is part of the coating, the fibrils are thinner and the coating more even. According to some previous studies, decorin takes part in the collagen monomer assembly and prevents lateral fusion of the fibrils. (**50**,**51**,**141**)

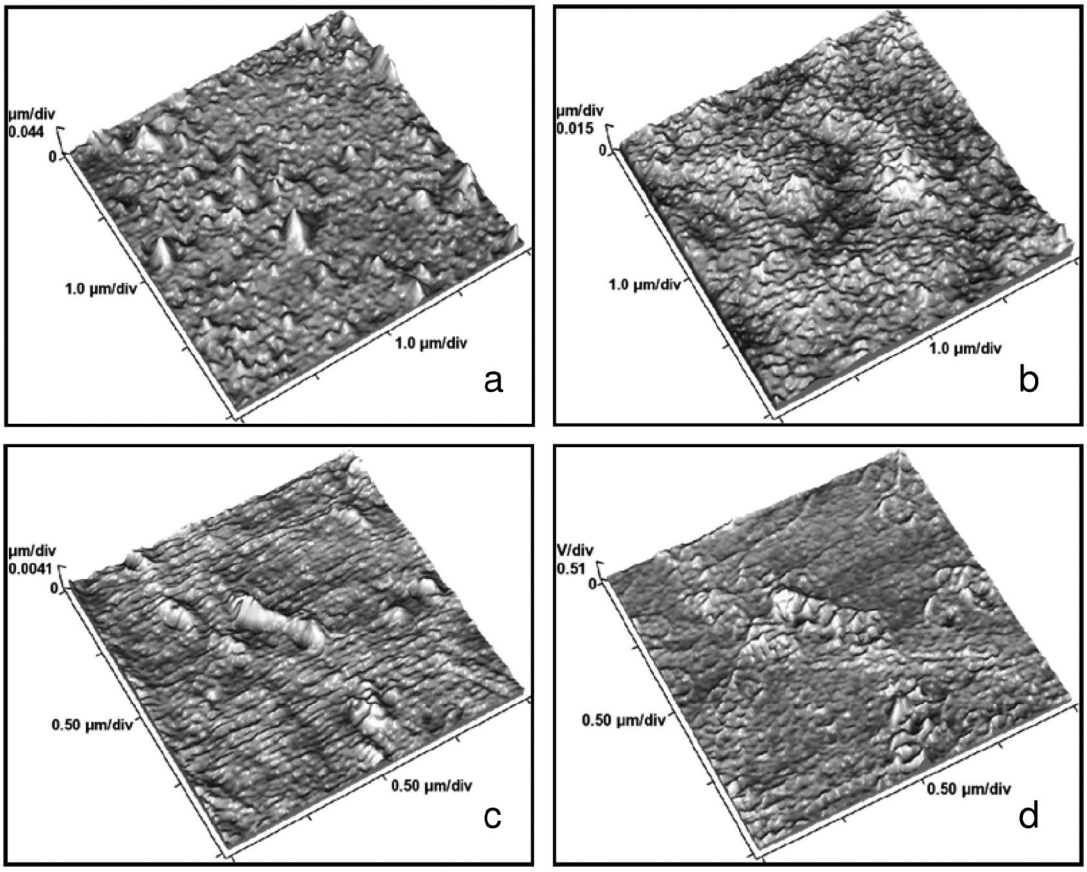

Figure 24. *Atomic force microscopy images of a) LDL particle coating, b) apoB-100 protein coating obtained after the delipidation of LDL particles with Nonidet P-40, c) height image and d) phase image for apoB-100 coating after rinsing of the capillary with 1M NaOH. For a detailed description of the procedures used for measurement of the AFM images, see the Experimental section.*

Atomic force microscopy images of glycated collagen I

For studies on glycated collagen I, capillaries were coated with collagen I and submitted to D-glucose-6-phosphate treatment for 0, 8, 16 or 24 h (Fig. 26, Fig. 3 paper V). The coating and treatment procedures are described in the Experimental section. As can be seen from Fig. 26, the thickness of the fibrils significantly decreases as a function of glycation time. As well, the collagen coverage becomes more even as glycation proceeds.

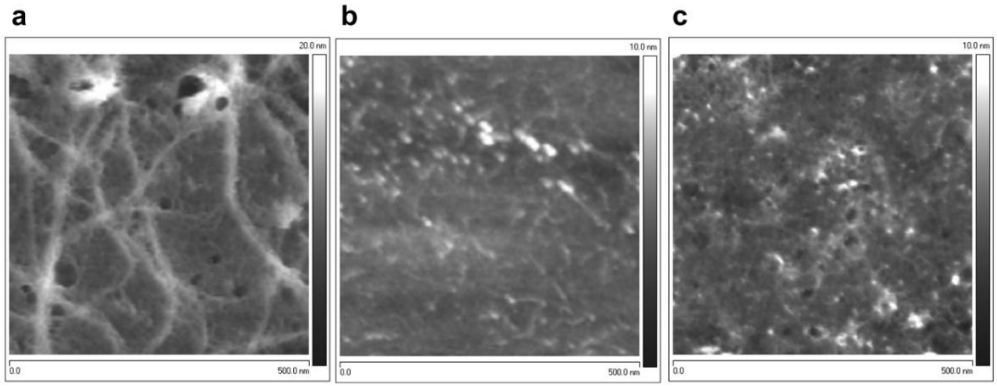

Figure 25. *AFM images of (a) collagen I, (b) collagen I–decorin and (c) collagen III coatings. For a detailed description of the conditions employed during the measurements, see the Experimental section. Area of the images 0.5 μm x 0.5 μm.*

These changes could be due to the glycation of collagen I and following cross-linking of the fibrils. (**84**,**87**) On this basis, we may conclude that glycation, the formation of AGEs and the reaction of AGEs with the lysine group of collagen seriously degrade the hierarchical structure of the fibrils.

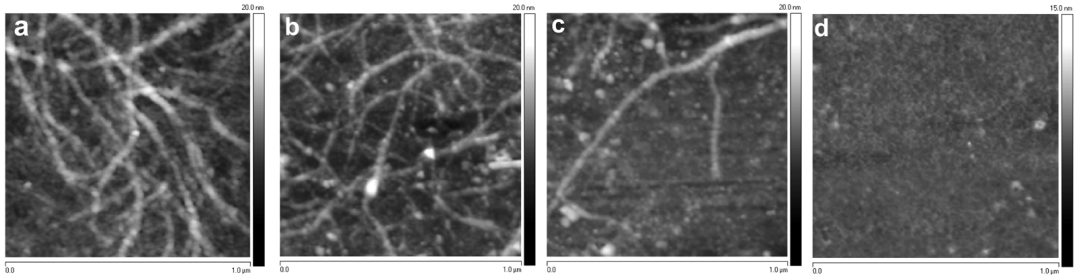

Figure 26. *AFM images of (a) collagen I, (b) glycated collagen I (8 h), (c) glycated collagen I (16 h), and (d) glycated collagen I (24 h) coatings. Area of images 1 μm x 1 μm.*

5.6.3 ζ-Potential measurements

The ζ-potential measurements, carried out in study I, showed an increase in the LDL negative charges as a function of oxidation time confirming the increasing degrees of oxidation of the LDL coating (see section 5.3.1).

5.6.4 Radioactivity measurements

Measurement of the number of ^{3}H-labelled LDL particles on the capillary wall (paper II) confirmed that LDLs prefer to interact with the capillary wall rather than each other and thus cover the silica surface as a monolayer.

5.7 QMC studies: development of new biological surfaces for interaction studies

The results obtained in CEC were exploited in QCM studies. An important aim of these investigations was to apply the CEC information to the preparation of chip surfaces useful for interaction studies between LDL and components of the ECM by QCM. Results for the PP and PP_2, and the collagen and C6S sensor chips are discussed separately below.

5.7.1 PP and PP_2 sensor chips

PP and PP_2 were immobilized on PS-derivatized gold-plated crystals as described in the Experimental section, and C6S was injected over the surface in concentrations ranging from 0.1 to 30 μg/mL for PP surfaces and from 0.5 to 2 μg/mL for PP_2 surfaces. As we can see from Figs. 27 and 28 (Figs. 1a and 2a paper VI), the C6S binding was concentration-dependent with both PP and PP_2 ligands. The binding was stronger on the PP_2-coated surface, while rather complex kinetics, with apparent biphasic dissociation, was observed on the PP surface. PP and PP_2 share part of the apoB-100 sequence involved in the interaction, and both bind C6S through electrostatic interactions. (**28**,**71**) It is possible, nevertheless, that the nonspecific interactions are enhanced with PP_2 because of the higher molecular weight. For both PP and PP_2 surfaces, the interaction with C6S is likely to occur as avidic binding. Moreover, the linear association curves suggest that the interactions between PP_2 and C6S are mass transport limited. The fitting of theoretical kinetic models to the data was difficult for the PP surface, and the binding constant could not be determined. For the PP_2 surface, on the other hand, the data fitting could be done according to a simple 1:1 model compensating for mass transport limitation, and the dissociation constant (0.23 nM) could be calculated. In control experiments carried out with BSA and $NeuP_2$ as ligands, no significant interactions occurred with C6S. Also, the injection of common sucrose instead of C6S did not provoke a response with either PP or PP_2 coated surfaces.

These results confirm that the binding of PP and PP_2 is relatively specific for C6S and is mediated by the positive lysine and arginine residues of apoB-100 peptide fragments.

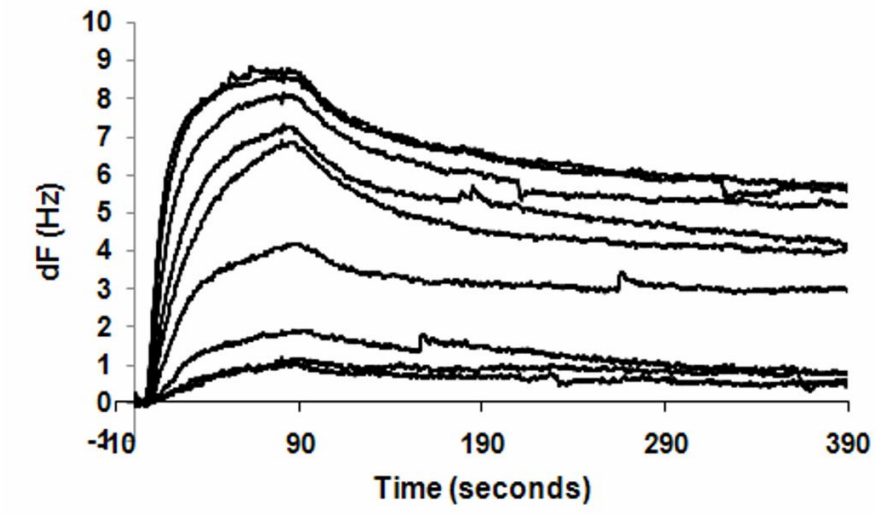

Figure 27. *C6S binding on PP sensor chip. C6S concentrations ranged from 0.1 to 30 μg/mL. Running buffer: 10 mM PBS pH 7.4. Flow rate: 25 μl/min. Experiments were carried out at room temperature.*

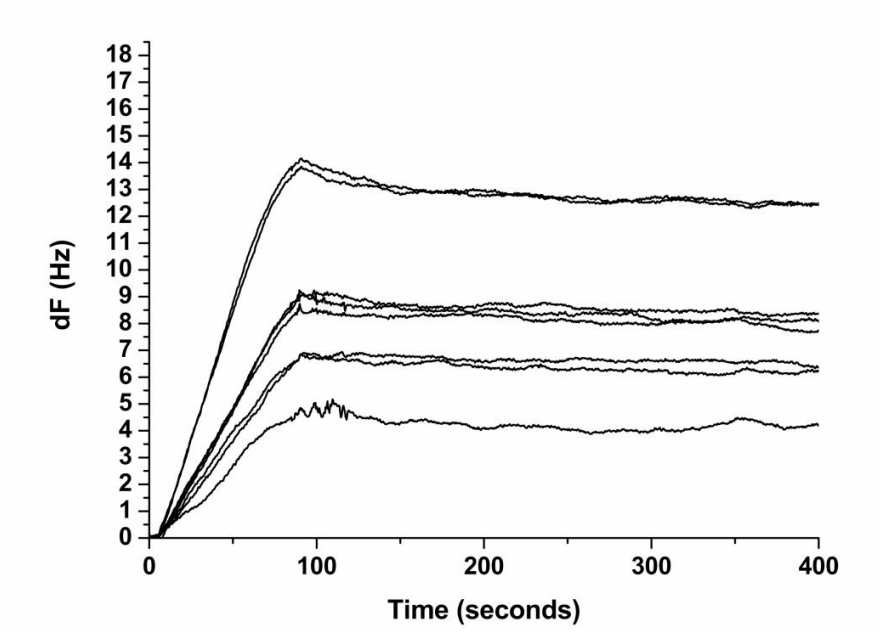

Figure 28. *C6S binding on PP_2 sensor chip. C6S concentrations ranged from 0.5 to 2 μg/mL. Running buffer: 10 mM PBS pH 7.4. Flow rates: 25 μl/min. Kinetic rate constants: k_a=2.3E+06 $M^{-1}s^{-1}$, k_d=5.2E-04 s^{-1}, K_d= 0.23 nM. Experiments were carried out at room temperature.*

5.7.2 Collagen and C6S sensor chips

PP was injected over a collagen or a C6S-coated surface at concentrations ranging from 5 to 50 μg/mL and from 50 to 250 μg/mL, respectively. PP interacted with the negative charges of collagen I and C6S through its positive lysine and arginine residues. With both surfaces, the frequency shift was concentration-dependent and the dissociation of the analyte fast (Figs. 29 and 30, figs. 3a and 4a paper VI). The stronger response with the C6S surface may be due to an amplification of the signal. The structure of C6S on the surface could be viewed as a matrigel-like structure, which enables the signal amplification The shape of the binding curve indicates that the interaction between PP and collagen I is of some complexity, evidently because collagen I can interact with PP through multiple sites and vice versa. Moreover, the fact that not all curves return to zero value of frequency, in particular at higher analyte concentrations, may indicate some rebinding of PP or some non-specific interactions with the collagen I surface.

A similar explanation is valid for C6S aldehyde coupled to the sensor chip (Fig. 30). Multi-site interactions of PP with the immobilized C6S may explain the complexity of the binding, and the incomplete dissociation suggests a possible rebinding of PP to the surface. In addition, a comparison of Figs. 30 and 27 suggests a decrease in the avidity effect when C6S is the ligand and PP the analyte. Control experiments resulted in poor binding of $NeuP_2$ to the C6S surface (Fig. 30, small plot on the right) and confirmed that positive residues are needed for the interactions.

The dissociation constants (K_d), ~9 μM for collagen I surfaces and ~13.3 μM for C6S surfaces, were estimated with equilibrium Scatchard plot analysis and should be treated with some care due to the complexity of the binding and not completely equilibrated state of the interaction. Although the affinity of PP is comparable for both surfaces, it should be remembered that the C6S sensor chip, experiments were carried out in the presence of salt (137 mM NaCl), which may hamper the interaction. Moreover, the negatively charged sulphate groups, which contribute to the interactions, are partly lost during the C6S oxidation. In addition, previous studies showed that collagen I has a much lower affinity for LDL and apoB-100 peptide fragments than when GAGs are part of collagen fibrils (**25,73**).

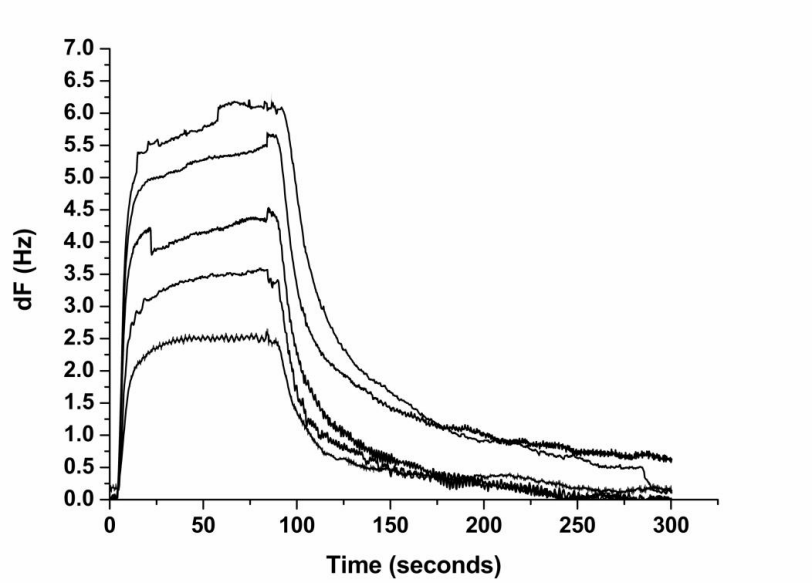

Figure 29. *PP binding on collagen I sensor chip. PP concentrations ranged from 5 to 50 µg/mL. Running buffer: 20 mM phosphate pH 7.4. Flow rate: 25 µl/min. Experiments were carried out at room temperature.*

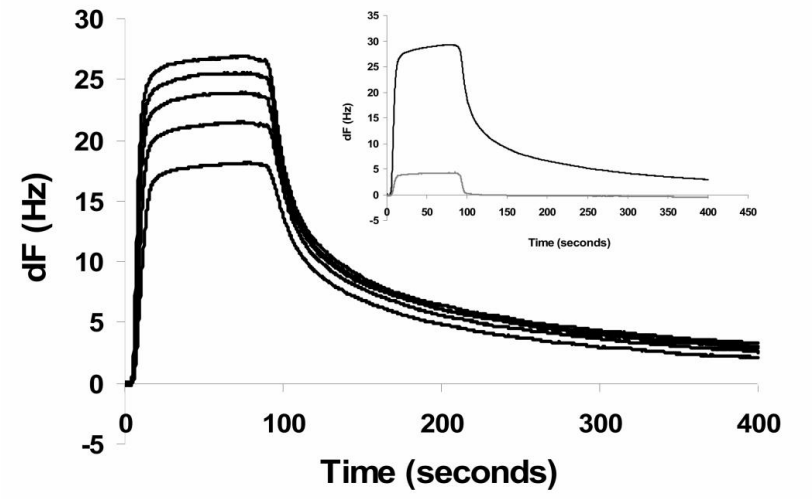

Figure 30. *PP binding on C6S sensor chip. PP concentrations ranged from 50 to 250 µg/mL. The small plot compares the binding of PP (black curve) and $NeuP_2$ (grey curve) at concentration 250 µg/mL Running buffer: 10 mM PBS pH 7.4. Flow rate: 25 µl/min. Experiments were carried out at room temperature.*

6 Conclusions

The goal of this doctoral research was to develop miniaturized analytical tools enabling interaction studies between nanodomains of biological importance. The primary technique investigated was capillary electrochromatography with diode array detection.

The focus of the investigations was modifications of LDL and the interactions of LDL with components of the extracellular matrix. Both processes are considered important in the development of atherosclerotic plaques. In the course of the work, methods were developed for coating of the fused silica capillary wall with lipoproteins or components of the ECM.

The first step was to optimize a procedure for coating LDL on the capillary wall. Although lipoproteins can interact with the capillary wall both electrostatically and hydrophobically, it is proposed here that the hydrophobic interactions play the major role in the adsorption. The optimized LDL coating was oxidized *in situ*, under various conditions, by flushing the capillary with copper sulphate. Neutral steroids, which interact hydrophobically with LDL particles, were introduced to the CE instrument as marker compounds, and their retention factors provided information about the modifications occurring in the LDL particle coating after oxidation.

The LDL coating was also treated *in situ* with selected enzymes present in the ECM: SMase, PLA_2 and α-chymotrypsin. The retention factors of steroids, indicating the affinity of the steroids towards modified LDL particles, gave information about the modification of LDL.

Capillary electrochromatography provided a useful platform for the removal of lipids from LDL particles resulting in a apolipoprotein B-100 surface suitable for interaction studies. ApoB-100 is the major apolipoprotein of LDL, and also the largest and most hydrophobic protein known. In this part of the work, both retention factors and distribution coefficients of steroids provided numerical information on interactions.

Since components of the ECM play a crucial role in the progression of atherosclerosis, collagen and collagen–decorin coatings were developed and optimized. Collagen types I and III were investigated, while selected apoB-100 peptide fragments acted as marker compounds. The retention factors of the peptides showed that interactions were strongest with the positive peptide (PP), including lysine and arginine groups, and that the interactions were enhanced by the presence of decorin.

The collagen I coating was then subjected to *in situ* glycation in CEC. The coating was treated with D-glucose-6-phosphate for different time periods, and native LDL, oxidized LDL, PP and $NeuP_2$ were introduced to evaluate their interactions with the modified collagen I coating. Oxidized LDL was completely retained on the collagen I, while the affinity of native LDL decreased with the degree of glycation of the coating. The negligible variation of the retention factor of PP and $NeuP_2$ suggested that another binding site, in addition to the positive one, mediates the interactions between LDL and glycated collagen.

Finally, QCM technique was introduced to provide complementary information on interactions between ECM components and LDL. Biosensor surfaces were derivatized with PP, PP_2 collagen I or C6S. The selected analytes were C6S for PP and PP_2 ligands, and PP for collagen I and C6S ligand. The sensitivity of this technique allowed very small amounts of analytes and biomaterials to be adsorbed onto the QCM chips. The results showed PP to have higher affinity for C6S than for collagen I, and the strongest binding was achieved for the sensor chip on which PP_2 was adsorbed.

All the methods developed in this work share some common features. They are suitable for surface interaction studies, they are easy to carry out, and, since just a small amount of material is required, they are relatively inexpensive. The flexibility and versatility of CEC make it a useful technique for miniaturization and for mimicking the physiological or pathological conditions that lead to the formation of atheroma. In addition, as a separation technique with high resolution, CEC can provide, within a single run, information about the interactions between several analytes and a biomaterial used as stationary phase. QCM, an excellent miniaturized technique, requires even smaller amounts of ligands and analytes than CEC. Although information is achieved for the interaction of only one analyte at a time, QCM allows quick changes in the experimental conditions. Despite the high mass sensitivity, however, QCM does not allow coupling with other detectors as CEC does. Most importantly, CEC has been shown to make an excellent microreactor for interaction studies, and the analytical CEC tools that were developed can easily be exploited in investigations on the interactions of many other biological nanodomains.

7 References

1) D. L. Sparks, M. C. Phillips, *J. Lipid Res*., 33 (1992) 123-130. Quantitative measurement of lipoprotein surface charge by agarose gel electrophoresis

2) E. Florentin, L. Lagrost, C. Lallemant, P. Gambert, *Anal. Biochem.*, 216 (1994) 352-357. Polyacrylamide gradient gel electrophoresis as a method to measure transfers of radiolabeled cholesteryl esters between several plasma lipoprotein fractions

3) R. D. Macfarlane, P. V. Bondarenko, S. L. Cockrill, I. D. Cruzado, W. Koss, C. J. McNeal, A. M. Spiekerman, L. K. Watkins, *Electrophoresis*, 18 (1997) 1796-1806. Development of a lipoprotein profile using capillary electrophoresis and mass spectrometry

4) H. Esterbauer, G. Striegl, H. Puhl, M. Rotheneder, *Free Radic. Res*., 6 (1989) 67-75. Continuous monitoring of in vitro oxidation of human low density lipoprotein

5) G. Yohannes, M. Sneck, S.Varjo, M. Jussila, S. K. Wiedmer, P. T. Kovanen, K. Öörni and M.-L. Riekkola, *Anal. Biochem.* 354 (2006) 255-265. Miniaturisation of asymmetrical flow-field flow fractionation and application to aggregation and fusion studies of lipoproteins

6) J. W. Jorgenson, K. D. Lukacs, *Anal. Chem.* 53 (1981) 1298-1302. Zone electrophoresis in open-tubular glass-capillaries;

7) A. Manz, D. J. Harrison, E. M. J. Verpoorte, J. C. Fettinger, A. Paulus, H. Ludi, H. M. Widmer, *J. Chromatogr*. 593 (1992) 253-258. Planar chips technology for miniaturization and integration of separation techniques into monitoring systems-capillary electrophoresis on a chip

8) S. Terabe, K. Otsuka, K. Ichikawa, A. Tsuchiya, T. Ando, *Anal. Chem.* 56 (1984) 111-113. Electrokinetic separations with micellar solutions and open-tubular capillaries

9) S. Terabe, *Annu. Rev. Anal. Chem.* 2 (2009) 99-120. Capillary separation: micellar electrokinetic chromatography

10) H. Watarai, *Chem. Lett.* 20 (1991) 391-394. Microemulsion capillary electrophoresis

11) R. Ryan, S. Donegan, J. Power, E. McEvoy, K. Altria, *Electrophoresis*, 30 (2009) 65-82. Recent advantages in methodology, optimization and application of MEEKC

12) J. W. Jorgenson, K. D. Lukacs, *J. Chromatogr.* 218 (1981) 209-216. High-resolution separations based on electrophoresis and electroosmosis

13) T. Tsuda, K. Nomura, G. Nakagawa, *J. Chromatogr.* 248 (1982) 241-247. Open-tubular microcapillary liquid chromatography with electroosmosis flow using a UV detector

14) K. Jinno, H. Sawada, *Trends Anal. Chem.* 19 (2000) 664-675. Recent trends in open-tubular capillary electrochromatography

15) IUPAC: M.-L. Riekkola, J. Å. Jönsson and R. M. Smith, *Pure Appl. Chem.* 76 (2004) 443-451. Terminology for analytical capillary electromigration techniques

16) M. G. Khaledi, John *Willey&Sons Inc.*, (1998). Hih-performance capillary electrophoresis: theory, techniques, and applications

17) Z. Deyl, F. Svec, Elsevier (2001). Capillary electrochromatography

18) J. P. Landers, *CRC Press, Tailor and Francis group* (2008). Capillary and microchip electrophoresis and associated microtechniques

19) K. W. J. Wahle, S. D. Heys, *Curr. Opin. Lipidol.*, 19 (2008) 435-437. Atherosclerosis: cell biology and lipoproteins

20) V. Z. Rocha, P. Libby, *Nat. Rev. Cardiol.*, 6 (2009) 399-409. Obesity, inflammation, and atherosclerosis

21) W. Khovidhunkit, M.-S. Kim, R. A. Memon, J. K. Shigenaga, A. H. Moser, K. R. Feingold, C. Grunfeld, *J. Lipid Res.*, 45 (2004) 1169-1196. Effects of infection and inflammation on lipid and lipoprotein metabolism: mechanisms and consequences to the host

22) W. J. Castellani, *Nutr. Res.*, 24 (2004) 681-693. Metabolic and nutritional aspects of the atherogenic atypical lipoproteins: lipoprotein(a), remnant lipoproteins, and oxidized low-density lipoprotein

23) R. Albertini, R. Moratti, G. De Luca, *Curr. Mol. Med.*, 2 (2002) 579-592. Oxidation of low-density lipoprotein in atherosclerosis from basic biochemistry to clinical studies

24) J. L. Goldstein, M. S. Brown, *Ann. Rev. Biochem.*, 46 (1977) 897-930. The low-density lipoprotein pathway and its relation to atherosclerosis

25) P. T. Kovanen, M. O. Pentikäinen, *Trends Cardiovasc. Med.*, 9 (1999) 86-91. Decorin links low-density lipoproteins (LDL) to collagen: a novel mechanism for retention of LDL in the atherosclerotic plaque

26) I. J. Goldberg, W. D. Wagner, L. Pang, L. Paka, L. K. Curtiss, J. A. DeLozier, G. S. Shelness, C. S. H. Young, S. Pillarisetti, *J. Biol. Chem.*, 273 (1998) 35355-35361. The NH_2-terminal region of apolipoprotein B is sufficient for lipoprotein association with glycosaminoglycans

27) G. Camejo, E. Hurt-Camejo, O. Wiklund, G. Bondjers, *Atherosclerosis*, 139 (1998) 205-222. Association of apo B lipoproteins with arterial proteoglycans: pathological significance and molecular basis

28) G. Camejo, S. O. Olofsson, F. Lopez, P. Carlsson, G. Bondjers, *Arterioscler. Thromb. Vasc. Biol.*, 8 (1988) 368-377. Identification of Apo B-100 segments mediating the interaction of low density lipoproteins with arterial proteoglycans

29) E. Hurt-Camejo, U. Olsson, O. Wiklund, G. Bondjers, *G. Camejo, Arterioscler. Thromb. Vasc. Biol.*, 17 (1997) 1011-1017. Cellular consequences of the association of apoB lipoproteins with proteoglycans

30) K. Öörni, M. O. Pentikäinen, M. Ala-Korpela, P. T. Kovanen, *J. Lipid Res.*, 41 (2000) 1703-1714. Aggregation, fusion, and vesicle formation of modified low density lipoprotein particles: molecular mechanism and effects on matrix interactions

31) G. M. Chisolm, D. Steinberg, *Free Radic. Biol. Med.*, 28 (2000) 1815-1826. The oxidative modification hypothesis of atherogenesis: an overview

32) H. M. Wilson, R. N. Barker, L.-P. Erwig, *Curr. Vasc. Pharmacol.*, 7 (2009) 234-243. Macrophages: promising targets for the treatment of atherosclerosis

33) P. Saha, B. Modarai, J. Humphries, K. Mattock, M. Waltham, K. G. Burnand, A. Smith, *Curr. Opin. Pharmacol.*, 9 (2009) 109-118. The monocyte/macrophage as a therapeutic target in atherosclerosis

34) N. Shibata, C. K. Glass, *J. Lipid Res.*, 50 (2009) S277-S281. Regulation of macrophage function in inflammation and atherosclerosis

35) K. J. Williams, I. *Tabas, Curr. Opin. Lipidol.*, 9 (1998) 471-474. The response to retention hypothesis of atherogenesis reinforced

36) C. Flood, M. Gustafsson, R. E. Pitas, L. Arnaboldi, R. L. Walzem, J. Borén, *Arterioscler. Thromb. Vasc. Biol.*, 24 (2004) 564-570

37) T. L. Innerarity, K. H. Weisgraber, K. S. Arnold, R. W. Mahley, R. M. Krauss, G. L. Vega, S. M. Grundy, *Proc. Natl. Acad. Sci.*, 84 (1987) 6919-6923. Familial defective apolipoprotein B-100: low density lipoproteins with abnormal receptor binding

38) N. B. Myant, J. J. Gallagher, B. L. Knight, S. N. McCarthy, J. Frostegard, J. Nilsson, A. Hamsten, P. Talmud, S. E. Humphries, *Arterioscler. Thromb. Vasc. Biol.*, 11 (1991) 691-703. Clinical signs of familial hypercholesterolemia in patients with familial defective apolipoprotein B-100 and normal low density lipoprotein receptor function

39) A. J. Whitfield, P. H. R. Barrett, F. M. van Bockxmeer, J. R. Burnett, *Clin. Chem.*, 50 (2004) 1725-1732. Lipid disorders and mutations in the APOB gene

40) T. Hevonoja, M. O. Pentikäinen, M. T. Hyvönen, P. T. Kovanen, M. Ala-Korpela, *Biochim. Biophys. Acta*, 1488 (2000) 189-210. Structure of low density lipoprotein (LDL) particles: basis for understanding molecular changes in modified LDL

41) K. D. Biggerstaff, J. S. Wooten, *Adv. Physiol. Educ.*, 28 (2004) 105-106. Understanding lipoproteins as transporters of cholesterol and other lipids

42) J. P. Kane, *Ann. Rev. Physiol.*, 45 (1983) 637-650. Apolipoprotein B: structural and metabolic heterogeneity

43) J. P. Segrest, M. K. Jones, H. De Loof, N. Dashti, *J. Lipid Res.*, 42 (2001) 1346-1367. Structure of apolipoprotein B-100 in low density lipoproteins

44) L. Chan, *J. Biol. Chem.*, 267 (1992) 25621-25624. Apolipoprotein B, the major protein component of triglyceride-rich and low density lipoproteins

45) A. Elenius, K. Simons, *Biochemistry*, 10 (1971) 2542-2547. Removal of lipids from human plasma low-density lipoprotein by detergents

46) L. Socorro, G. Camejo, *J. Lipid Res.*, 20 (1979) 631-638. Preparation and properties of soluble, immunoreactive apoLDL

47) L. L. Kilgore, B. W. Patterson, W. R. Fisher, *J. Biol. Chem.*, 261 (1986) 8842-8848. Immunologic comparison of the conformations of apolipoprotein B

48) C.-Y. Yang, S.-H. Chen, S. H. Gianturco, W. A. Bradley, J. T. Sparrow, M. Tanimura, W.-H. Li, D. A. Sparrow, H. Deloof, M. Rosseneu, F.-S. Lee, Z.-W. Gu, A. M. Gotto Jr., L. Chan, *Nature*, 323 (1986) 738-742. Sequence, structure, receptor-binding domains and internal repeats of human apolipoprotein B-100

49) J. R. McNamara, G. R. Warnick, G. R. Cooper, *Clin. Chim. Acta*, 369 (2006) 158-167. A brief history of lipid and lipoprotein measurements and their contribution to clinical chemistry

50) W. T. Friedewald, R. I. Levy, D. S. Fredrickson, *Clin. Chem.*, 18 (1972) 499-502. Estimation of the concentration of low-density lipoprotein cholesterol in plasma, without use of the preparative ultracentrifuge

51) J. D. Otvos, E. J. Jeyarajah, D. W. Benett, *Clin. Chem.*, 37 (1991) 377-386. Quantification of plasma lipoproteins by proton nuclear magnetic resonance spectroscopy

52) P. Li, M. Hansen, J. C. Giddings, *J. Liq. Chrom. & Rel. Technol.*, 20 (1997) 2777-2802. Separation of lipoproteins from human plasma by flow field-flow fractionation

53) H. Kurosawa, H. Yoshida, H. Yanai, Y. Ogura, Y. Hirowatari, N. Tada, *Clin. Biochem.*, 40 (2007) 1291-1296. Comparative study between anion-exchange HPLC and homogeneous assay methods in regard to the accuracy of high- and low-density lipoprotein cholesterol measurement

54) T. Manabe, S. Visvikis, J. Steinmetz, M. M. Galteau, T. Okuyama, G. Siest, Electrophor. '86, *Proc. Meet. Int. Electrophor. Soc.*, 5th (1986) 579-582. Combined technique of micro 2-D electrophoresis for analysis of serum lipoproteins and apolipoproteins

55) G. Bittolo-Bon, G. Cazzolato, *J. Lipid Res.*, 40 (1999) 170-177. Analytical capillary isotachophoresis of total plasma lipoproteins: a new tool to identify atherogenic low density lipoproteins

56) G. Nowicka, T. Bruning, B. Grothaus, G. Kahl, G. Schmitz, *J. Lipid Res.* 31 (1990) 1173-1186. Characterization of apolipoprotein B-containing lipoproteins separated by preparative free low isotachophoresis

57) G. Schmitz, C. Mollers, *Electrophoresis* 15 (1994) 31-39. Analysis of lipoproteins with analytical capillary electrophoresis

58) G. Schmitz, C. Mollers, V. Richter, *Electrophoresis* 18 (1997) 1807-1813. Analytical capillary isotachophoresis of human serum lipoproteins

59) A Bottcher, J. Schlosser, F. Kronenberg, H. Dieplinger, G. Knipping, K. J. Lackner, G. Schmitz, *J. Lipid Res.* 41 (2000) 905-915. Preparative free-solution isotachophoresis for separation of human plasma lipoproteins: apolipoprotein and lipid composition of HDL subfractions

60) A. D. Dergunov, A Hoy, E. A. Smirnova, S. Visvikis, G. Siest, *Int. J. Biochem. Cell Biol.* 35 (2003) 530-543. Charged-based heterogeneity of human plasma lipoproteins at hypertriglyceridemia: capillary isotachophoresis study

61) T. N. Wight, *Arteriosclerosis*, 9 (1989) 1-20. Cell biology of arterial proteoglycans

62) R. V. Iozzo, A. D. Murdoch, *FASEB J.*, 10 (1996) 598-614. Proteoglycans of extracellular environment: clues from the gene and the protein side offer novel perspectives in molecular diversity and function

63) J. Engel, H. P. Bächinger, *Top. Curr. Chem.*, 247 (2005) 7-33. Structure, stability and folding of the collagen triple helix

64) S. E. Paramonov, J. D. Hartgerink, in: C. S. S. R. Kumar, J. Hormes, C. Leuschner, (Eds.), Nanofabrication towards biomedical applications, *Wiley-VCH* (2005) 95-117

65) M. G. Venugopal, J. A. M. Ramshaw, E. Braswell, D. Zhu, B. Brodsky, *Biochemistry*, 33 (1994) 7948-7956. Electrostatic interaction in collagen-like triple-helical peptides

66) E. Schönherr, H. Hausser, L. Beavan, H. Kresse, *J. Biol. Chem.*, 270 (1995) 8877-8883. Decorin-type I collagen interaction. Presence of separate core protein–binding domains

67) M. Raspanti, A. Alessandrini, V. Ottani, A. Ruggeri, *J. Struct. Biol.*, 119 (1997) 118-122. Direct visualization of collagen-bound proteoglycans by tapping-mode atomic force microscopy

68) T. Douglas, S. Heinemann, S. Bierbaum, D. Scharnweber, H. Worch, *Biomacromolecules*, 7 (2006) 2388-2393. Fibrillogenesis of collagen types I, II, and III with small leucine-rich proteoglycans decorin and biglycan

69) S. Bierbaum, T. Douglas, T. Hanke, D. Scharnweber, S. Tippelt, T. K. Monsees, R. H. W. Funk, H. Worch, *J. Biomed. Mater. Res.*, 77A (2006) 551-562. Collageneous matrix coatings on titanium implants modified with decorin and chondroitin sulfate: characterization and influence on the osteoblastic cells

70) M. Raspanti, M. Viola, M. Sonaggere, M. E. Tira, R. Tenni, *Biomacromolecules*, 8 (2007) 2087-2091. Collagen fibril structure is affected by collagen concentration and decorin

71) K. Skålen, M. Gustafsson, E. K. Rydberg, L. M. Hultén, O. Wiklund, T. L. Innerarity, J, Borén, *Nature*, 417 (2002) 750-754. Subendothelial retention of atherogenic lipoproteins in early atherosclerosis

72) G. Camejo, U. Olosson, E. Hurt-Camejo, N. Baharamian, G. Bondiers, *Atheroscler. Suppl.*, 3 (2002) 3-9. The extracellular matrix on atherogenesis and diabetes-associated vascular disease

73) M. O. Pentikäinen, K. Öörni, R. Lassila, P. T. Kovanen, J. Biol. Chem., 272 (1997) 7633-7638. The proteoglycan decorin links low density lipoproteins with collagen type I

74) H. Esterbauer, M. Dieber-Rotheneber, G. Waeg, G. Striegl, G. Jürgens, *Chem. Res. Toxicol.*, 3 (1990) 77-92. Biochemical, structural, and functional properties of oxidized low-density lipoprotein

75) M. Torzewski, K. J. Lackner, *Clin. Chem. Lab. Med.*, 44 (2006) 1389-1394. Initiation and progression of atherosclerosis enzymatic or oxidative modification of low-density lipoprotein?

76) K. Öörni, P. Posio, M. Ala-Korpela, M. Jauhiainen, P. T. Kovanen, *Arterioscl. Thromb. Vasc. Biol.*, 25 (2005) 1678-1683. Sphingomyelinase induces aggregation and fusion of small very low-density lipoprotein and intermediate-density lipoprotein particles and increases their retention to human arterial proteoglycans

77) P. Sartipy, E. Hurt-Camejo, *Trends Cardiovasc. Med.*, 9 (1999) 232-238. Modification of plasma lipoproteins by group IIA phospholipase A_2. Possible implication for atherogenesis

78) M. Piha, L. Lindstedt, P. T. Kovanen, *Biochemistry*, 34 (1995) 10120-10129. Fusion of proteolyzed low-density lipoprotein in the fluid phase: a novel mechanism generating atherogenic lipoprotein particles

79) K. Öörni, J. K. Hakala, A. Annila, M. Ala-Korpela, P. T. Kovanen, *J. Biol. Chem.*, 273 (1998) 29127-29134. Sphingomyelinase induces aggregation and fusion, but phospholipase A_2 only aggregation, of low density lipoprotein (LDL) particles

80) A. J. Guarino, S. P. Lee, T. N. Tulenko, S. P. Wrenn, *J. Colloid Interface Sci.*, 279 (2004) 109-116. Aggregation kinetics of low density lipoproteins upon exposure to sphingomyelinase

81) K. Paananen, J. Saarinen, A. Annila, P. T. Kovanen, *J. Biol. Chem.*, 270 (1995) 12257-12262. Proteolysis and fusion of low density lipoprotein particles strengthen their binding to human aortic proteoglycans

82) P. Sartipy, G. Camejo, L. Svensson, E. Hurt-Camejo, *J. Biol. Chem.*, 274, (1999) 25913-25920. Phospholipase A_2 modification of low density lipoproteins forms small high density particles with increased affinity for proteoglycans and glycosaminoglycans

83) J. van Asten, B. O. Bingen, E. A. B. J. Broeders, E. S. Hoogeveen, F. van Hout, V. A. Kwee, B. Laman, F. Malgo, M. Mohammadi, M. Nijenhuis, M. Rijkée, M. M. van Tellingen, M. Tromp, Q. Tummers, L. de Vries, *Eur. J. Intern. Med.*, 20 (2009) 253-260. The role of inflammation on atherosclerosis, intermediate and clinical cardiovascular endpoints in type 2 diabetes mellitus

84) R. G. Paul, A. J. Bailey, *Int. J. Biochem. Cell. Biol.*, 28 (1996) 1297-1310. Glycation of collagen: the basis of its central role in the late complications of ageing and diabetes

85) A. G. Huebschmann, J. G. Regensteiner, H. Vlassara, J. E. B. Reusch, *Diabetes Care*, 29 (2006) 1420-1432. Diabetes and advanced glycoxidation end products

86) N. Ahmed, *Diabetes Res. Clin. Pract.*, 67 (2005) 3-21. Advanced glycation endproducts-role in pathology of diabetic complications

87) V. M. Monnier, M. Glomb, A. Elgawish, D. R. Sell, *Diabetes*, 45, 1996, S67-72. The mechanism of collagen cross-linking in diabetes: a puzzle nearing resolution

88) M-X. Fu, K. J. Knecht, S. R. Thorpe, J. W. Baynes, *Diabetes*, 41 (1992) 42-48. Role of oxygen in cross-linking and chemical modification of collagen by glucose

89) M. Brownlee, H. Vlassara, A. Cerami, *Diabetes*, 34 (1985) 936-941. Nonenzymatic glycosylation products on collagen covalently trap low-density lipoprotein

90) S. Jimi, N. Sakata, A. Matunaga, S. Takebayashi, *Atherosclerosis*, 107 (1994) 109-116. Low density lipoproteins bind more to type I and III collagens by negative charge-dependent mechanisms than to type IV and V collagens

91) E. Kenndler, Theory of capillary zone electrophoresis, in: *High-performance capillary electrophoresis*, Wiley-VHC (1998), 25-76)

92) A. S. Rathore, C. Horváth, *Electrophoresis*, 23 (2002) 1211-1216. Chromatographic and electrophoretic migration parameters in capillary electrochromatography

93) S. K. Wiedmer, M. Jussila, R. M. S. Hakala, K.-H. Pystynen, M.-L. Riekkola, *Electrophoresis*, 26 (2005) 1920-1927. Piperazine-based buffers for liposome coating of capillaries for electrophoresis

94) Karin Walhagen, Klaus K. Unger, Milton T. W. Hearn, *Anal. Chem.* 73 (2001) 4924-4936. Capillary electrochromatography analysis of hormonal cyclic and linear peptides

95) J. Chen, A. Fallarero, A. Mättänen, M. Sandberg, J. Peltonen, P. M. Vuorela, M.-L. Riekkola, *Anal. Chem.*, 80 (2008) 5103-5109. Living cells of staphylococcus aureus immobilized onto the capillary surface in electrochromatography: a tool for screening of biofilm

96) E. Nemutlu, N. Özaltin, Anal. Bioanal. Chem., 383 (2005) 833-838. Determination of magnesium, calcium, sodium, and potassium in blood plasma by capillary zone electrophoresis

97) A.-C. Servais, J. Crommen, M. Fillet, Electrophoresis, 27 (2006) 2616-2629. Capillary electrophoresis-mass spectrometry, an attractive tool for drug bioanalysis and biomarker discovery

98) J. R. Petersen, A. O. Okorodudu, A. Mohammad, D. A. Payne, *Clin. Chim. Acta*, 330 (2003) 1-30. Capillary electrophoresis and its application in the clinical laboratory

99) P. W. Hawkes, (ed.)., *Adv. Elec. Elec. Phys. Suppl. 16*, Academic Press, London 1985, pp 1-21

100) G. Binnig, C. F. Quate, Ch. Gerber, *Phys. Rev. Lett.* 56 (1986) 930-933. Atomic force microscope;

101) M. Radmacher, R. W. Tillamnn, M. Fritz, H. E. Gaub, *Science* 257 (1992) 1900-1905. From molecules to cells: imaging soft samples with the atomic force microscope

102) S. Magonov, *Handbook of Surfaces and Interfaces of Materials*, 2 (2001) 393

103) T. W. Kelley, P. A. Schorr, K. D. Johnson, M. Tirrell. C. D. Frisbie, *Macromolecules*, 31 (1998) 4297-4300. Direct force measurement at polymer brush surfaces by atomic force microscopy

104) P. K. Hansma, J. P. Cleveland, M. Radmacher, D. A. Walters, P. E. Hillner, M. Bezanilla, M. Fritz, D. Vie, H. G. Hansma, C. B. Prater, J. Massie, L. Fukunage, J. Gurley, V. Elings, *Appl. Phys. Lett*., 64 (1994) 1738-1740. Tapping mode atomic force microscopy in liquids

105) M. A. Cooper, *Anal. Bioanal. Chem.*, 377 (2003) 834-842. Label-free screening of bio-molecolar interactions

106) M. Muratsugu, F. Ohta, Y. Miya, T. Hosokawa, S. Kurosawa, N. Kamo, H. Ikeda, *Anal. Chem*., 65 (1993) 2933-2937. Quartz crystal microbalance for the detection of microgram quantities of human serum albumin: relationship between the frequency change and the mass of protein adsorbed

107) K. A. Marx, *Biomacromolecules*, 4 (2003) 1099-1120, Quartz crystal microbalance: a useful tool for studying thin polymer films complex biomolecular systems at the solution-surface interface

108) G. Z. Sauerbrey, *Z. Phys.*, 155 (1959) 206-222. The use of quartz crystal oscillators for weighing thin layers and for micro-weighing

109) M. Johnsson, N. Bergstrand, K. Edwards, J. J. R. Stålgren, *Langmuir*, 17 (2001) 3902-3911. Adsorption of a PEO-PPO-PEO triblock copolymer on small unilamellar vesicles: equilibrium and kinetic properties and correlation with membrane permeability

110) F. Höök, B. Kasemo, T. Nylander, C. Fant, K. Sott, H. Elwing, *Anal. Chem.*, 73 (2001) 5796-5804. Variations in coupled water, viscoelastic properties, and film thickness of a

Mefp-1 protein film during adsorption and cross-linking: a quartz crystal microbalance with dissipation monitoring, ellipsometry, and surface plasmon resonance study

111) Y. S. Fung, Y. Y. Wong, *Anal. Chem.*, 73 (2001) 5302-5309. Self-assembled monolayers as the coating in a quartz piezoelectric crystal immunosensor to detect salmonella in aqueos solution

112) M. Thompson, G. L. Hayward, *IEEE Int. Frequency Control Symposium* (1997)

113) A. Janshoff, H. J. Galla, C. Steinem, *Angew. Chem. Int. Ed.*, 39 (2000) 4004-4032. Piezoelectric mass-sensing devices as biosensor—an alternative to optical biosensors?

114) J. C. Giddings, *Sep. Sci.*, 1 (1966) 123-125. New separation concept based on a coupling of concentration and flow nonuniformities

115) B. Roda, A. Zattoni, P. Reschiglian, M. H. Moon, M. Mirasoli, E. Michelini, A. Roda, *Anal. Chim. Acta*, 635 (2009) 132-143. Field flow fractionation in bioanalysis: a review of recent trends

116) K. H. Weisgraber, S. C. Rall, Jr., *J. Biol. Chem.*, 262 (1987) 11097-11103. Human apolipoprotein B-100 heparin-binding sites

117) C. M. Radding, D. Steinberg, *J. Clin. Invest.*, 39 (1960) 1560-1569. Studies on the synthesis and secretion of serum lipoproteins by rat liver slices

118) R. J. Havel, H. A. Eder, J. H. Bragdon, *J. Clin. Invest.*, 34 (1955) 1345-1353. The distribution and chemical composition of ultracentrifugally separated lipoproteins in human serum

119) O. H. Lowry, N. J. Rosebrough, A. L. Farr, R. J. Randall, *J. Biol. Chem.*, 193 (1951) 265-275. Protein measurement with the folin phenol reagent

120) E. G. Bligh, W. J. Dyer, *Biochem. Cell Biol.*, 37 (1959) 911-917. A rapid method of total lipid extraction and purification

121) N. Meechai, A. M. Jamieson, J. Blackwell, *J. Colloid Interface Sci.*, 218 (1999) 167-175. Translational diffusion coefficients of bovine serum albumin in aqueous solution at high ionic strength

122) A. E. Bolton, W. M. Hunter, *Biochem. J.*, 133 (1973) 529-539. The labeling of proteins to high specific radioactivities by conjugation to a ^{125}I-containing acylating agent

123) D. G. Myszka, T. A. Morton, *Trends Biochem. Sci.*, 23 (1998) 149-150. Clamp: a biosensor kinetic data analysis program

124) R. Kuldvee, S. K. Wiedmer, K. Öörni, M.-L. Riekkola, *Anal. Chem.*, 77 (2005) 3401-3405. Human low-density lipoprotein-coated capillaries in electrochromatography

125) C. C. Dupont-Gillain, E. Pamula, F. A. Denis, V. M. De Cupere, Y. F. Dufrene, P. G. Rouxhet, *J. Mater. Sci. Mater. Med.*, 15 (2004) 347-353. Controlling the supramolecular organization of adsorbed collagen layers

126) R. Müller, J. Abke, E. Schnell, D. Scharnweber, R. Kujat, C. Englert, D. Taheri, M. Nerlich, P. Angele, *Biomaterials*, 27 (2006) 4059-4068. Influence of surface pretreatment of titanium- and cobalt-based biomaterials on covalent immobilization of fibrillar collagen

127) M. Morra, C. Cassinelli, G. Cascardo, L. Mazzucco, P. Borzini, M. Fini, G. Giavaresi, R. Giardino, *J. Biomed. Mater. Res.*, 78A (2006) 449-458. Collagen I-coated titanium surfaces: mesenchymal cell adhesion and *in vivo* evaluation in trabecular bone implants

128) S. E. Woodcock, W. C. Johnson, Z. Chen, *J. Colloid. Interface Sci.*, 292 (2005) 99-107. Collagen adsorption and structure on polymer surfaces observed by atomic force microscopy

129) E. Gurdak, P. G. Rouxhet, C. C. Dupont-Gillain, *Colloids Surf. B. Biointerfaces*, 52 (2006) 76-88. Factors and mechanisms determining the formation of fibrillar collagen structures in adsorbed phases

130) J. T. Hautala, M. V. Lindén, S. K. Wiedmer, S. J. Ryhänen, M. J. Säily, P. K. J. Kinnunen, M.-L. Riekkola, J. Chromatogr. A, 1004 (2003) 81-90. Simple coating of capillaries with anionic liposomes in capillary electrophoresis

131) B. R. Williams, R. A. Gelman, D. C. Poppke, K. A. Piez, *J. Biol. Chem.*, 253 (1978) 6578-6585. Collagen fibril formation

132) A. J. Rodríguez-Malaver, D. S. Leake, C. A. Rice-Evans, *FEBS Lett.*, 406 (1997) 37-41. The effect of pH on the oxidation of low-density lipoprotein by copper and metmyoglobin are different

133) B. Kalyanaraman, W. E. Antholine, S. Parthasarathy, *Biochim. Biophys. Acta*, 1990, 1035, 286-292. Oxidation of low-density lipoprotein by Cu^{2+} and lipoxygenase: an electron spin resonance study

134) R. J. Deckelbaum, G. G. Shipley, D. M. Small, *J. Biol. Chem.*, 252 (1977) 744-754. Structure and interactions of lipids in human plasma low density lipoproteins

135) M. Sneck, P. T. Kovanen, K. Öörni, *J. Biol. Chem.*, 280 (2005) 37449-37454. Decrease in pH strongly enhances binding of native, proteolyzed, lipolyzed, and oxidized low density lipoprotein particles to human aortic proteoglycans

136) F. Ghomashchi, S. Schüttel, M. K. Jain, M. H. Gelb, *Biochemistry*, 31 (1992) 3814-3824. Kinetic analysis of a high molecular weight phospholipase A_2 from rat kidney: divalent metal-dependent trapping of enzyme on product-containing vesicles

137) R. R. Baker, H. Y. Chang, *Biochem. Cell Biol.*, 69 (1991) 358-365. Properties of phospholipase A_2 isolated from rat serum

138) R. Shireman, L. L. Kilgore, W. R. Fisher, *Proc. Natl. Acad. Sci. USA*, 74 (1977) 5150-5154. Solubilization of apolipoprotein B and its specific binding by the cellular receptor for low density lipoprotein

139) I. D. Cruzado, S. L. Cockrill, C. J. McNeal, *J. Lipid Res.*, 39 (1998) 205-217. Characterization and quantitation of apolipoprotein B-100 by capillary electrophoresis

140) A. Johs, M. Hammel, I. Waldner, R. P. May, P. Laggner, *J. Biol. Chem.*, 281 (2006) 19732-19739. Modular structure of solubilized human apolipoprotein B-100

141) Z. Pei, H. Anderson, T. Aastrup, O. Ramström, *Biosens. Bioelectron.*, 21 (2005) 60-66. Study of real-time lectin-carbohydrate interactions on the surface of a quartz crystal microbalance

142) I. Jacquemart, E. Pamula, V. M. De Cupere, P. G. Rouxhet, C. C. Dupont-Gillain, *J. Colloid Interface Sci.*, 278 (2004) 63-70. Nanostructured collagen layers obtained by adsorption and drying;

143) J. T. Elliott, M. Halter, A. L. Plant, J. T. Woodward, K. J. Langenbach, A. Tona, *Biointerphases*, 3 (2008) 19-28. Evaluating the performance of fibrillar collagen films formed at polystyrene surfaces as cell culture substrates

144) U. P. Steinbrecher, *J. Biol. Chem.*, 262 (1987) 3603-3608. Oxidation of human low density lipoprotein results in derivatization of lysine residues of apolipoprotein B by lipid peroxide decomposition products

145) I. Jialal, S. Devaraj, *Clin. Chem.*, 42 (1996) 498-506. Low-density lipoprotein oxidation, antioxidants, and atherosclerosis: a clinical biochemistry perspective

146) J. Stocks, N. E. Miller, *J. Lipid Res.*, 39 (1998) 1305-1309. Capillary electrophoresis to monitor the oxidative modification of low density lipoproteins

147) E. Hurt-Camejo, G. Camejo, P. Sartipy, *Curr. Opin. Lipidol.*, 11 (2000) 465-471. Phospholipase A_2 and small dense low-density lipoprotein

148) P. Bernfeld, T. F. Kelley, *J. Biol. Chem.*, 239 (1964) 3341-3346. Proteolysis of human serum β-lipoprotein

149) L. J. Siskind, M. Colombini, *J. Biol. Chem.*, 275 (2000) 38640-38644. The lipids C_2- and C_{16}-ceramide form large stable channels

150) L. J. Siskind, R. N. Kolesnick, M. Colombini, *J. Biol. Chem.*, 277 (2002) 26796-26803. Ceramide channels increase the permeability of the mitochondrial outer membrane to small proteins

151) U. Westphal, B. D. Ashley, *J. Biol. Chem.*, 233 (1958) 57-62. Steroid-protein interactions: IV. Influence of functional groups in Δ^4-3-ketosteroids on interaction with serum and β-lactoglobulin

152) T. J. Berg, O. Snorgaard, J. Faber, P. A. Torjesen, P. Hildebrandt, J. Mehlsen, K. F. Hanssen, *Diabetes Care*, 22 (1999) 1186-1190. Serum levels of advanced glycation end products are associated with left ventricular diastolic function in patients with type 1 diabetes

153) D. A. Slatter, R. G. Paul, M. Murray, A. J. Bailey, *J. Biol. Chem.*, 274 (1999) 19661-19669. Reactions of lipid-derived malondialdehyde with collagen

154) S. Lund-Katz, J. A. Ibdah, J. Y. Letizia, M. T. Thomas, M. C. Phillips, *J. Biol. Chem.*, 263 (1988) 13831-13838. A ^{13}C NMR characterization of lysine residues in apolipoprotein B and their role in binding to low density lipoprotein receptor

155) J. Ruiz-Jimenez, R. Kuldvee, J. Chen, K. Öörni, P. Kovanen, M.-L. Riekkola, *Electrophoresis*, 28 (2007) 779-788. Open tubular CE for *in vitro* oxidation studies of human very-low-density lipoprotein particles

156) K. Vainikka, J. Chen, J. Metso, M. Jauhiainen, M.-L. Riekkola, *Electrophoresis*, 28 (2007) 2267-2274. Coating of open tubular capillaries with discoidal and spherical high-density lipoprotein particles in electrochromatography

157) S. Ghosh, M. K. Basu, J. S. Schweppe, *Anal. Biochem.*, 50 (1972) 592-601. Agarose gel electrophoresis of serum lipoproteins: determination of true mobility, isoelectric point, and molecular size

158) E. Hurt-Camejo, G. Camejo, B. Rosengren, F. Lopez, O. Wiklund, G. Bondjers, *J. Lipid Res.*, 31 (1990) 1387-1398. Differential uptake of proteoglycan-selected subfractions of low density lipoprotein by human macrophages